

INVESTIGATING CONTROLS OVER METHANE PRODUCTION AND BUBBLING
FROM INTERIOR ALASKAN LAKES USING STABLE ISOTOPES AND
RADIOCARBON AGES

By

Laura S. Brosius

RECOMMENDED:

M. J. Woods

Katey Walter Anthony

Advisory Committee Co-Chair

M. Sydonia Bret Horle

Advisory Committee Co-Chair

Richard D. Boone
Chair, Department of Biology and Wildlife

APPROVED:

Paul W. Sayer
Dean, College of Natural Science and Mathematics

Lamorne K. Suffy
Dean of the Graduate School

April 8, 2010
Date

INVESTIGATING CONTROLS OVER METHANE PRODUCTION AND BUBBLING
FROM INTERIOR ALASKAN LAKES USING STABLE ISOTOPES AND
RADIOCARBON AGES

A
THESIS

Presented to the Faculty
of the University of Alaska Fairbanks
in Partial Fulfillment of the Requirements
for the Degree of

MASTER OF SCIENCE

By

Laura S. Brosius, B.S.

Fairbanks, Alaska

May 2010

Abstract

Large uncertainties in first-order estimates of the magnitude of CH₄ emissions from lakes (global lakes: 8-48 Tg CH₄ yr⁻¹, Bastviken et al. 2004) result from variation in ebullition (bubbling) rates between and within lakes. Based on a comparison of two interior Alaska thermokarst lakes, I suggest that variation in CH₄ ebullition observed within and between lakes can be explained by a few key differences in substrate quality and sediment density. Killarney Lake, which has a 130 cm-thick modern sediment package, emitted 120 mg CH₄ m⁻² day⁻¹ produced from a mixture of modern C and permafrost C sources, while Goldstream Lake, a younger lake with only 2-5 cm of modern lake sediment, emitted more CH₄ (183 mg CH₄ m⁻² day⁻¹) produced mostly from thawed permafrost. Incubated thawed permafrost supported production of substantially more CH₄ (0.25 ± 0.04 mg CH₄ g TC⁻¹ d⁻¹) than did taberal lake sediments (0.08 ± 0.02 mg CH₄ g TC⁻¹ d⁻¹). Together, these lines of evidence support the importance of permafrost C availability as control on CH₄ production and bubbling in thermokarst lakes.

Stable isotope and radiocarbon values of contemporary interior Alaska thermokarst lake CH₄ emissions reported in this study could help constrain contributions of thermokarst lakes to the global atmospheric CH₄ budget. I show here that methanogens in close proximity to thermokarst utilized pore water derived from melted permafrost ice as a hydrogen source, and that δD_{CH₄} values reflected ancient δD of precipitation. δD_{CH₄} values from Alaskan thermokarst lakes were less-depleted than δD_{CH₄} values from Siberian lakes. Thus, thermokarst lake contributions to early Holocene atmospheric CH₄ concentrations were likely higher than originally thought.

Table of Contents	Page
Signature Page	i
Title Page	ii
Abstract	iii
Table of Contents	v
List of Figures	viii
List of Tables	ix
Acknowledgements	x
Chapter 1: Introduction and Overview	1
1.1 Introduction	1
1.2 The Interior Environment	2
Permafrost	2
Organic matter inputs to Alaskan lake sediments	4
Vegetation	5
Study Sites	5
1.3 Methanogenesis	8
Physical and biological controls	10
Pathway controls	12
Methane oxidation	13
1.4 Stable Isotopes	16
Carbon isotopes	16
Hydrogen isotopes	17
1.5 CH ₄ Bubbling in Northern Lakes	18
1.6 Conclusion	22
References	24
Tables	33
Chapter 2: A comparison of CH ₄ production and bubbling from two interior Alaskan thermokarst lakes	34
Abstract	34

2.1 Introduction	35
2.2 Methods	38
Physiography of study area	38
Study lakes	40
Sample collection and analysis	42
Geophysics	43
Anaerobic laboratory incubation	44
Calculations	45
2.3 Results	46
Whole-lake CH ₄ production	46
Bubble fluxes and composition	46
Production Pathway	48
Anaerobic incubation results	48
Permafrost and sediment characteristics	49
Geophysics	50
Limnology	51
2.4 Discussion	52
Temperature and production pathway	52
Bubble gas composition variation	52
Whole-lake CH ₄ production	55
2.5 Conclusion	59
Acknowledgements	60
References	60
Figures	66
Tables	84
Chapter 3: Implications of δD_{CH_4} from Alaskan thermokarst lakes for past and present atmospheric CH ₄ budgets	95
Abstract	95
3.1 Introduction	95

3.2 Methods.....	99
Study site	99
Sample collection and analysis.....	99
Calculations	99
3.3 Results.....	100
Bubble isotopic and elemental composition.....	100
Water isotopes and H mixing model	100
3.4 Discussion	103
3.5 Conclusion.....	104
Acknowledgements	104
References.....	105
Figures.....	109
Tables	112
Appendix.....	113

List of Figures	Page
2.1: During the Last Glacial Maximum, aeolian silt accumulated on hillsides.....	65
2.2: Similarities and differences between valley-bottom Alaskan.....	66
2.3: Approximate coring locations (A,B,C) and approximate transect locations.....	67
2.4: Seep locations.....	68
2.5: Average CH ₄ concentrations for all ebullition point seeps.....	69
2.6: Study lake ¹⁴ C-CH ₄ radiocarbon ages of bubbling.....	70
2.7: The result of 1) upscaling lake ice bubble survey results.....	71
2.8: Changes in bubble CH ₄ concentration of discreet seeps.....	72
2.9: Bimodal graph of bubble flux vs. CH ₄ concentration	73
2.10: High-emission ebullition seeps were dominated by CO ₂ reduction.....	74
2.11: Production potentials of anaerobically incubated lake sediments sections.....	75
2.12: Down-core gamma density.....	76
2.13: Deep resistivity data collected using 5 m electrode spacing.....	77
2.14: Shallow resistivity data collected using 2 m electrode spacing.....	78
2.15: Goldstream Lake's 1949 margin.....	79
2.16: Range of potential permafrost C contributions to specific seep bubbling.....	80
2.17: Schematic of Killarney Lake and its talik.....	81
2.18: Schematic of the eastern end of Goldstream Lake and its talik.....	82
3.1: Seep CH ₄ was more enriched in δD with increased distance.....	108
3.2: Schematic of Goldstream Lake showing varying H contributions.....	109
3.3: δD and δ13C of CH ₄ emissions from Siberian lakes, Alaskan lakes	110
A.1: The measured resistivity of Fairbanks silt.....	113
A.2: Lake temperature profiles.....	114

List of Tables	Page
1.1: Major research gaps in understanding interior Alaskan thermokarst lake methane	33
2.1: Summary of past studies measuring CH ₄ concentrations in bubbling	83
2.2: Anaerobic incubation substrate characteristics and methane production potentials	84
2.3: Elemental and isotopic composition of lake bubbles	85
2.4: Sediment core photo, interpretation	86
2.5: Permafrost and sediment isotopic and elemental composition	92
2.6: Predicted bubble gas composition for bubbles of different sizes	93
3.1: Source water isotopic composition	111
A.1: Explanation of whole lake bubbling estimates	115
A.2: Goldstream Lake hydrological data	116
A.3: Killarney Lake hydrological data	117
A.4: Isotopic and elemental composition of all bubbling seeps sampled	118
A.5: Isotopic and elemental composition of all other bubbling seeps	119
A.6: Water isotope data from lakes and sediment pore water	120
A.7: Coordinates of coring locations	121

Acknowledgements

First, I would like to give thanks to Katey Walter Anthony for her patience and belief in my ability to mature into a capable scientist. Her high expectations challenged me to live up to my potential and the hard-working example she set as a researcher, communicator and professional inspired me in many ways. I would also like to thank Donie Bret-Harte for her gentle support and guidance, as well as many wonderful meals and relaxing evenings at Tamarack Knoll. As co-advisors, Katey and Donie were perfectly balanced. I have greatly appreciated Mat Wooller's infectious enthusiasm and inspiration as an "isotopist," and Jay Jones' humor and perspective. Thanks to both Mat and Jay for completing an excellent committee that provided an abundance of helpful feedback to my research.

I owe many thanks to Jeff Chanton for his guidance, knowledge of methane and isotopes, and collaboration on bubble gas stable isotope determination at Florida State University. Thanks also to: Dragos Vas for sharing the graduate school experience with me and keeping me sane with indefatigable humor and laughter; Mat and Ben Gagliotti for their assistance in retrieving sediment cores from Killarney and Goldstream lakes, and for their help, along with Nancy Bigelow in interpreting them; Bill Lee, Bill Schnabel, Jens Monk and Jay Nolan for sharing their expertise in geophysics and for their assistance in collecting and processing electrical resistivity data. The tireless assistance of Dragos, Laurel McFadden, Brian Sweeney, Melissa Smith and Edda Mutta made field work a joy. The extra effort made by Louise Farquarson and Laura Oxtoby to process lake cores from my field sites at LacCore greatly improved my research results; and Melanie Engram's GIS assistance strengthened the presentation of my work. Finally, thank you to Guido Grosse, Benjamin Jones and Mary Edwards for sharing dialog that enhanced my graduate school experience.

Thank you to my Mother, Father and sisters, Emily and Michelle, whose love and support have meant a great deal. I credit my father for provoking at an early age my curiosity

about the world and for instilling in me an appreciation of scientific thought and reason. Being far away from home, Mother's care packages were endlessly uplifting.

Thanks to Alaska ESPSoR for one year of partial funding, the Center for Global Change for two Global Change Grants, the Institute of Northern Engineering for 1.3 years of funding, the Institute of Arctic Biology for providing a summer research fellowship and one semester of funding, and the Department of Biology and Wildlife for providing three TA awards. Additional funding for this research came from IARC, DOE #DE-NT0005665, and NSF grants IPY #0732735 and OPP #0632264.

Chapter 1: Introduction and Overview

1.1 Introduction

Recent emphasis on climate change has brought study of atmospheric methane (CH_4) sources and sinks to the forefront. Methane has a radiative effect about 25 times that of CO_2 (Wuebbles & Hayhoe 2002). Though a large fraction of atmospheric CH_4 is of modern bacterial (non-thermogenic) origin, controls on CH_4 production and emission are only moderately understood. Past studies have focused on CH_4 emissions from prominent biological sources such as wetlands, agriculture (rice paddies, ruminant animals) and termites that comprise the majority of CH_4 release. Recent work has added CH_4 produced under aerobic conditions in terrestrial plants and bubbling from northern lakes to this list of sources. Lake CH_4 is produced largely by microbes living in anoxic lake sediments. Global first-order estimates of lake emissions range from 8-55 $\text{Tg CH}_4 \text{ yr}^{-1}$ (Smith & Lewis 1992, Bastviken et al. 2004, Walter et al. 2007). Siberian lakes alone contribute as much as 3.6 $\text{Tg CH}_4 \text{ y}^{-1}$ to the atmosphere, largely via ebullition (bubbling) (Walter et al. 2006). Walter (2006) and others (Casper et al. 2000, Huttunen et al. 2003a, 2003b, Juutinen et al. 2003, Bastviken et al. 2004) have investigated rates of lake CH_4 bubbling and Walter et al. (2006) attributed high bubbling rates to high organic matter availability from thawing permafrost in Siberian lakes. While strong spatial patchiness associated with bubbling frequency and composition both within and between lakes has been observed, the causes of, and controls over spatial heterogeneity in bubbling, with respect to temperature, sediment characteristics and hydrology, have yet to be explained. My thesis research used field studies and isotopic analyses to investigate controls over methane bubbling from two interior Alaska lakes, providing information for a region where lake CH_4 emissions have been largely unstudied.

This chapter will give a basic overview of 1) the climate, environment and landscape processes of interior Alaska, 2) methanogenesis and its apparent controls, 3) the use of stable isotopes as biogeochemical tracers of physical and microbial processes and 4) CH_4

bubbling in northern lakes. Gaps in the current state of knowledge will be identified and addressed with respect to my work.

1.2 The Interior Environment

Permafrost

Interior Alaska lies within a 4.3 million ha circumpolar zone of discontinuous permafrost, which covers 3.9% of earth's land area (Brown et al. 1997). Present day mean annual air temperatures for the region average -3.3°C . During the Last Glacial Maximum, despite cooler temperatures ($\sim -7.0^{\circ}\text{C}$) (P  w   1975), interior Alaska remained largely unglaciated due to a drier climate. Glaciation during this period was constrained to mountain ranges and high altitudes. The unglaciated interior landscape collected aeolian loess, blown primarily from the Tanana River to the south, and secondarily from the Yukon River to the north and Nenana River to the southeast, which in some cases accumulated on hillsides over the course of the late-Quaternary (Muhs et al. 2003, Muhs and Budhan 2006). Colluvial forces and frost action gradually eroded loess down slope, redepositing it as ice-rich permafrost that formed syngenetically (concurrent with deposition) and now fills area valley bottoms to a thickness of 10-30 m (P  w   1975). Based on age (14,860-56,900 y.b.p., all radiocarbon dates are presented in this thesis as uncalibrated radiocarbon years before present) and relatively high organic carbon content (0.38 – 2.39% C) (P  w   1952), loess deposits appear to have originated in the productive Pleistocene steppe environment where fast-growing graminoid roots and leaf litter rapidly accumulated.

Alaskan Pleistocene-aged loess deposits are similar in character to Siberian yedoma, and are termed hereafter “yedoma-like.” Late Pleistocene-aged Siberian yedoma also consists of loess and loess-like sediments, is ice-supersaturated, and contains large quantities of organic carbon (2-20% C) owing to its steppe origin (Zimov et al. 2001, 2006b). Yedoma-like permafrost in interior Alaska, due to its retransportation from hill tops to valley bottoms, is of mixed late-Pleistocene age and lacks the chronology and continuity of Siberian yedoma, which was not widely redeposited. Because of these similarities in

character, permafrost-related studies conducted in Siberia can inform and often parallel work conducted in interior Alaska.

Thermokarst activity (ground surface subsidence resulting from icy permafrost thaw) affects the majority of periglacial lowlands throughout the Arctic. 78% and 72% of Siberia's coastal lowlands and Alaska's Barrow Peninsula investigated via Landsat-7 have been influenced by thermokarst processes, respectively (Grosse et al. 2006, Hinkel et al. 2003). Thermokarst lakes occupy a relatively large area of Interior Alaska (5.5-14.3% land area, Arp & Jones 2009). These lakes formed as Holocene warming thawed ice-rich permafrost, resulting in ground subsidence and depressions that filled with water. Thermokarst processes continue to erode lake shores, drain, recreate and form new lakes – generating a dynamic, changing landscape. Understanding these landscape processes is important because they can both result from, and act as positive feedbacks to climate warming.

Permafrost-driven landscape processes affect decomposition and alter the quantity and quality of organic matter contained in permafrost. Loess permafrost in the Fairbanks area exhibits varying C and N concentrations. The history of these permafrost deposits may explain such differences. 'Virgin' yedoma permafrost (yedoma permafrost that has remained frozen since initial formation), contains large amounts of highly reactive organic matter, as determined by laboratory incubations of thawed Siberian yedoma permafrost (Zimov et al. 1997, 2006a, Dutta et al. 2006). Permafrost that thaws beneath a lake (termed taberal sediment), is subject to decomposition in the benthic environment. These taberal sediments become increasingly depleted in C and N as the labile fraction of organic matter is decomposed. Up to 30% of organic C can be lost from beneath Siberian yedoma lakes due to microbial decomposition (Kholodov et al. 2003, Walter et al. 2007). Upon eventual lake drainage or migration, subaerial (ground surface) exposure of drained lake sediments to mean annual atmospheric temperatures below zero causes taberal sediments to refreeze. The remaining organic matter, which is more recalcitrant, becomes sequestered in the reforming 'non-virgin' permafrost.

Forest fire also impacts a high percentage of interior Alaskan loess permafrost, altering permafrost C and N content. Severe forest fires, by destroying insulating vegetative ground cover in black spruce stands, can significantly increase active layer depth and soil temperature (O'Neill et al. 2002, 2003, Yoshikawa et al. 2003). As C stored in the newly-thawed active layer becomes bioavailable, rates of microbial decomposition increase (O'Neill et al. 2002, 2003). Mass balance models based on field measurements indicate that recently burned soils may release $1.8 - 11.0 \text{ Mg C ha}^{-1}$, or 12.4% - 12.6% of total soil organic C matter (O'Neill et al. 2003) for 7-15 y after fire. Similar to the process of organic matter depletion and refreezing of taberal sediments in thermokarst lakes, fire may leave C- and N-depleted soils which also refreeze into "non-virgin" permafrost as the burned environment recovers.

Organic matter inputs to Alaskan lake sediments

Interior Alaskan lakes are typically productive and often, though not always, affected by thermokarst. A mid-summer survey of 15 interior Alaskan lakes revealed slightly basic pH values (8.17 ± 0.7), low conductivity ($155 \pm 94 \text{ uS}$), super-saturated dissolved oxygen concentrations ($9.64 \pm 3.0 \text{ mg/L}$), moderate dissolved organic carbon (DOC, $73.5 \pm 78.0 \text{ mg/L}$), dissolved inorganic carbon (DIC, $20.1 \pm 13.6 \text{ mg/L}$) and total phosphorus (TP, $58.0 \pm 118.0 \text{ mg/L}$) concentrations, and low total nitrogen ($0.96 \pm 0.67 \text{ mg/L}$) (Gregory-Eaves et al. 2000). Thermokarst activity in these lakes was not assessed by Gregory-Eaves et al.; however all of eleven interior Alaskan lakes surveyed by our laboratory group from 2007 to 2009 showed evidence of thermokarst along margins (Walter Anthony et al. *pers. comm.*).

A variety of C sources are present in lake environments and occur in three forms: particulate organic carbon (POC), DOC and DIC. Possible DOC sources include root exudates of aquatic or terrestrial macrophytes, leachate from modern soils and recently thawed permafrost, and extra- or intracellular compounds liberated from algae and zooplankton. POC is supplied in the form of modern terrestrial leaf litter and plant

detritus deposited via wind or water, aquatic plant detritus, ancient plant detritus liberated via thermokarst processes, and structural components of other dead aquatic organisms. DIC can be produced within the lake via heterotrophic respiration and CH₄ oxidation, can be mineralized from rock or carbonate shells of aquatic organisms, or can diffuse into the lake from the atmosphere.

In productive lakes with little to no thermokarst activity, modern C sources drive microbial activity. Aquatic primary production by photosynthetic algae and macrophytes constitutes an important carbon source to microbes in many eutrophic lakes in interior Alaska (Corcoran et al. 2009). However, many arctic lakes are oligotrophic (Engstrom 1987, Tranvik 1988), and receive much of their C inputs from allochthonous sources (Hobbie et al. 1999). This means that modern terrestrial inputs (e.g. leachate and litter) in oligotrophic lakes, and aquatic primary production in interior Alaska's eutrophic lakes, constitute important carbon sources to lake microbes and benthic organisms in lakes with little to no thermokarst activity.

Vegetation

The northern boreal forest, which dominates in interior Alaska, exhibits spatial variations in temperature, soil moisture and permafrost characteristics that largely govern vegetation cover. White spruce (*Picea glauca*) and early successional species including paper birch (*Betula papyrifera*), aspen (*Populus tremuloides*), and balsam poplar (*P. balsamifera*), dominate warm, dry south-facing slopes. Cool, wet, north-facing slopes and lowlands are populated by black spruce (*Picea mariana*), larch (*Larix laricina*) and mosses. Alder (*Alnus crispa*), bog birch (*B. glandulosa*), dwarf birch (*B. nana*) and willow (*Salix spp.*) shrubs may also be present (Viereck and Little 1986). Thermokarst lakes are found most often in low-elevation areas, such as valley bottoms.

Study Sites

I studied two shallow (~2.0 m) thermokarst lakes near Fairbanks, Alaska. Killarney Lake (64.86°N, 147.90°W, elev. 162 m), situated in Goldstream Valley at the base of the

Happy Creek watershed (draining the eastern slopes of Ester Dome) is 2.1 m deep and underlain by discontinuous permafrost. Triangular in shape, the lake is bordered on two sides by emergent grasses and on the third side by a moderately eroding bank dotted with black spruce (*Picea mariana*). A seasonal inlet and outlet flow adjacent to one another at the southern apex, carrying substantial volumes of water and detritus during spring thaw. Sediment cores reveal a 130 cm-thick modern to Holocene-aged sediment package consisting of alternating organic and mineral layers of varying thickness – presumably the result of fluvial deposition of terrestrial organic matter and mineral sediments, thermokarst erosion, and in-lake production. A 10 cm-thick detritus-rich “trash layer” forms a possible lower boundary of the modern sediment package and is composed of well preserved terrestrial organic material that was likely inundated at the onset of lake formation. A spruce needle from the trash layer (137 cm below sediment surface) was radiocarbon dated at 290 y.b.p. Below this trash layer I found 60 cm of dense, mineral loess that makes up the surface tens of meters of discontinuous permafrost in interior Alaska (discussed above). Due to the relatively young age and small size of Killarney Lake, it is likely that this mineral horizon constitutes the top of the tabular unit; however, the length of our sediment core was insufficient to confirm this. In Siberian coastal exposures of drained thermokarst lake profiles, similar alternating mineral and organic-rich horizons (<1-50 cm thick each), which together comprised packages of lake sediments up to 15 m thick, were observed (Walter Anthony, *pers. comm.*).

Goldstream Lake (64.92°N, 147.85°W, elev. 177 m) is 2.2 m deep and is also located in Goldstream Valley, a region of discontinuous permafrost north of Fairbanks. Unlike Killarney, it has no significant surface water connectivity. Goldstream’s longitudinal lake shores consist of wide (2-5 m) cattail (*Typha spp.*) stands. Large ground fissures (caused by freeze-thaw cycling and permafrost thaw), freshly eroded surfaces and inundated vegetation on the eastern lake margin are evidence of acute thermokarst activity eroding loess permafrost. Aerial photos of 1949 revealed that the lake was larger on the N-S axis than it was in 2007-2009 during my study period, but smaller on the E-W axis (Chapter 2, Figure 2.15). On the lake bottom, an extremely thin (< 3 cm) modern organic sediment

layer, composed mainly of aquatic detritus of locally dominant *Ceratophyllum demersum*, overlies a thick package of silty loess. Near the eastern thermokarst margin, peaty units containing fragments of *Drepanocladus spp.* were interspersed with mineral sediments in our 0.95 m lake core (Chapter 2, Table 2.4c). These units, however, were not observed in the 0.55 and 0.60 m cores from the lake center. Loess sediments are thought to be of the same origin as Pleistocene-aged retransported loess permafrost that fills many area valleys. Dating by ^{210}Pb suggested Goldstream may be a very young lake, less than 100 year old (Turner 2009).

Beneath both lakes, permafrost has been locally thawed by heat transferred from surface waters, forming thaw bulbs (taliks). The benthos of both lakes in this study were dominated almost exclusively by coon tail (*C. demersum*) small patches of *Potamogeton spp.* Aquatic mosses (*Drepanocladus spp.*) were present in the littoral zones, and water lilies (*Nuphar spp.*) were found in Goldstream Lake.

Killarney Lake, due to its lower elevation, protected location and shorter fetch appears to have a slightly cooler mean annual temperature regime and maintains more dramatic temperature differences between the hypolimnion and epilimnion throughout the summer than does Goldstream Lake, which is longitudinally oriented in the direction of prevailing winds and therefore better mixed. Maximum summer surface water temperatures for Killarney and Goldstream were 18.4°C and 19.6°C, respectively. Both lakes had similar summer pH values of 8.0 for Goldstream and 7.9 for Killarney, and similar oxidation reduction potentials of 381 mV for Goldstream and 353 mV for Killarney. Goldstream had higher average summer conductivity (770 uS), and lower summer dissolved oxygen (DO) concentrations (5.33 mg/L) than Killarney (cond: 350 uS, DO: 7.61 mg/L). Both lakes had higher summer conductivity but similar summer pH values, on average, than the 15 interior Alaskan lakes in Gregory-Eaves et al.'s study (2000).

1.3 Methanogenesis

Methanogenesis is an important microbial process that contributes globally significant volumes of CH₄ to the atmosphere. Because CH₄ is a potent greenhouse gas, it is important that we understand methanogenesis and its controls in order to more accurately evaluate the role of bacterial CH₄ in global C cycling and climate warming.

Methanogenesis occurs via two major pathways. The first is by oxidation of H₂ and reduction of CO₂ to CH₄:



The second is by fermentation of acetate (CH₃COOH) or other methylated compounds to CH₄:



In each process, CO₂ or acetate serves as terminal electron acceptor, and hydrogen serves as an energy source. A proton gradient created across a cell membrane, on the other side of which the hydrogenase is located, is used to produce ATP via electron transfer, or reducing power in the form of NADPH. Both NADPH and ATP are used to fix C via the Calvin Cycle. Additionally, ATP provides energy for cell growth and maintenance.

A syntrophic relationship exists between methanogens and fermenting bacteria.

Methanogens depend on other bacteria for hydrolysis of complex carbon polymers to smaller molecules and subsequent fermentation of these products to even smaller carbon units (acetate, CO₂ and H₂). Fermenters also depend on methanogens. While common end products of isolated chemoheterotrophic fermentation include butyrate, propionate, ethanol, butanol, propanol, acetate, acetone, and some H₂ and CO₂, oxidation of H₂ by methanogens provides H⁺ for use as a terminal electron acceptor in fermentation reactions and eliminates the need for other electron acceptors. This augmentation of lone chemoheterotrophic fermentation and subsequent fueling of methanogenesis is termed interspecies H₂ transfer. Chemoheterotrophs also depend on hydrogenotrophic

methanogens to lower the concentration of H₂, thereby changing equilibrium conditions and creating an environment in which certain reactions, such as transformation of butyrate to acetate and H₂, can proceed. Many reactions would not otherwise be thermodynamically viable (Mah et al. 1982).

Methanogenesis is thought to be carried out exclusively by anaerobic archaea. Recent studies suggest that methane may also be aerobically produced in large quantities (up to 176 Tg y⁻¹) from pectins in living plants tissues and senescent leaves (Keppler et al. 2006, Ferretti et al. 2007, McLeod et al. 2008).

Twenty-six genera and up to 80 species of methanogenic archaea have been identified (Garcia et al. 2000). All methanogens contain methyl coenzyme M reductase (MCR) genes. Because no other group of microorganisms possesses this functional operon, it is useful for identifying methanogens. Most methanogenic clones belong to the orders: *Methanosarcinaceae*, *Methanosaetaceae*, *Methanomicrobiaceae*, *Methanobacteriacea*, *Methanothermus*, *Methanopyrus* and the yet uncultured kingdom, *Crenarchaeota* (Chin et al. 1999, Metje and Frenzel 2007). Thermophilic methanogens found in thermal vents represent the families *Methanococcoceae* and include *methanohyperthermococcus*, *methanothermococcus* and *methanocaldococcus* (Nercessian et al. 2005). Genera from all families except for *Methanosarcinaceae* and *Methanosaetaceae* can use the CO₂/H₂ reduction pathway. *Methanosarcinales* and *Methanosaetaceae* are obligate acetoclasts (methanogens which utilize the acetate fermentation pathway).

Methanogenesis occurs in a variety of anoxic environments, including wetlands, lake sediments, soils and unique marine environments such as spreading centers and seeps. However, the rate of CH₄ production in the greater ocean is significantly lower than in freshwater environments due to high concentrations of sulfate. Sulfate availability favors energetically more profitable sulfate reduction, and leads to dominance of sulfate-reducing bacteria (SRB) over methanogens. Methanogenesis can also occur in the guts of

termites and ruminant animals; however, my thesis will focus explicitly on methanogenesis in anaerobic lake sediments.

Physical and biological controls

A suite of physical and biological factors control CH₄ production and pathway dominance in natural and laboratory environments. These include: soil saturation, temperature, organic substrate quality and availability, competition (i.e., presence of other electron acceptors and the microbes that utilize them), and the availability of other inhibiting compounds.

Methanogenesis requires anoxic conditions to proceed, making soil/sediment saturation a straightforward control mechanism based on the fact that diffusion rates of O₂ through water are very slow ($1.8 \times 10^{-4} \text{ cm s}^{-1}$). Rates of methanogenesis within the soil column varied with saturation in a study comparing Scottish and Swedish peat cores (Beckmann and Llyod 2001). Water table height also explained the majority of CH₄ flux variation in a chamber study conducted in northern Ontario (Bubier et al. 1993).

After anoxic conditions have been met, organic substrate availability and quality are considered the major limiting factors for CH₄ production (Segers 1998). Soil carbon content was shown to be positively correlated with CH₄ production ($r^2=0.83$) in a study by Ramakrishnan et al. (2000), supporting the importance of substrate availability. Declining organic material quality and quantity with depth were found to decrease CH₄ production over incubated peat core depths of 10 cm to 40 cm (Galand et al. 2002). Addition of direct methanogenic precursors (acetate, CO₂, H₂) to incubated soils boosted production of CH₄ in studies by Valentine et al. (1994) and Sorrell et al. (1997). Indirect precursor addition (leaf leachate, glucose) has also been shown to increase CH₄ production (Bachoon & Jones 1992, Amaral & Knowles 1994). Root decay and root exudates supply highly labile C that enhanced CH₄ production in the rooting zone of plants (King et al. 2002). Whiting and Chanton (1993) posited net ecosystem production as a master variable controlling CH₄ production, noting a conversion factor of 3% NEP as

CH₄ released in wetlands. This work, however, was criticized for its low repetition and use of an explanatory variable that in its very nature ties together many different mechanisms of control on ecosystem processes. Together, these studies present a compelling case for the importance of organic matter availability as a factor controlling CH₄ production. However, all of these studies were conducted in wetland soils. Less is known about the controls on CH₄ production in lake sediments.

The presence of other nutrients available in oxidized form may decrease CH₄ production because of their kinetically-preferred status as electron acceptors for other carbon-competitive microbes. Sulfate greatly reduces the extent of methanogenesis in oceans because of sulfates reducing bacteria's competitive advantage. Even small additions (0.2 mM) of SO₄ were shown to inhibit CH₄ production in incubated Lake Mendota sediments (Winfrey and Zeikus 1977). Stable isotope studies revealed NO₃, SO₄ and Fe(II) as inhibitors of CH₄ production to some extent, due to the competitive advantage of nitrate-reducing, sulfate-reducing and iron-reducing microbes over methanogens for carbon resources (Chidthaisong & Conrad 2000). Iron, where present, is especially inhibiting and often affects freshwater systems. Frenzel et al. (1999) showed that CH₄ production in rice paddy microcosms was variable between soil layers where ferric iron was present (upper layer) and absent (lower layer). After complete reduction of iron in the upper soil layer, a dramatic increase in rates of methanogenesis was observed (Frenzel et al. 1999). The same was true in incubations of subarctic peat: CH₄ concentrations increased as Fe(II) concentrations decreased over time (Metje and Frenzel 2007).

Finally, temperature controls rates of methane production. Laboratory incubations of soils and sediments from a variety of environments have yielded different thermal optima for CH₄ production. In subarctic peat, the optimum reaction temperature for methanogens is around 27°C (Metje and Frenzel 2007). Temperature optima in other incubations were 30°C for methanogens from a Russian mire (Simankova et al. 2001), 35°C for those from Lake Constance (Switzerland) (Schultz et al. 1997), and 20-25°C (Kotsyurbenko et al. 2004) and 50°C (Nozhevnikova et al. 1997) for microbial communities in a Siberian peat

bog (at depth) and in lake sediments, respectively. Ganzert et al. (2006) showed that mesophiles and psychrophiles do inhabit different soil horizons in Siberian permafrost; however, Metje & Frenzel (2007) point out both that it is not uncommon for thermal optima to deviate from *in situ* temperatures, and that high temperature optima do not preclude successful function of organisms even at cold temperatures. This body of work demonstrates the thermodynamic control over methanogenesis *in vitro*: warmer temperatures support higher rates of methanogenesis.

Pathway controls

Temperature, in part, also appears to control which CH₄ reaction pathway dominates production. Metje and Frenzel (2007) note that at optimum temperatures for overall CH₄ production (20–50°C), acetoclastic methanogens dominated, while at lower temperatures (0–4°C), CO₂-reducing methanogens were far more productive. Methane dated to 25,000 y.b.p. with a $\delta^{13}\text{C}_{\text{CH}_4}$ value of < -80‰ was recovered from inside an ice wedge in the Fox permafrost tunnel (Katayama et al. 2007). This suggests that microbes also operate at subzero temperatures, albeit slowly, and that permafrost itself (rather than thawed permafrost) can form CH₄ that is stored in permafrost and released upon warming or thaw (Katayama et al. 2007). However, the total amount of CH₄ from this source annually is 3–5 orders of magnitude lower than other natural and anthropogenic sources. Along with temperature, depth within the soil/sediment column appears to determine relative rates of CH₄ production from CO₂ and acetate. In an analysis of Siberian peat cores, an increasing contribution from CO₂-reducing microbes was observed with increasing depth (Kotsyurbenko et al. 2004). This could be a function of substrate quality and availability, which can decrease with depth, or the result of shifts in microbial community structure toward those species adapted to cooler temperatures closer to permafrost at greater depth.

In some environments CO₂ reduction has been shown to completely dominate CH₄ production. Duddlestone et al. (2002) reported on an oligotrophic, acidic peat bog Anchorage, Alaska, where CO₂ reduction dominated CH₄ production, and acetate actually accumulated, despite the fact that acetate fermentation is energetically favored over CO₂

reduction. Further investigation of the microbial community present at the site showed an absence of acetotrophic methanogens *methanosarcinaceae* and *methanosaetaceae* (Rooney-Varga et al. 2007), suggesting that the CO₂-reducing methanogens dominate under cold, oligotrophic conditions. Ordination of field data from this and other Alaskan study sites linked CH₄ production pathway most strongly to vegetation type, with acidic *sphagnum*-dominated wetlands accumulating acetate and *carex*-dominated wetlands consuming it (Rooney-Varga et al. 2007). Other studies have also linked production pathway to modern vegetation cover in other biomes (Chanton et al. 1995, King et al. 2002).

Presence or absence of specific compounds appears also to determine which pathway is favored. Phosphate inhibits acetoclastic methanogenesis in rice paddies where CH₄ production from acetate usually represents 50-60% of the total flux (Lehmann-Richter et al. 1999). Experimental additions of as little as 20 mM PO₄⁻³ led to complete dominance by CO₂-reducing microbes and total inhibition of the acetoclastic pathway in soil incubations (Conrad et al. 2000). The mechanism of acetotroph inhibition is unknown, but is thought to be related to the adaptation of acetate-fermenting microbes to phosphate-limited conditions (Conrad et al. 2000). Yedoma soils are known for their high P contents (Dutta et al. 2006); so P cycling could be a control over acetotrophic CH₄ production in thermokarst lakes where Fe III, or other controls over P availability limit PO₄⁻³ concentrations in lake sediments.

Methane oxidation

CH₄ is produced and also consumed by microbes. Both anaerobic and aerobic methane oxidizing bacteria (MOB) consume CH₄, producing H₂ and CO₂. Net CH₄ emission is the balance of CH₄ produced and CH₄ consumed. In wetlands, CH₄ oxidation rates vary with water table depth and soil saturation. Most CH₄ oxidation observed in wetlands occurs near the oxic/anoxic boundary where oxygen becomes available to aerobic MOB.

Reeburgh et al. (1993) estimates that in high latitude wetlands up to 30% of all CH₄ produced is oxidized prior to reaching the atmosphere. An average of 43% of evolved

CH₄ in a Maine marsh was found to be consumed by MOB, and consumption shifted from 15-32% to 48-76% with seasonal drying (Roslev & King 1994). As much as 91% of CH₄ produced in peat soils in Florida was also oxidized in a subtropical wetland study (King et al. 1990). Evidence for association of MOB with plant roots and the rhizosphere has been found for several species of emergent macrophytes in Florida and elsewhere. Researchers propose that plants not only serve as conduits carrying CH₄ to the atmosphere, but also transport atmospheric gases, including O₂, to roots, rhizomes and the surrounding soils/sediments where it can be used in aerobic consumption of CH₄ (King et al. 1991, Wagatsuma et al. 1992, Epp & Chanton 1993). Variations in the fraction of CH₄ that is produced in wetlands and consumed prior to emission can therefore be attributed to differences in vegetation and hydrological regimes (Hanson & Hanson 1996). Due to large variability of these factors it is difficult to assign an overall rate of methane oxidation for wetlands.

In lakes, oxidation of dissolved CH₄ occurs at the oxycline, a region of the water column analogous to the oxic/anoxic boundary in soils. The effect of oxidation on CH₄ produced in lake sediments has been studied primarily on CH₄ that has diffused out of sediments and into the hypolimnion, the ultimate fate of which is oxidation or diffusion into the atmosphere. Highly stratified lakes may store hundreds of g C m⁻² yr⁻¹ in the form of CH₄ in anoxic hypolimnia, depending on rates of CH₄ production and diffusion into overlying, oxic waters (Michmerhuizen et al. 1996, Striegl & Michmerhuizen 1998, Huttunen et al. 2003a, Bastviken et al. 2004). Stored CH₄ may be rapidly released during mixing events, and become susceptible to oxidation as the water column become more uniformly oxygenated. In this manner, 60%, 74% and 94% of CH₄ stored in Lake 227, Canada (Rudd & Hamilton 1975), Lake Kasumigaura, Japan (Utsumi et al. 1998a) and Lake Nojiri, Japan (Utsumi et al. 1998b) (respectively) was oxidized during fall turnover (mixing of lake water). Bastviken et al. (2002) determined rates of ¹⁴CH₄ transformation, which revealed high summer rates of oxidation in two Swedish lakes (11-82 mg C m⁻² day⁻¹, or 57-100% of CH₄ produced). A third, oligotrophic lake supported much lower oxidation rates (0.22-0.47 mg C m⁻² day⁻¹). Oxidation rates also varied seasonally and

were higher in summer months than in winter. The authors attributed seasonal variation and variation of oxidation rates between lakes to differences in productivity (Bastviken et al. 2002). Oxidation of CH₄ emitted from lakes via ebullition has not been studied explicitly, but is thought to be modest because of the rapid transport of bubbles through the water column to the atmosphere.

Up to 90% of CH₄ produced in marine sediments is consumed by anaerobic MOB (Reeburgh et al. 1993). Geochemical analyses of lake and ocean sediment suggest that anaerobic methane oxidation is mediated by sulfate reduction where sulfate is abundant (Iversen and Jorgensen 1985, Reeburgh 1989). Though the syntrophic relationship between methane-oxidizing archaea and sulfate-reducing bacteria near the sulfate-methane transition zone in marine sediments is apparent, the bacterial and archaeal assemblages present and responsible for anaerobic methane oxidation are not yet well characterized (Harrison et al. 2009). This process is not considered important in freshwater environments where SO₄⁻² is often present in only very low concentrations.

Evidence for anaerobic methane oxidation coupled with denitrification has also been found during laboratory incubations of lake sediment, in which CH₄, nitrate and nitrite were consumed and N₂ was evolved (Raghoebarsing et al. 2006). In Raghoebarsing et al.'s study, ¹³C-labeled lipid biomarkers and 16S rRNA sequence analyses were used to isolate and identify two new microorganisms believed to be involved in this process. Though incubation studies of sludge from a denitrifying reactor also support this finding (Islas-Lima et al. 2004), little is known about how or where coupled nitrate reduction and methane oxidation occurs in nature (Raghoebarsing et al. 2006).

Despite extensive soil, peat and sediment core incubation studies, it is unclear how the many factors that appear to control CH₄ production in the laboratory interact in the natural environment. Of the combined effect of temperature, organic matter quality, quantity and bioavailability, microbial community structure, CH₄ oxidation rates and presence of other nutrients, it is unknown which of these factors most strongly influence

CH₄ production and emission *in situ*. Thus, continued field studies, informed by laboratory incubations, are necessary to accurately gauge and predict CH₄ production and consumption at the ecosystem level and beyond.

1.4 Stable Isotopes

Isotopic fractionation occurs when molecules containing different isotopes of a single element are preferentially selected because of their difference in mass. Fractionation signatures develop as a result of unidirectional processing, in which case they are driven by reaction kinetics, or through a process of equilibration in which molecules with higher bond force constants are more apt to contain heavier isotopes.

Ratios of ¹³C/¹²C and D/H (D = ²H), expressed as δ¹³C (‰) and δD (‰) values, are calculated:

$$\delta (\text{‰}) = ((R_{\text{sample}}/R_{\text{standard}})-1) \times 10^3 \quad (1.3)$$

Where R = ¹³C/¹²C or D/H. Standards refer to the Vienna Pee Dee Belemnite (VPDB) for C and Vienna Standard Mean Ocean Water (VSMOW) for H.

Carbon isotopes

Using the ratio of various hydrocarbons and δ¹³C, one can classify CH₄ as either thermogenic (non-microbial) or bacterial in origin. High temperatures associated with thermogenic processes generate CH₄ that is more enriched in δ¹³C (-20‰ to -50‰). The δ¹³C signature of bacterial CH₄ is more depleted and ranges from -50‰ to -110‰.

Carbon isotope ratios are also useful for determining the production pathway by which CH₄ evolves (CO₂ reduction or acetate fermentation), because each pathway imparts a different fractionation. An estimation of this fractionation, called the apparent fractionation factor (α_C), is calculated from dissolved inorganic carbon and evolved CH₄:

$$\alpha_C = \frac{(\delta^{13}\text{C}_{\text{CH}_4} + 10^3)}{(\delta^{13}\text{C}_{\text{CO}_2} + 10^3)} \quad (1.4)$$

This ratio has been used repeatedly throughout the literature in pathway studies of methanogenesis both *in situ* and *in vitro* (Valentine et al. 1994, Nakagawa et al. 2002, Beckman & Llyod 2001, Mikaloff-Fletcher et al. 2004, Metje & Frenzel 2005). A widely-adopted rule of thumb [$1.055 < \alpha_C < 1.090 = \text{CO}_2$ reduction, $1.040 < \alpha_C < 1.055 =$ acetate fermentation] developed by Whiticar (1999) is used to assign the relative production of CH_4 via each pathway.

Hydrogen isotopes

δD ranges for bacterial and thermogenic CH_4 are less constrained and are -150‰ to -400‰ and -100‰ to -275‰, respectively. This makes δD less useful as an isolated parameter for distinguishing between CH_4 of different origins (Whiticar 1999).

However, both C and H isotopes can be used to track methanogenic pathway. Daniels et al. (1980) demonstrated that CO_2 -reducing methanogens derive all four of their H atoms from water, but that during acetate fermentation, three hydrogen atoms are transferred intact (as a methyl group) from the parent molecule and only one H is gained from environmental water. If given a known water source, and the fractionation factor of hydrogen between H_2O and CH_4 ($\epsilon_h = -160$ ‰ for CO_2 reduction), one can calculate the fraction of CH_4 produced *via* each pathway (f) as follows:

$$\delta\text{D}_{\text{CH}_4} = f (\delta\text{D}_{\text{H}_2\text{O}} - 160) + (1-f)[(0.75 \times \delta\text{D}_{\text{methyl}}) + (0.25 \times \delta\text{D}_{\text{hydrogen}})] \quad (1.5)$$

Where $\delta\text{D}_{\text{methyl}}$ is the isotopic value of the intact methyl group and $\delta\text{D}_{\text{hydrogen}}$ is the isotopic value of the remaining hydrogen (Whiticar 1999). $\delta\text{D}_{\text{methyl}}$ and $\delta\text{D}_{\text{hydrogen}}$, however, are difficult values to measure, and are parameters to which literature ranges are often assigned (Whiticar 1999).

Equation (1.5) is also useful for determining source water to methanogens in cases where microbes may gain protons from more than one source (i.e., permafrost water vs. surface water). This approach works only in cases where CO_2 reduction dominates CH_4

production, or when one can assign an accurate production ratio determined via another means (e.g. from α_C). If CO_2 reduction is dominant, such as is the case in my Alaskan study lakes and the majority of Alaskan wetlands (Rooney-Varga et al. 2007), one may drop the entire second term, eliminating the problematic $\delta\text{D}_{\text{methyl}}$ and $\delta\text{D}_{\text{hydrogen}}$ values.

In conclusion, stable isotopes are excellent biogeochemical tracers. They may be used to identify the origin and production pathway of CH_4 , as well as the water and (potentially) carbon sources utilized by methanogens in various environments.

1.5 CH_4 Bubbling in Northern Lakes

Ebullition from northern lakes has recently been recognized as a globally significant source of atmospheric CH_4 , a potent greenhouse gas (Casper et al. 2000, Huttunen et al. 2003a, 2003b, Juutinen et al. 2003, Bastviken et al. 2004, Walter et al. 2006, 2007, 2008). Three major transport mechanisms convey CH_4 produced in anoxic soils and sediments to the atmosphere: diffusion, ebullition and movement through emergent plants (Schutz et al. 1991, Chanton 2005). Though diffusive fluxes of CH_4 from northern streams, wetlands and lakes have been fairly well documented (Kling et al. 1992, Striegl & Michmerhuizen 1998, Casper et al. 2000, Huttunen et al. 2003a, 2003b, Juutinen et al. 2003, Bastviken et al. 2004, Prater et al. 2007), only a few, isolated studies describe ebullition dynamics in lakes in Siberia, Scandinavia and the Midwestern U.S. (Casper et al. 2000, Huttunen et al. 2003a, 2003b, Juutinen et al. 2003, Bastviken et al. 2004, Walter et al. 2006, 2007, 2008). Walter et al. (2008) and Walter Anthony et al. (in prep) surveyed methane ebullition in 75 lakes in Alaska but the dominant pathway and drivers of CH_4 production and ebullition in Alaskan lakes remain poorly known.

Methane bubbling exhibits large spatial and temporal heterogeneity within and between lakes. Bubbling is classified into three categories (hotspot, point-source and background bubbling), based on fluxes and major gas composition. Gas samples collected from Siberian thermokarst lakes suggest that $\delta^{14}\text{C}$, $\delta^{13}\text{C}$ and δD values of bubbles vary by category (Walter et al. 2008) and are a function of organic matter source, pathway, and

depth of CH₄ production in lake sediments. In Siberian lakes, background was a low rate of bubbling of CH₄ formed in surface lake sediments by a mixture of acetate fermentation and CO₂ reduction. Relatively modern radiocarbon ages of CH₄ in background bubbles suggested modern organic matter source contributions. Point-source and hotspot bubbling had older radiocarbon ages, (up to 43,000 years) that reflected the late Pleistocene age of organic matter in permafrost. Point sources and hotspots were produced purely by CO₂ reduction, and higher bubbling rates from these seep types are thought to be the result of production at depth in densely packed sediments with emission occurring through discrete bubble tubes. **My thesis research aimed to examine isotopic values of gases from similar bubbling seeps to examine if the same isotopic patterns hold for ebullition in interior Alaskan lakes, and to determine the dominant pathway and drivers of methanogenesis using field work and laboratory incubations.**

Radiocarbon dating of CH₄ from point-source and hotspot seeps in Siberian thermokarst lakes suggested mineralization of ancient carbon that until recently had been sequestered in permafrost (Walter et al. 2006). Do Alaskan lakes behave in the same manner as Siberian lakes? Alaska spans several biomes, which vary in their permafrost regimes (continuous to sporadic), but nearly all of the 75 lakes investigated to date support CH₄ ebullition to some extent (Walter Anthony pers. comm.). Initial preliminary radiocarbon data suggest that ¹⁴C-depleted organic C released to lake bottoms does, at least in part, drive CH₄ production in thermokarst lake seeps in interior Alaska (Walter et al. 2008). **My thesis research aimed to determine the relative contribution of modern vs. ancient organic matter sources to methanogenesis using field work and laboratory incubations. I determined radiocarbon ages for CH₄ bubbling from seeps in interior Alaskan thermokarst lakes, and H contributions from modern surface waters and late-Pleistocene permafrost water using the stable hydrogen isotope techniques outlined in section 1.4.**

Prior studies have noted the episodic nature of bubbling events, which may be controlled in large part by fluctuations in barometric pressure (Chanton et al. 1989, Casper et al.

2000, Tokida et al. 2007, Vas et al. in prep). The majority of seep ebullition data has been collected manually by measuring volumes of gas trapped by an overlying chamber or bubble trap (Casper et al. 2000, Huttunen et al. 2003b, Bastviken et al. 2004, Walter et al. 2006). Depending on the frequency of sampling, this method often yields low-temporal-resolution data sets. The strenuous nature of this work (especially during winter months when surface lake ice is up to 2 m thick) has led researchers to either take less frequent measurement (1-2 times per week) over long periods of time or more frequent measurements spanning shorter time periods (Walter et al. 2006). These winter data sets fail to capture the high-temporal resolution (minutes-hours) CH₄ flux dynamics that have been observed through higher frequency sampling during the open water season and thin-ice conditions. Variations in flux likely results from hourly to seasonal changes in temperature and pressure, and may also be related to water depth, wind and wave action, and physical and biological sediment properties. In a few cases, long-term high-temporal resolution flux measurements using automated bubble traps have provided better temporal resolution on low background bubbling in a temperate Massachusetts lake (Varadharajan 2009) and for higher rates of ebullition from point-source and hotspot bubbling seeps in the interior Alaskan Goldstream Lake (Vas et al. in prep). Such data sets will be useful in resolving the flux dynamics of CH₄ bubbling from Alaskan and other lakes globally.

Bubble gas composition appears to vary between and within Siberian and Alaskan lakes. Differences between “fresh” (CH₄: 80%, CO₂: 0.9%, N₂: 16.6%, O₂: 3.9%) bubbling and bubbles trapped in ice (CH₄: 54%, CO₂: 0.3%, N₂: 43.7%, O₂: 4.4%) have been attributed to diffusion of gases between water and free-phase bubbles, as well as to oxidation of CH₄ in bubbles trapped under ice prior to ice formation and bubble enclosure (Walter et al. 2008). Bubble mixing ratios may also be correlated with bubble flux rates. CH₄ and N₂ concentrations in bubbles were negatively correlated in two different types of aquatic ecosystems (Chanton et al. 1989, Walter et al. 2008). Both Chanton et al. (1989) and Walter et al. (2008) observed an inverse relationship between bubble N₂ concentrations and rates of bubbling, and postulated that diffusion rates of N₂ into sediment pore water

could not keep pace with high rates of bubbling that quickly stripped gases from the sediment, resulting in lower overall concentrations of N_2 and higher concentrations of CH_4 in each bubble. **Data from Alaskan lakes in this study indicate that CH_4 concentration is not correlated with bubbling rates within lakes, and that point-source and hotspot seeps of similar flux between lakes may emit bubbles of drastically different composition due to differences in sediment organic matter and density. Information on bubble size and sediment texture is needed to resolve the factors controlling constituent gas concentrations in bubbles.**

Organic matter availability has been identified as a key driver of CH_4 production in aquatic environments. Among Alaskan lakes, organic matter sources include those released from thawing permafrost and those produced by modern ecosystems. Until now, crude assumptions have been made to assess relative contributions of each. Chanton et al. (1995), Zimov et al. (1997), Nakagawa et al. (2002) and Walter et al. (2008) assigned modern photosynthetic and permafrost C contributions based on $^{14}C_{CH_4}$ emitted from lakes and wetlands. Only Walter et al. (2007) and Zimov et al. (1997) posited permafrost C contributions of 60-95% to Siberian lakes based on radiocarbon ages ranging from 1,345 to 42,900 y.b.p. Methane emitted from three interior Alaskan lakes via ebullition was also found to be ^{14}C -depleted (Walter et al. 2008). **The effect of different abundances and bioavailability of OM sources on CH_4 production has not yet been evaluated. Improving understanding of these is a main objective of my thesis research. Understanding controls over CH_4 production and ebullition dynamics in Alaskan lakes is important because projections of warming and permafrost thaw have indirect implications for enhancing emissions, thereby exacerbating climate warming.**

Questions of permafrost organic matter quality, uniformity and history further complicate theories about thermokarst inputs driving CH_4 production in Alaskan lakes. Virgin and non-virgin permafrost OM should have different qualities and bioavailability, and thus different potentials for supporting CH_4 production. In a landscape heavily influenced by

thermokarst, lakes may have a lower CH₄ production potential because of the abundance of low quality, non-virgin permafrost in the region; whereas, lakes in a less dynamic permafrost region may overlay and erode highly labile, virgin permafrost which could support high rates of methanogenesis. An ongoing project by Walter Anthony et al. (2008) addresses these differences by comparing CH₄ fluxes from first and second generation lakes in yedoma regions of Siberia and the Northern Seward Peninsula using field studies, remote sensing, numerical modeling and laboratory incubations. The influence of periglacial history and permafrost organic matter quality on CH₄ production in Alaskan lakes is little understood. Further study is needed to determine how permafrost dynamics influence CH₄ production in northern lakes.

Interior Alaskan loess permafrost contains significant amounts of preserved N and P. Thus, it is possible that permafrost degradation and thermokarst activity have a fertilizing effect that stimulates primary production in lakes, making greater amounts of modern photosynthate available to methanogens. It is also possible that physical disturbances caused by thermokarst slumping initiate growth of productive, early successional plant communities that in turn drive CH₄ production, as Prater et al. (2007) found in a northern Alberta beat bog. While work on Siberian lakes and rivers suggest that thaw of yedoma has a fertilizing affect by releasing nutrients to these ecosystems (Finlay et al. in prep), no study has yet investigated the former in interior Alaskan lakes.

1.6 Conclusion

Understanding the role of CH₄ as a positive feedback to climate warming is crucial to our ability to construct accurate climate models and mitigate climate change. Further study will enable prediction of future lake CH₄ emissions through assessment of changes likely to occur in the availability of the organic carbon sources that drive CH₄ production.

Examination of carbon transport from terrestrial to aquatic systems and from lakes to the atmosphere will also improve our understanding of material and energy transfer in arctic ecosystems, allowing us to classify different ecosystem components as C sources or sinks. Finally, isotopic investigation of evolved gases will allow calculation of a regional

isoflux value for CH₄ ebullition from Alaskan lakes, which, in turn, can be used in inverse modeling to evaluate past, present and future contributions of lake CH₄ to climate warming (Mikaloff-Fletcher et al. 2004, Walter et al. 2008).

Major research gaps in the current understanding of controls over CH₄ production and emission dynamics from northern lakes are shown in Table 1.2. My thesis research addressed some of these gaps (also described in Table 1.2). The effect of different abundances and bioavailability of OM sources on CH₄ production in interior Alaskan thermokarst lakes has not yet been evaluated. In Chapter 2, I determined the relative contribution of modern vs. ancient organic matter sources to methanogenesis using field work and laboratory incubations. I determined radiocarbon ages for CH₄ bubbling from Alaskan lakes and used them in a mixing model to determine ranges of relative contributions of modern and ancient permafrost-derived OM to CH₄ production. I also evaluated potential physical controls over variability in CH₄ ebullition between two different lakes. In Chapter 3, I quantified H contributions from modern surface waters and late-Pleistocene permafrost water using stable hydrogen isotope techniques, and discussed the implications of these data for determining past and present atmospheric CH₄ budgets. Finally, my thesis research examined the stable isotopic values of bubble gases to determine the dominant pathway and drivers of methanogenesis.

References

- Arp CD, Jones BM (2009) Geography of Alaska lake districts: Identification, description, and analysis of lake-rich regions of a diverse and dynamic state. U.S. Geological Survey Scientific Investigations Report 2008–5215. 40 pp.
- Amaral JA, Knowles R (1994) Methane metabolism in a temperate swamp. *Appl Environ Microbiol* 60:3945-3951.
- Bachoon D, Jones RD (1992) Potential rates of methanogenesis in sawgrass marshes with peat and marl soils in the Everglades. *Soil Biol Biochem* 24:21-27.
- Bastviken D, Ejlertsson J, Tranvik L (2002) Measurement of methane oxidation in lakes: a comparison of methods. *Environ Sci Technol* 36:3354-3361.
- Bastviken D, Cole J, Pace M, Tranvik L (2004) Methane emissions from lakes: dependence of lake characteristics, two regional assessments, and a global estimate. *Global Biogeochem Cycles* 18 DOI 10.1029/2004GB002238.
- Beckmann M, Llyod D (2001) Mass spectrometric monitoring of gases (CO₂, CH₄, O₂) in a mesotrophic peat core from Kopparas Mire, Sweden. *Global Change Biol* 7:171-180.
- Brown J, Ferrians OJ Jr, Heginbottom JA, Melnikov ES (1997) Circum-Arctic Map of Permafrost and Ground-Ice Conditions, U.S. Geol. Surv., Washington, D.C., Circum-Pacific Map Series CP-45.
- Bubier JL, Moore TR, Roulet NT (1993) Methane emissions from wetlands in the midboreal region of Northern Ontario, Canada. *Ecology* 74:2240-2254.
- Casper P, Maberly SC, Hall GH, Finlay BJ (2000) Fluxes of methane and carbon dioxide from a small productive lake to the atmosphere. *Biogeochem* 49:1-19.
- Chanton JP, Martens CS, Kelley CA (1989) Gas transport from methane-saturated, tidal freshwater and wetland sediments. *Limnol Oceanogr* 34:807-819.
- Chanton JP, Bauer JE, Glaser PA, Siegel DI, Kelley CA, Tyler SC, Romanoicz EH, Lazarus A (1995) Radiocarbon evidence for the substrates supporting methane formation within northern Minnesota peatlands. *Geochim Cosmochim Acta* 59:3663-3668.
- Chanton JP (2005) The effect of gas transport on the isotope signature of methane in wetlands. *Org Geochem* 36:753-768.

- Chidthaisong A, Conrad R (2000) Turnover of glucose and acetate coupled to reduction of nitrate, ferric iron and sulfate and to methanogenesis in anoxic rice field soil. *FEMS Microbiol Ecol* 31:78-86.
- Chin KJ, Lukow T, Conrad R (1999) Effect of temperature on structure and function of the methanogenic archaeal community in an anoxic rice field. *Appl Environ Microbiol* 65:2341-2349.
- Conrad R, Klose M, Claus P (2000) Phosphate inhibits acetotrophic methanogenesis on rice roots. *Appl Environ Microbiol* 66:828-831.
- Corcoran RM, Lovvorn JR, Heglung PJ (2009) Long-term change in limnology and invertebrates in Alaskan boreal wetlands. *Hydrobiologia* 620:77-89.
- Daniels L, Fulton G, Spencer RW, Orme-Johnson WH (1980) Origin of hydrogen in methane produced by *Methanobacterium thermoautotrophicum*. *J Bacteriol* 141:694-698.
- Duddleston KN, Kinney MA, Keine RP, Hines ME (2002) Anaerobic microbial biogeochemistry on a northern bog: acetate as a dominant metabolic end product. *Global Biogeochem* 16 DOI 10.1029/201GB001402.
- Dutta K, Schuur EAG, Neff JC, Zimov SA (2006) Potential carbon release from permafrost soils of northeastern Siberia. *Global Change Biol* 12:2336-2351.
- Epp MA, Chanton JP (1993) Rhizospheric methane oxidation determined via the methylfluoride inhibition technique. *J Geophys Res* 98:18413-18422.
- Engstrom DR (1987) Influence of vegetation and hydrology on the humus budgets of Labrador lakes. *Can J Fish Aquat Sci* 44: 1306-1314.
- Ferretti DF, Miller JB, White JWC, Lassey KR, Lowe DC, Etheridge DM (2007) Stable isotopes provide revised global limits of aerobic methane emissions from plants. *Atmos Chem Phys* 7:237-241
- Finlay, JC, Mack M, Neff JC, Chapin FS, Davydov SA, Davydova A, Walter Anthony KM, Zimov SA (2010) Aquatic response to phosphorus release from thawing permafrost. *Science* (in review).
- Frenzel R, Bosse U, Janssen PH (1999) Rice roots and methanogenesis in a paddy soil: ferric iron as an alternative electron acceptor in the rooted soil. *Soil Biol Biochem* 31:421-430.
- Galand PE, Saarnio S, Fritze H, Yrjala K (2002) Depth related diversity of methanogen archaea in finnish oligotrophic fen. *FEMS Microbiol Ecol* 42:441-449.

- Ganzert L, Jurgens G, Munster U, Wagner D (2006) Methanogenic communities in permafrost-affected soils of the Laptev Sea coast, Siberian Arctic, characterized by 16S rRNA gene fingerprints. *FEMS Microbiol Ecol* 59:476-488.
- Garcia JL, Patel BKC, Ollivier B (2000) Taxonomic phylogenetic and ecological diversity of methanogenic archaea. *Anaerobe* 6:205-226.
- Gregory-Eaves I, Smol JP, Finney BP, Lean DRS, Edwards ME (2000) Characteristics and variation in lakes along a north-south transect in Alaska. *Arch Hydrobiol* 147:193-223.
- Grosse G, Schirrmeister L, Malthus TJ (2006) Application of Landsat-7 satellite data and a DEM for the quantification of thermokarst-affected terrain types in the periglacial Lena-Anabar coastal lowland. *Polar Res* 25:51-67.
- Hanson RS, Hanson TE (1996) Methanotrophic bacteria. *Microbiol Res* 60:439-470.
- Harrison BK, Zhang H, Berelson W, Orphan VJ (2009) Variations in archaeal and bacterial diversity associated with the sulfate-methane transition zone in continental margin sediments (Santa Barbara Basin, California). *Appl Environ Microbiol* 75:1487-1499.
- Hinkel KM, Eisner WR, Bockheim JG, Frederick EN, Peterson KM, Dai X (2003) Spatial extent, age, and carbon stocks in drained thaw lake basins on the Barrow Peninsula, Alaska. *Arct Alp Res* 35:291-300.
- Hobbie JE, Bahr M, Bettezi N, Rublee PA (1999) Microbial food webs in oligotrophic arctic lakes. *Proceedings of the 8th International Symposium on Microbial Ecology*, Halifax, 1999.
- Horn MA, Matthies C, Kusel K, Schramm A, Drake HL (2003) Hydrogenotrophic methanogenesis by moderately acid-tolerant methanogens of a CH₄-emitting acidic peat. *Appl Environ Microbiol* 69:74-83.
- Huttunen JT, Alm J, Saarigarvi E, Lappalainen KM, Silvola J, Martikainen PJ (2003a) Contribution of winter to the annual CH₄ emission from a eutrophied boreal lake. *Chemosphere* 50:247-250.
- Huttunen JT, Alm J, Liikanen A, Juutinen S, Larmola T, Hammar T, Silvola J, Martikainen PJ (2003b) Fluxes of methane, carbon dioxide and nitrous oxide in boreal lakes and potential anthropogenic effects on the aquatic greenhouse gas emissions. *Chemosphere* 52:609-621.

- Islas-Lima S, Thalasso F, Gomez-Hernandez (2004) Evidence of anoxic methane oxidation couples to denitrification. *Water Res* 38:13-16.
- Iversen N, Jorgensen BB (1985) Anaerobic methane oxidation rates at the sulfate-methane transition in marine sediments from Kattegat and Skagerrak (Denmark). *Limnol Oceanogr* 30:944–955.
- Juutinen S, Alm J, Larmola T, Huttenen JT, Morero M, Martikainen PJ, Silvola J (2003) Major implication of the littoral zone for methane release from boreal lakes. *Global Biogeochem Cycles* 17 DOI 10.1029/2003GB002105.
- Katayama T, Tanaka M, Moriizumi J, Nakamura T, Brouckov A, Douglas TA, Fukuda M, Tomita F, Asano K (2007) Phylogenetic analysis of bacteria preserved in a permafrost ice wedge for 25,000 years. *Appl Environ Microbiol* 73:2360-2363.
- Keppler F, Hamilton JTG, Brass M, Rockmann T (2006) Methane emissions from terrestrial plants under aerobic conditions. *Nature* 429:187-191.
- Kholodov AL, Rivkina EM, Gilichinsky DA, Fyodorov-Davydov DG, Gubin SV, Sorokovikov VA, Ostroumov VE, Maksimovich SV. (2003) Estimation of the organic carbon input into Arctic ocean due to erosion of the East-Siberian seashore. *Kriosphera Zemli* (Russian).
- King GM, Skovgaard H, Roslev P (1990) Methane oxidation in sediments and peats of a subtropical wetland, The Florida Everglades. *Appl Environ Microbiol* 56:2902–2911.
- King GM, Roslev P, Adamsen APS (1991) Controls of methane oxidation in a Canadian wetland and forest soils. *Trans Am Geophys Union* 72:79.
- King JY, Reeburgh WS, Thieler KK, Kling GW, Loya WM, Johnson LC, Nadelhoffer KJ (2002) Pulse-labeling studies of cycling in Arctic tundra ecosystems: The contribution of photosynthates to methane emission. *Global Biogeochem Cycles* 16:1062-1070.
- Kling GW, Kipphut GW, Miller MC (1992) Arctic lakes and streams as gas conduits to the atmosphere: implications for tundra carbon budgets. *Science* 251:154-156.
- Kotsyurbenko OR, Chin KJ, Glagolev MV, Stubner S, Simankova MV, Nozhevnikova AN, Conrad R (2004) Acetoclastic and hydrogenotrophic methane production and methanogenic populations in an acidic West-Siberian peat bog. *Environ Microbiol* 6:1159–1173.
- Lehmann-Richter S, Großkopf R, Liesack W, Frenzel P, Conrad R (1999) Methanogenic archaea and CO₂ –dependent methanogenesis on washed rice roots. *Environ Microbiol* 1:156-166.

- Mah RA, Keunen JG, Quayle JR (1982) Methanogenesis and methanogenic partnerships [and discussion]. *Phil Trans R Soc Lond* 297:599-616.
- McLeod AR, Fry SC, Loake GJ, Messenger DJ, Reay DS, Smith KA, Yun B-W (2008) Ultraviolet radiation drives methane emissions from terrestrial plant pectins. *New Phytol* 180:124-132.
- Metje M, Frenzel P (2005) The effect of temperature on anaerobic ethanol oxidation and methanogenesis in an acidic peat from a northern wetland. *Appl Environ Microbiol* 71:8191-8200.
- Metje M, Frenzel P (2007). Methanogenesis and methanogenic pathways in a peat from subarctic permafrost. *Environ Microbiol* 9:954-964.
- Michmerhuizen CM, Striegl RG, McDonald ME (1996) Potential methane emission from north-temperate lakes following ice melt. *Limnol Oceanogr* 41:985-991.
- Mikaloff -Fletcher SE, Tans PP, Bruhwiler LM, Miller JB, Heimann M (2004) CH source estimated from atmospheric observations of CH₄ and its ¹³C/¹²C isotopic ratios. *Global Biogeochem Cycles* 18 DOI 10.1029/2004GB002223.
- Muhs DR, Ager TA, Bettis EA III, McGeehin J, Been JM, Beget JE, Pavich MJ, Stafford TM Jr, Stevens DSP (2003) Stratigraphy and palaeoclimatic significance of Late Quaternary loess-palaeosol sequences of the last interglacial-glacial cycle in central Alaska. *Quat Sci Reviews* 22:1947-1986.
- Muhs DR, Budahn JR (2006) Geochemical evidence for the origin of late Quaternary loess in central Alaska. *Can J Earth Sci* 43:323-337.
- Nakagawa F, Yoshida N, Nojiri Y, Makarov VN (2002) Production of methane from alasses in eastern Siberia: implications from its ¹⁴C and stable isotope compositions. *Global Biogeochem Cycles* 16 DOI 10.1029/2000GB001384.
- Nercessian O, Bienvenu N, Moreira D, Prieur D, Jeanthon C (2005) Diversity of functional genes of methanogens, methanotrophs and sulfate reducers in deep-sea hydrothermal environments. *Environ Microbiol* 7:118-132.
- Nozhevnikova AN, Holliger C, Ammann A, and Zehnder AJB (1997) Methanogenesis in sediments from deep lakes at different temperatures (2–70°C). *Water Sci Technol* 36:57-64.
- O'Neill KP, Kasischke ES, Richter DD (2002) Environmental controls on soil CO₂ flux following fire in black spruce, white spruce, and aspen stands of interior Alaska. *Can J For Res* 32:1525-1541.

- O'Neill KP, Kasischke ES, Richter DD (2003) Seasonal and decadal patterns of soil carbon uptake and emission along an age sequence of burned black spruce stands in interior Alaska. *J Geophys Res* 108 DOI 10.1029/2001JD004443.
- Péwé TL (1952) Geomorphology of the Fairbanks area, Alaska. Dissertation, Stanford University
- Péwé TL (1975) Quaternary Geology of Alaska. United States Government Printing Office, Washington.
- Prater JL, Chanton JP, Whiting GJ (2007) Variation in methane production pathways associated with permafrost decomposition in collapse scar bogs of Alberta, Canada. *Global Biogeochem Cycles* 21 DOI 10.1029/2006GB002866.
- Raghoebarsing AA, Pol A, van de Pas-Schoonen KT, Smolders AJP, Ettwig KF, Rijpstra WIC, Schouten S, Sinninghe Darneste JS, Op den Camp HJM, Jetten MSM, Strous M (2006) A microbial consortium couples anaerobic methane oxidation to denitrification. *Nature* 440:918-921.
- Ramakrishnan B, Lueders T, Conrad R, Friedrich M (2000) Effect of soil aggregate size on methanogenesis and archaeal community structure in anoxic rich field soil. *FEMS Microbiol Ecol* 32:261-270.
- Reeburgh WS, Whalen SC, Alperin MJ (1993) The role of methylotrophy in the global methane budget. In: Murrell JC, Kelly DP (ed.), *Microbial growth on C1 compounds*. Proceedings of the 7th International Symposium of the American Society for Microbiology, Washington, D.C.
- Reeburgh WS (1989) Coupling of the carbon and sulphur cycle through anaerobic methane oxidation, p 149–159. In: P. Brimblecombe and A. Y. Lein (ed.), *Evolution of the global biogeochemical sulphur cycle*. John Wiley & Sons, Inc., New York
- Roslev P, King GM (1994) Survival and recovery of methanotrophic bacteria starved under oxic and anoxic conditions. *Appl Environ Microbiol* 60:2602–2608.
- Rooney-Varga JN, Giewat MW, Duddleston KN, Chanton JP, Hines ME (2007) Links between archaeal community structure, vegetation type and methanogenic pathway in Alaskan peatlands. *FEMS Microbiol Ecol* 60:240-251.
- Rudd JWM, Hamilton RD (1975) Factors controlling rates of methane oxidation and the distribution of methane oxidizers in a small stratified lake. *Arch Hydrobiol* 4:522–538.

- Schultz S, Matsuyama H, Conrad R (1997). Temperature dependence of methane production from different precursors in a profundal sediment (Lake Constance). *FEMS Microbiol Ecol* 22:207-213.
- Schutz H, Schroder P, Rennenberg H (1991) Role of plants in regulating the methane flux to the atmosphere. In: Mooney H, Holland E, Sharkey T (eds) Trace gas emissions from plants. Academic Press, San Diego, CA. 29-64.
- Segers R (1998) Methane production and methane consumption: a review of processes underlying wetland CH₄ fluxes. *Biogeochem* 41:23-51
- Simankova MV, Parshina SN, Tourova TP, Kolganova TV, Zehnder AJB, Nozhevnikova AN (2001) *Methanosarcina lacustris* sp. nov., a new psychrotolerant methanogenic archaeon from anoxic lake sediments. *Syst Appl Microbiol* 24: 362–367.
- Smith LK, Lewis JWM (1992) Seasonality of methane emissions from five lakes and associated wetlands of the Colorado Rockies. *Global Biogeochem Cycles* 6:323–338.
- Sorrell BK, Brix H, Schierup HH, Lorenzen B (1997) Die-back of *Phragmites australis*: influence on the distribution and rate of sediment methanogenesis. *Biogeochem* 36:173-188.
- Striegl RG, Michmerhuizen CM (1998) Hydrologic influence on methane and carbon dioxide dynamics at two north-central Minnesota lakes. *Limnol Oceanogr* 43:1519-1529.
- Tokida T, Miyazaki T, Mizoguchi M, Nagata O, Takakai F, Kagemoto A, Hatano R (2007) Falling atmospheric pressure as a trigger for methane ebullition from peatland. *Global Biogeochem Cycles* 21 DOI 10.1029/2006GB002790
- Tranvik LJ (1988) Availability of dissolved organic carbon for planktonic bacteria in oligotrophic lakes of differing humic content. *Microbiol Ecol* 16:311-322.
- Turner H (2009) An investigation into the formation and evolution of two lakes in Fairbanks, AK. B.S. Sr. Honors Thesis, University of Southampton.
- Utsumi M, Nojiri Y, Nakamura T, Nozawa T, Otsuki A, Seki H (1998a) Oxidation of dissolved methane in a eutrophic, shallow lake: Lake Kasumigaura, Japan. *Limnol Oceanogr* 43:471-480.
- Utsumi M, Nojiri Y, Nakamura T, Nozawa T, Otsuki A, Takamura A, Watanabe M, Seki H (1998b) Dynamics of dissolved methane and methane oxidation in dimictic Lake Nojiri during winter. *Limnol Oceanogr* 43:10-17.

- Valentine DW, Holland EA, Schimel DS (1994) Ecosystem and physiological controls over methane production in northern wetlands. *J Geophys Res* 99:1563-1571.
- Varadharajan C (2009) Magnitude and spatio-temporal variability of methane emissions from a eutrophic freshwater lake. Dissertation, Massachusetts Institute of Technology.
- Vas DA (2010) Methane seep dynamics in an interior Alaska thermokarst lake using high-temporal resolution automated bubble traps. M.Sc. Thesis. University of Alaska Fairbanks.
- Viereck LA, Little EL Jr. (1986) Alaska trees and shrubs. U.S. Dept. of Agriculture, Forest Service, Agricultural Handbook no. 410, 265.
- Wagatsuma T, Jujo K, Tawaraya K, Sato T, Ueki A (1992) Decrease of methane concentration and increase of nitrogen gas concentration in the rhizosphere by hydrophytes. *Soil Sci Plant Nutr* 38:467-476.
- Walter Anthony K, Grosse G, Edwards M, Plug L, Slater L (2008) NSF IPY #0732735: IPY: Understanding the impacts of permafrost degradation and thermokarst lake dynamics in the Arctic on carbon cycling, CO₂ and CH₄ emissions, and feedbacks to climate change July 2008-June 2011.
- Walter KM, Zimov SA, Chanton JP, Verbyla D, Chapin FS III (2006) Methane bubbling from siberian thaw lakes as a positive feedback to climate warming. *Nature* 443:71-75.
- Walter KM, Smith LC, Chapin FS III (2007). Methane bubbling from northern lakes: present and future contribution to the global CH₄ budget. *Phil Trans R Soc Lond* 365:1657-1676.
- Walter KM, Chanton JP, Chapin FS III, Schuur AG, Zimov SA (2008) Methane production and bubble emissions from arctic lakes: isotopic implications for source pathways and ages. *J Geophys Res* 113 DOI 10.1029/2007JG000569.
- Walter Anthony KM, Chapin FS III, Zimov SA, Zhuang Q (2010) Estimating methane emissions from northern lakes using ice-bubble surveys. *Limnol Oceanogr* (in review).
- Whiticar MJ (1999) Carbon and hydrogen isotope systematic of bacterial formation and oxidation of CH₄. *Chem Geol* 161:291-314.
- Whiting, G.J. and J.P. Chanton. 1993. Primary production control of methane emission from wetlands. *Nature* 364:794-795.
- Winfrey MR, Zeikus JG (1977) Effect of sulfate on carbon and electron flow during microbial methanogenesis in freshwater sediments. *Appl Environ Microbiol* 33:275-281.

Wuebbles DJ, Hayhoe K (2002) Atmospheric methane and global change. *Earth Sci Rev* 57: 177–210.

Yoshikawa K, Bolton WR, Romanovsky VE, Fukuda M, Hinzman LD (2003) Impacts of wildfire on the permafrost in boreal forests of Interior Alaska. *J Geophys Res* 108 DOI 10.10292001JD00438.

Zimov SA, Voropaev YV, Semiletov IP, Davidov SP, Prosiannikov SF, Chapin FS III, Chapin MC, Trumbore S, Tyler S (1997) North Siberian lakes: a methane source fueled by Pleistocene carbon. *Science* 277 DOI 10.1126/science.277.5327.800.

Zimov SA, Voropaev YV, Davydov SP, Zimova GM, Davydova AI, Chapin FS III, Chapin MC (2001) Flux of methane from north Siberian aquatic systems: influence on atmospheric methane. In: Paepe R, Melnikov V (ed) *Permafrost response on economic development, environmental security and natural resources*. Kluwer Academic Publishers, Netherlands

Zimov SA, Davydov SP, Zimova GM, Davydova AI, Schuur EAG, Dutta K, Chapin FS III (2006a) Permafrost carbon: stock and decomposability of a globally significant carbon pool. *Geophys Res Lett* 33 DOI 10.1029/2006GL027484.

Zimov, SA, Schuur, EAG, Chapin FS III (2006b) Climate change: permafrost and the global carbon budget. *Science* 312 DOI 10.1126/science.11289.

Tables

Table 1.1: Major research gaps in understanding interior Alaskan thermokarst lake methane production and emission, and means for addressing these gaps in my thesis research.

Knowledge gap	Addressed in thesis?	Research method
Magnitude of bubbling	Partially	Ice-bubbles surveys via PALIMMN (http://www.alaska.edu/uaf/cem/ine/walter/index_docs/PALIMMN_background.pdf)
Environmental controls on production and bubbling rates		
Temperature	Partially	Manual flux measurements related to temperature; laboratory incubation of permafrost, and mineral and organic lake sediment at different temperatures
C quality and bioavailability	Yes	
Availability of other nutrients	No	
Barometric pressure	No	
Isotopic values of CH ₄	Yes	Isotopic analysis of $\delta^{13}\text{C}_{\text{CO}_2}$, $\delta^{13}\text{C}_{\text{CH}_4}$ and $\delta\text{D}_{\text{CH}_4}$ of bubbles from different flux categories
OM sources fueling CH ₄ production (ancient vs. modern)	Yes	Radiocarbon dating; stable isotope and ^{14}C mixing model; laboratory incubations
Controls on bubble gas composition	Partially	Field measurements of bubbling flux rates (manual) and sediment properties related to composition, measurement of sediment bulk density in lake cores.
Production pathway	Yes	α_c calculated from $\delta^{13}\text{C}_{\text{CO}_2}$ and $\delta^{13}\text{C}_{\text{CH}_4}$
CH ₄ oxidation in lake bubbles	No	-

Chapter 2: A comparison of CH₄ production and bubbling from two interior Alaskan thermokarst lakes¹

Abstract

Large uncertainty in the magnitude of methane (CH₄) emissions from lakes exists. Much of the uncertainty in first order estimates (northern lakes: 24.2 ± 10.5 Tg CH₄ yr⁻¹ (Walter et al. 2007); global lakes: 11-55 Tg CH₄ yr⁻¹ (Smith & Lewis 1992), 8-48 Tg CH₄ yr⁻¹ (Bastviken et al. 2004)) results from variation in ebullition (bubbling) rates between and within lakes. This study compares two similar thermokarst (thaw) lakes near Fairbanks, AK, which display different bubbling dynamics and bubble characteristics. Killarney Lake, a low-elevation lake that has a large accumulation of organic detritus in the lake bottom from seasonal stream throughput, released bubbles containing low concentrations ($39.9 \pm 11.8\%$) of ¹³C-depleted ($-82.2 \pm 3.7\%$) CH₄. Radiocarbon ages of CH₄ 8,290-12,950 radiocarbon years before present (y.b.p.) showed that a mixture of modern and ancient organic C substrates fuels anaerobic decomposition and methanogenesis in lake sediments. Goldstream Lake seeps had high CH₄ concentrations ($86.4 \pm 8.3\%$), and the methane was more enriched in ¹³C ($-67.7 \pm 5.7\%$) and more depleted in ¹⁴C (725-30,800 y.b.p.). Using an isotope mixing model we determined that ¹⁴C-depleted permafrost organic C contributed more (98%) to total CH₄ production near the thermokarst margin of Goldstream than in Killarney (85%), where Holocene-aged organic detritus in the thick lake sediment package also contributed to CH₄ production (up to 27%). Trends toward high bubbling rates and CH₄ concentrations, and relatively lower $\delta^{13}\text{C}_{\text{CH}_4}$ and $^{14}\text{C}_{\text{CH}_4}$ values were more exaggerated in bubbling near Goldstream's actively thermokarsting eastern margin than in other non-thermokarst areas of the lake. Goldstream Lake exhibited higher rates of bubbling on the whole ($183 \text{ mg CH}_4 \text{ m}^{-2} \text{ d}^{-1}$) than Killarney Lake ($120 \text{ mg CH}_4 \text{ m}^{-2} \text{ d}^{-1}$) according to early winter lake-ice bubble surveys. To inform these observations, we conducted anaerobic laboratory incubations of lake and taberal sediments from Killarney and Goldstream as well as of representative Pleistocene loess

¹ Brosius LS, Walter Anthony KM, Chanton JP. In preparation for publication in JGR Biosciences as part of a forthcoming special issue on thermokarst lakes.

permafrost from Rosie Creek. Thawed permafrost soil inoculated with lake microbes and incubated at 21-23°C supported production of substantially more CH₄ (0.25 ± 0.04 mg CH₄ g TC⁻¹ d⁻¹) than did mineral lake sediments (0.07 - 0.09 mg CH₄ g TC⁻¹ d⁻¹) over 39 weeks at 4°C. While incubation temperatures were not identical and therefore production rates should not be directly compared, applying the mean of the low range of Q₁₀ values reported for lake sediments in other studies (mean = 2.7, range = 0.9-4.5 for incubations at 4-10°C; Duc et al. in review) suggests that at 4°C, the thawed permafrost soil would have produced 0.05 ± 0.01 mg CH₄ g TC⁻¹ d⁻¹, which is comparable to rates of CH₄ production supported by mineral lake sediments and thawed Siberian yedoma permafrost (0.01 mg CH₄ g C⁻¹ d⁻¹, Zimov et al. 1997). Considering the thickness of the lake sediment units (3 or 130 cm) and underlying thawed yedoma-like permafrost (up to 22 m), it is clear that labile permafrost C availability is an important control on CH₄ production and bubbling in interior Alaska thermokarst lakes. Here we suggest that the variation in CH₄ ebullition observed within and between lakes in our system can be explained by a few key differences in substrate quality and sediment density. Assigning accurate CH₄ flux estimates to lakes is important for extrapolating to larger scales, and for generating estimates for use in global climate models. Knowledge of sediment packages and contributions of permafrost vs. modern organic matter inputs to lakes could improve the accuracy of scaling up CH₄ flux estimates from ground-based bubble surveys to regions or lake districts when geographical information about lakes is known.

2.1 Introduction

Methane has a radiative effect ~25 times that of CO₂ (Wuebbles & Hayhoe 2002). Recent studies have identified lake ebullition (bubbling) as an important source of atmospheric CH₄ (Casper et al. 2000, Huttunen et al. 2003a, 2003b, Juutinen et al. 2003, Bastviken et al. 2004, Walter et al. 2006). Siberian lakes alone were shown to contribute as much as 3.6 Tg CH₄ y⁻¹ to the atmosphere (Walter et al. 2006), and to compose 7-45% of global lake CH₄ emissions. Yet, controls on CH₄ production and emission from lakes are only moderately understood. Organic matter (OM) contained in Siberian Pleistocene-aged

yedoma permafrost has been shown through laboratory incubations to be highly bioreactive (Zimov et al. 1997, 2006a, Dutta et al. 2006). Using field studies of ebullition and thermokarst together with stable and radiocarbon isotopes of CH₄, Walter et al. (2006) attributed high rates of bubbling in Siberian thermokarst (thaw) lakes to the large quantity of labile organic matter (OM) available when yedoma thaws beneath lakes.

Few studies have characterized methane (CH₄) bubbling dynamics in lakes, and most have focused on individual (Casper 2000, Varadharajan 2009) or small numbers of lakes in the same region (Huttunen et al. 2003b, Bastviken et al. 2004, Walter et al. 2006). Early investigations recorded isolated ebullition events using short-term, randomly deployed floating chambers or inverted funnel traps (Casper 2000, Huttunen et al. 2003b, Juutinen et al. 2003, Bastviken et al. 2004). However, random deployment of collection traps, even within particular zones of lakes, cannot be used to adequately describe ebullition dynamics on a whole lake basis, owing to the observed spatial and temporal heterogeneity of discrete seep bubbling (Walter et al. 2006, Walter Anthony et al. in review). Using on-ice surveys of the distribution of methane seeps observed as clusters of bubbles trapped in lake ice, Walter et al. (2006) determined that the probability of capturing seep ebullition through random placement of traps in lakes was <0.001%, yet year-round monitoring of ebullition through seeps revealed that discrete seeps dominated CH₄ flux from two Siberian lakes. Given the importance of discrete seep ebullition as a pathway for methane release from lakes, sources of variability in seep emissions among different kinds of lakes need to be better understood.

Regional lake CH₄ emission estimates have been based on extrapolation of early winter ice-bubble surveys conducted in Siberia and Alaska (Walter Anthony et al. in review). Individual clusters of bubbles in lake ice were classified into one of four categories based on bubble cluster geometry and size (Walter et al. 2006). Using statistical analysis of long and short term flux monitoring (<21 days, 15-30 seeps per category; >1 year, 7-8 seeps per category), and gas composition of bubbles collected from 35-182 seeps per category,

seasonal and annual emissions were assigned to thousands of seeps mapped in the surveys of 85 lakes in Alaska and Siberia (Walter Anthony et al. in review).

Understanding variation in bubble CH_4 concentrations is important for purposes of scaling up based on lake ice bubble survey data. Studies of ebullition from lakes and coastal environments found significant variation in the gas composition of bubbles over time and space (Table 2.1). CH_4 and N_2 concentrations in bubbles were negatively correlated in many studies (Chanton et al. 1989, Walter et al. 2008, Varadharajan 2009); and Chanton et al. (1989) and Walter et al. (2008) both observed a positive relationship between bubble CH_4 concentration and bubbling rates. They postulated that high rates of bubbling stripped pore water N_2 faster than it could be replenished by diffusion from the atmosphere, resulting in high CH_4/N_2 ratios in bubbles. Chanton et al. (1989) also reported higher CH_4 concentrations in summer bubbling compared to winter bubbling, and attributed differences to seasonal shifts in CH_4 production and bubbling rates, which allowed pore water N_2 to accumulate in winter. Casper et al. (2000) observed a positive correlation of bubble CH_4 concentration with water depth at seven trap locations in Priest Pot Lake. Possibly, there was more organic matter available to fuel CH_4 production at deeper locations within the lake due to sediment transport and focusing. Other studies have placed traps randomly or at loosely tethered positions from lake bottoms (Poissant et al. 2007, Varadharajan 2009). Traps that are not fixed at a single location, but which are allowed to roam even over short distances, will naturally experience differences in flux and composition due to variations in the subsurface and distributions of fixed seeps, prohibiting rigorous interpretation of temporal variation in ebullition.

This study focused on understanding sources of uncertainty to estimates of CH_4 production and bubbling in northern lakes due to differences in organic matter availability and sediment texture. This was accomplished by investigating two interior Alaskan thermokarst lakes which are similar to one another in location, size, genesis, and rates of ebullition, but which display different rates of CH_4 production, seep distribution, bubble gas composition, hydrology and sediment characteristics. We suggest that

variation in CH₄ emission rates within and between the two lakes can be explained by a few key differences in organic substrate bioavailability and sediment density.

Specifically, we assess: (a) the availability of different sources of organic matter (thawed, Pleistocene-aged yedoma-like permafrost OM vs. Holocene-aged terrestrial and aquatic OM) as a control over rates of CH₄ production and (2) sediment density as a control on bubble size and gas content, influencing the patterns of release in the two lakes.

Knowledge of sediment characteristics and thermokarst activity in different lake districts could improve extrapolation of lake-ice CH₄ seep survey data for better estimates of regional lake CH₄ emissions.

2.2 Methods

Physiography of study area

We studied methane production, ebullition and limnology in two shallow thermokarst lakes in Goldstream Valley, near Fairbanks, Alaska. Goldstream Valley is underlain by discontinuous, retransported Pleistocene-aged loess permafrost. During the last glacial maximum, arid interior Alaska remained largely unglaciated despite 4°C cooler mean annual temperatures (Péwé 1975). The unglaciated interior landscape collected aeolian silt, blown mainly from the Tanana River (south), with some inputs from the Yukon River (north) and Nenana River (southeast), which accumulated on hillsides over the course of the late-Quaternary (Muhs and Budhan 2006). Colluvial forces and frost action gradually eroded loess down slope, redepositing it as ice-rich permafrost that formed syngenetically (concurrent with deposition) with massive ice wedges that are up to several meters wide. Redeposited loess now fills valley bottoms to a thickness of 10-30 m (Péwé 1975) (Figure 2.1). Loess deposits appear, because of their age [14,860-56,900 years before present (y.b.p.)] and relatively high organic carbon content (0.38-2.39 % C) (Péwé 1952), to have originated in the productive Pleistocene steppe environment where fast-growing grass roots and leaf litter rapidly accumulated and were incorporated into permafrost.

Muhs et al. (2003) described and dated several distinct ~29,000-30,000 year old, interstadial organic horizons in three hillslope loess deposits near Fairbanks. Similarly-aged organic units were found in the Fox permafrost tunnel, which extends into hillslope loess deposits on the edge of Goldstream Valley (Hamilton et al. 1988). Atop these palaeosols, Muhs et al. noted a surprisingly thin unit of Pleistocene-aged loess (<4 m, despite model predictions of high contemporary silt production), and a relatively thick unit of Holocene-aged loess. A similar nonconformity in the permafrost tunnel may be evidenced by a break in ice wedge formation and a paucity of radiocarbon ages of OM from 14-30 ka (Sellmann 1967). Though this finding has been debated in more recent studies of tunnel cryostratigraphy (Shur et al. 2004, Bray et al. 2006), Sellmann (1967) suspected that the nonconformity was the result of a depositional or erosional event that washed loess into valley bottoms. The dominance of low herb vegetation evidenced by pollen records from this time period was suspected to have buffered loess accumulation rates by promoting erosion and transport of material into valley bottoms. When rough, loess-trapping spruce forests returned to interior Alaska 8-9 ka, loess accumulation rates increased (Muhs et al. 2003). However, there is some discrepancy in the date at which redeposition slowed. Fan-like deposits found at the mouth of the permafrost tunnel are thought to mark the end of the period of widespread downslope erosion ~ 12,000 years ago (12 ka) (Hamilton et al. 1988). From these analyses, we can predict that valley bottom retransported loess permafrost likely contains a large amount of 12-30 ka old material.

Valley bottom Alaskan Pleistocene-aged loess permafrost deposits are ice-rich (8-42 % excess ice, Jorgenson et al. 2001) and similar in character to Siberian yedoma (Figure 2.2). Siberian yedoma also consists of aeolian silt, is ice-supersaturated, and contains high concentrations of organic C (2.6%) owing to its similar steppe origin (Zimov et al. 2001, 2006a). Occasional layers have exceptionally high organic C content (up to 20%) (Schirrmeister et al. 2002, Dutta et al. 2006, Zimov et al. 2001, 2006a). Ice wedges in the Fox permafrost tunnel are 0.5-3 m wide and smaller than Pleistocene-aged Siberian yedoma ice wedges. Interior Alaska valley bottom loess permafrost, due to its

retransported nature, is of mixed age and lacks the chronology and continuity of Siberian lowland yedoma, which was not widely redeposited. Despite these differences, notable similarities in the organic matter and ice contents, and palaeoclimates at the time of formation of Alaskan yedoma-like loess and Siberian yedoma allow cryosphere-related studies conducted in Siberia and Alaska yedoma and yedoma-like regions to inform and parallel one another.

Study lakes

In areas of Goldstream Valley, thaw of massive ground ice has caused land surface subsidence, pooling of water, and the formation of thermokarst lakes. Killarney Lake (64.86°N, 147.90°W, elev. 162 m, depth 2.1m, 0.72 ha, hereafter: Killarney) is situated at the base of Happy Creek, in a watershed 1521 ha in size. Roughly triangular in shape, the lake is bordered on two sides by emergent grasses and on the third side by a thermokarst-eroding bank covered by black spruce (*Picea mariana*) forest. A seasonal inlet and outlet flow adjacent to one another at the southern apex, carrying large volumes of water with organic detritus during spring melt. Killarney's northern margin is ~ 3 m from the top of the bluff to the lake surface.

Goldstream Lake (64.92°N, 147.85°W, elev. 177 m, 0.99 ha, hereafter: Goldstream) is a 2.2 m deep thermokarst lake. Despite sitting at the bottom of a watershed that is ten times larger (19,458 ha) than that of Killarney, there was no apparent surface water connectivity to Goldstream Lake. Most likely patchy thaw of discontinuous permafrost throughout the valley has altered the hydrology, redirecting flow through disappearing and re-appearing channels into Goldstream Creek, located <1 km south of the lake. Goldstream's longitudinal N and S shores consist of wide, emergent sedge (*Carex spp.*), and cattail (*Typha spp.*) stands. On the eastern lake margin, 0.3-1.0 m fissures in the surface soil were observed. These formed by freeze-thaw cycling and ground surface subsidence associated with melting excess ice in thawing permafrost adjacent to the lake, a process which causes expansion of the lake in this direction and which deposits organic-rich loess from thawed permafrost, and the overlying modern terrestrial

vegetation and soils into the lake bottom. The relief along this margin is ~2 m from the top of the bluff to the water surface.

Sample collection and analysis

Using winter lake ice as a platform, we recovered three intact 0.55-1.90 m sediment cores in 5.5 cm diameter polycarbonate tubes from each lake using a piston hammer corer (Aquatic Research Instruments). The locations of the coring sites are provided in Figure 2.3. We sampled permafrost adjacent to the lake shores by chiseling frozen ground from >10 cm below the bottom of the seasonal active layer when active layer depth was greatest (72 cm, late September 2008). We measured gamma density along each Core B using a Geotek multi-sensor core logger (MSCL-S, 1% accuracy) at the National Lacustrine Core Repository. We also measured total C and N, and $\delta^{13}\text{C}$ and $\delta^{15}\text{N}$ on sediment core subsamples taken every 8 cm (Goldstream Cores A and C, Killarney Cores A and B), and on subsamples of incubated core sections (described below) using a Costech ECS 4010 elemental analyzer attached to a Thermo Finnigan Deltaplus XL isotope ratio mass spectrometer (IRMS) at the Alaska Stable Isotope Facility, University of Alaska Fairbanks. Instrument precision was <0.2‰. Permafrost samples were acid fumed for >24 h in a sealed chamber with 12 M HCl prior to analysis for organic C, N, $\delta^{13}\text{C}$ and $\delta^{15}\text{N}$ as above. Lake sediment samples were not acidified, however, and only total C contents are reported for lake sediments throughout this thesis. Application of 6 M HCl to a subset of sediment samples did not cause any visible CO_2 off-gassing from reaction with carbonate. It is therefore likely that the majority of measured total C is organic in nature.

We collected gas samples and measured fluxes from seeps using submerged umbrella-style traps (Walter Anthony et al. in review). Five to six seeps in each lake were sampled frequently (once every 3-12 days) from March through October 2008, while 1-3 samples were collected from 33 additional seeps in either April or October 2008. Figure 2.4 shows the location of sampling points in our lakes. We stored samples in the dark at 4°C in clear glass serum bottles sealed with butyl rubber stoppers and aluminum crimp caps until analysis. Gas composition of each sample was determined using a Shimadzu-2014 gas chromatograph fitted with both thermal conductance (TCD) and flame ionization (FID)

detectors (instrument accuracy = 1%). We measured gas phase $\delta^{13}\text{C}_{\text{CH}_4}$ and $\delta^{13}\text{C}_{\text{CO}_2}$ using a paired gas chromatograph and Delta V IRMS at Florida State University (precision = 0.2‰). $\delta\text{D}_{\text{CH}_4}$ was determined at the National High Magnetic Field Laboratory in Tallahassee, FL (precision = 3‰). ^{14}C radiocarbon ages of graphite derived from bubble CH_4 were determined by accelerator mass spectrometry (AMS) at the Keck-Carbon Cycle AMS Laboratory at University of California, Irvine and at the National Ocean Sciences AMS Facility in Woods Hole, MA. Radiocarbon data is reported in uncalibrated radiocarbon years before present (y.b.p.), normalized to $\delta^{13}\text{C}$ and relative to an oxalic standard (Stuiver & Polach 1977). Immediately after ice formed on lakes in 2007 and 2009 we estimated whole-lake emissions for both lakes according to the ice-bubble survey methods of Walter Anthony et al. (in review). We applied average CH_4 concentrations measured in bubble gas collected from each of the lakes separately to scale seep distributions to daily emission rates (Figure 2.5).

Geophysics

We collected electrical resistivity data using an 84 electrode Wenner array along two transects crossing Killarney Lake and three transects crossing Goldstream Lake during the open water season in 2008 and 2009 to determine the freeze-thaw boundary beneath and adjacent to the study lakes. The location of each transect is provided in Figure 2.6. Electrode spacing was 2 or 5 m. The 2 m spacing produced a shallow (~25 m below ground surface), high resolution inversion image, while the 5 m spacing allowed for deeper penetration (~68 m), but caused some loss of precision. Resistivity data were collected with a SuperSting R1/IP (Advanced Geosciences Inc). This technique has previously been used in discontinuous permafrost regions to detect the presence of ice bodies and to differentiate between permafrost and thawed soil (Fortier et al. 2008, Lee pers. comm.). Interpretation of geophysical data was based on resistivity values of retransported loess permafrost in the Fairbanks area measured and reported by the Cold Regions Research and Engineering Laboratory (CRREL, Hoekstra et al. 1973) to be 500 to >2000 ohm.m. This study noted the strong dependence of permafrost resistivity values

on temperature (Appendix Figure A.1), given that the presence of even a small amount of liquid water changes resistivity dramatically, and that liquid water can exist in permafrost at temperatures well below zero due to the presence of solutes.

Anaerobic laboratory incubation

We conducted anaerobic laboratory incubations of lake sediments and interior Alaska yedoma-like permafrost to determine the CH₄ production potentials of various organic matter sources that may contribute to the observed bubbling in lakes. Incubations were set up in triplicate vials containing: Yedoma-like permafrost from the Rosie Creek area (Yoshikawa *pers. comm.*); modern gyttja (organic-rich lake mud, 0-3 cm), and mineral-rich sediments (55-60 cm) from the center of Goldstream Lake; fluvial mineral sediments (55-65 cm) and taberal sediments (180-190 cm) below the sediment surface in Killarney Lake; and organic-rich debris from a lower trash layer in Killarney. Prior to incubation, we thawed and gently homogenized the yedoma-like permafrost by stirring. Lake sediments were not homogenized, but remained moist and intact, in the dark, in polycarbonate tubes, at 4°C for 12 hours prior to the start of the incubation. Sediment characteristics, including percent total C (TC) and N are provided in Table 2.2. Organic carbon was not analyzed on incubation materials or lake cores. To triplicate 120 ml clear glass serum bottles we added either 15.9-23.8 g dry weight (DW) mineral sediment (0.7-1.2% TC), 2.2-5.3 g DW organic sediment (9.3-20.1% TC), or 44.0-54.8 g DW permafrost (3.5% TC). We added 50 ml deionized water and 1 ml of slurried lake sediment to inoculate each vial with the same lake-sediment microbes. Vials were sealed with butyl rubber stoppers and aluminum crimps caps, shaken for 2 minutes, and purged with ultra-high purity N₂ for 20 minutes. Every 5 minutes during purging bottles were shaken again for 1 minute to purge any remaining O₂ from the vials. Though microbes may have been exposed to O₂ during this process, we are confident (based on the success of the experiment) that some anaerobic microbes remained intact and preserved a healthy population of methanogens. Vials contained approximately 28 ml of headspace. Incubation vials were sampled at time zero for initial headspace composition and

incubated in the dark at 4°C, with the exception of the thawed permafrost. We initiated the incubation of all samples in Fairbanks. After 8 weeks, bottles were mailed to Florida State University for isotopic analysis. Inadvertently, the permafrost incubation vials were left to incubate at 21-23°C for 31 weeks, while the lake core samples remained at 4°C. After 39 weeks we injected 5 ml of deionized water to each vial to create positive headspace pressure, then sampled headspace gases to determine long-term rates of CH₄ production. We analyzed headspace gas for composition.

Calculations

We calculated the apparent fractionation factor (α_C) using the following equation:

$$\alpha_C = (\delta^{13}\text{C}_{\text{CO}_2} + 10^3) / (\delta^{13}\text{C}_{\text{CH}_4} + 10^3) \quad (2.1)$$

In this and other studies (Whiticar et al. 1986, 1999; Hornibrook et al. 1997, 2000a, 2000b; Conrad 2005, Chanton 2005, others), α_C is used to approximate methanogenic pathway (CO₂ reduction or acetate fermentation). We used Whiticar's proxy values, $1.055 < \alpha_C < 1.090 = \text{CO}_2$ reduction, $1.040 < \alpha_C < 1.055 = \text{acetate fermentation}$, to assess the relative production of methane via each pathway (Whiticar 1999).

We determined the proportion of permafrost C that was incorporated into bubble CH₄ using two independent mixing models. In the first model (2.2), we used $\Delta^{14}\text{C}$ end members equivalent to 150 radiocarbon y.b.p. (representing modern ecosystem C of mixed age and degree of decomposition deposited in our lakes, "MOD"), and 12,000 radiocarbon y.b.p. (representing the upper bound of possible retransported permafrost C ages, young permafrost "YP"). The second model (2.3) used the same modern C end member and the $\Delta^{14}\text{C}$ equivalent of 30,000 radiocarbon y.b.p. (representing the lower bound of possible retransported permafrost C ages, old permafrost "OP").

$$\Delta^{14}\text{C}_{\text{CH}_4} = x \Delta^{14}\text{C}_{\text{YP}} + (1-x) \Delta^{14}\text{C}_{\text{MOD}} \quad (2.2)$$

$$\Delta^{14}\text{C}_{\text{CH}_4} = x \Delta^{14}\text{C}_{\text{OP}} + (1-x) \Delta^{14}\text{C}_{\text{MOD}} \quad (2.3)$$

Modern C contributions to CH₄ production were calculated by scaling experimental production potentials of incubated modern organic sediment sections by the volume of total carbon contained in each lake's modern sediment package according to down core gamma density and total C content. We assumed for these calculations that organic carbon dominated the total carbon content and that organic matter throughout Killarney's modern sediment package (a composite of terrestrial and aquatic OM) had the same production potential as incubated detritus from the trash layer (primarily terrestrial in origin).

2.3 Results

Whole-lake CH₄ production

Killarney and Goldstream Lakes exhibited differences in overall CH₄ production, seep distribution and gas bubble composition. In Goldstream, the density of seeps was greater near the active thermokarst margin than in the rest of the lake, though patches of dense seeps were also observed near in the littoral zone of all other margins and in the NW corner of the lake. In contrast, seeps were more evenly distributed across Killarney Lake. Lake-wide average ebullition was estimated to be $120 \pm 30 \text{ mg CH}_4 \text{ m}^{-2} \text{ day}^{-1}$ for Killarney (n=6 transects) and $183 \pm 56 \text{ mg CH}_4 \text{ m}^{-2} \text{ day}^{-1}$ for Goldstream (n=6 transects), with as much as $445 \text{ mg CH}_4 \text{ m}^{-2} \text{ day}^{-1}$ bubbling from the area of the lake nearest the active thermokarst margin surveyed in 2007 (Figure 2.7).

Bubble fluxes and composition

Elemental gas composition of bubbles varied considerably between our two study lakes, and from one end of the lake to the other in Goldstream Lake. Bubbles emitted from Killarney Lake averaged $39.8 \pm 11.8\% \text{ CH}_4$ (n=26), with a balance of primarily N₂ and small amounts of O₂ and CO₂, while those emitted from Goldstream averaged $86.4 \pm 8.3\% \text{ CH}_4$ (n=17) (Table 2.3). In Killarney, CH₄ concentrations did not vary spatially with any distinguishable pattern. However, in Goldstream, CH₄ concentrations averaged 90.2

$\pm 2.9\%$ (n=11) for bubbling nearer to the eastern thermokarst margin and $79.5 \pm 11.9\%$ (n=6) for bubbling nearer to the western margin (Figure 2.5).

On occasion, seep bubbling varied in absolute CH₄ concentration over time by as much as 50%, but most often by ~20-30% (Figure 2.8). Temporal variability (expressed in standard deviation) in bubble CH₄ concentration within individual seeps over time was weakly correlated with seepage rates (Goldstream, $R^2 = 0.4$; Killarney $R^2 = 0.2$). Lower flux seeps in both lakes exhibited more variability in bubble CH₄ concentration. High CH₄-concentration (>85% CH₄) seeps in Goldstream showed relatively little variation over time (3-8%). We observed similar bubble flux rates from each lake, with the exception of a few high-flow seeps near Goldstream's thermokarst margin, which exhibited bubbling rates of over 7,500 ml day⁻¹ on average, and over 20,000 ml day⁻¹ on some sampling dates. Figure 2.9 illustrates the bimodal pattern of bubble gas composition found in our study lakes and shows the lack of correlation between bubbling rate and CH₄ concentration that was previously observed in other studies (Chanton et al. 1989, Walter et al. 2008).

$\delta^{13}\text{C}_{\text{CH}_4}$, $\delta^{14}\text{C}_{\text{CH}_4}$ and $\delta^{13}\text{C}_{\text{CO}_2}$ isotopic analysis of lake bubbles (Table 2.3) revealed significant differences between the carbon isotope composition of CO₂ and CH₄ emitted from each lake (n = 43, $P < 0.001$). δD of CH₄ in bubbles also varied significantly by lake (n = 43, $P < 0.001$). Overall, $\delta^{13}\text{C}$ values were lower in Killarney than Goldstream for both CH₄ and CO₂. δD values were lower in Goldstream ($-333 \pm 19\text{‰}$) than in Killarney ($-306 \pm 13\text{‰}$). ¹⁴C radiocarbon dating of CH₄ revealed older ages of bubbling near Goldstream's thermokarst margin (14,800-30,800 y.b.p.), intermediate ages of bubbling from Killarney (8,290-12,290 y.b.p.), and relatively young ages of bubbling near Goldstream's stable western margin (725-8,110 y.b.p.) (Figure 2.6). Radiocarbon ages of CH₄ emitted from bubbling sources radiating away from Goldstream's thermokarst margin suggest declining contribution of ¹⁴C-depleted permafrost C into seep CH₄ over distance.

Production Pathway

Alpha C (α_C) suggested that 88% of the total CH₄ produced in Goldstream Lake (mean α_C = 1.056) and 98% of the total methane produced in Killarney Lake (mean α_C = 1.061) were from CO₂ reduction. Methane emitted from higher flux seeps in each lake also appeared to be produced entirely by CO₂ reduction (Figure 2.9).

Anaerobic incubation results

Incubation of yedoma-like permafrost in this study yielded 68 ± 12 mg CH₄ g TC⁻¹ (n=6) at room temperature (21-23°C) after only 39 weeks (0.25 mg CH₄ g TC⁻¹ d⁻¹). Shallow mineral sediments from Killarney exhibited production rates of 0.07 ± 0.04 mg CH₄ g TC⁻¹ d⁻¹ (n=3) and taberal sediments Goldstream and Killarney produced 0.07 ± 0.00 mg CH₄ g TC⁻¹ d⁻¹ (n=3) and 0.09 ± 0.05 mg CH₄ g TC⁻¹ d⁻¹ (n=3), respectively, when incubated at 4°C. Potential explanations for 70% lower CH₄ production rates of mineral sediments compared to rates of production of freshly thawed permafrost are (1) difference in incubation temperature (4°C vs. 21-23°C), and (2) bioavailability of organic substrate for methanogenesis. Applying a temperature correction factor to CH₄ production potentials of thawed permafrost using a mean Q₁₀ for arctic lake sediments of 2.7 (Duc et al. in review) at 4°C, we would expect production of 0.05 mg CH₄ g TC⁻¹ d⁻¹. This result is roughly comparable to rates of CH₄ production by our mineral lake sediments and by thawed Siberian yedoma incubated anaerobically at nearly the same temperature (3.5°C, 0.01 mg CH₄ g C⁻¹ d⁻¹, Zimov et al. 1997). Modern organic gyttja from Goldstream and organic material from Killarney's trash layer had higher production rates of 0.52 and 0.24 mg CH₄ g TC⁻¹ d⁻¹, respectively (Figure 2.11). If there is appreciable inorganic carbon in the modern sediments sections, then these production rates may be higher than would have otherwise expected. Though we measured only total C content, we suspect the fraction of inorganic C in these sediments is small (see methods section 2.2).

Permafrost and sediment characteristics

Over time, fluvial processes have deposited persistent terrestrial OM such as spruce needles, leaf litter, and wood on Killarney's lake bottom. Growth and senescence of highly productive submerged macrophytes, periphyton and benthic mats observed in Killarney Lake contribute higher quality organic substrates annually to the lake bottom, but may not be present in great enough quantity to support high rates methanogenesis. Killarney Lake sediment C:N ratios probably reflect a mixture of these high and low quality substrates (C:N=12.4 ± 1.8). Layering of organic matter and silt in sediment cores also suggests inwashing of mineral material, presumably originating from Pleistocene-aged loess, which has been re-worked in cryogenic, fluvial, and thermokarst processes throughout the Holocene, and subjected to decomposition in the modern terrestrial environment prior to deposition in the lake. During the past few hundred years, these allochthonous materials have formed a thick (130 cm), Holocene-aged organic sediment package that contains a high percentage of total C (1.0-9.3%, Table 2.4). A 10 cm-thick detritus-rich trash layer at 120-130 cm composed of well-preserved terrestrial organic material (likely inundated at the onset of thermokarst lake formation) formed the lower boundary of the modern sediment package. The radiocarbon age of a spruce needle from this layer was 290 ± 25 y.b.p., representing a minimum possible lake age (assuming lake formation occurred immediately after the needle's senescence). The absence of siliceous diatom frustule remains (Farquarson *pers. comm.*) is consistent with the interpretation that the massive, mineral layer found directly below the trash layer, at 130-190 cm, is the top of the taberal sediment package. However, we were not able to core below 190 cm to determine whether this was a true lake initiation trash layer or simply an organic-rich layer representing an erosion/deposition event in the lake. Thick alternating units of mineral and organic-rich trash-like horizons comprised sediment packages up to 15 m thick in thermokarst lakes in Siberia (K. Walter Anthony, *pers. comm.*).

In Goldstream Lake cores, an extremely thin (< 5 cm) modern organic sediment layer (TC = 19.1 ± 1.4%, C:N = 20.3 ± 0.4, Table 2.4) composed mainly of aquatic detritus of

locally dominant *Ceratophyllum demersum*, also overlaid a thick package of dense silt. This silt was presumed to be of the same origin as retransported yedoma-like permafrost. Goldstream's taberal sediments had a lower total TC content (0.6-0.9%, Table 2.4, C:N = 10.8 ± 1.2) than the overlying organic-rich layer, and than any of the lakes sediments and taberal material in Killarney Lake. Late Pleistocene loess deposition buried and incorporated steppe graminoids, roots, root exudates, soil fauna and other soil decomposition products that may have survived the relatively short period of soil genesis prior to erosion, redeposition and permafrost formation. The Pleistocene steppe environment was mediated by large grazer populations, which, through physical disturbance and grazing pressure, sustained grassland vegetation and fostered rapid accumulation of graminoid remains. As in Siberia, slow decomposition rates in cold Pleistocene soils allowed this material to be fairly well preserved (Zimov 2005).

Average down-core gamma densities for Goldstream core B and most of Killarney core B were $1.86 \pm 0.30 \text{ g cm}^{-3}$ and $1.77 \pm 0.13 \text{ g cm}^{-3}$, respectively (Figure 2.12). Goldstream core B sediments were quite homogenous and dense (1.92 g cm^{-3}), with the exception of a 1 cm surface organic sediment layer (1.53 g cm^{-3}). In Killarney, frequent shifts in density from 1.83 - 1.92 g cm^{-3} for dense mineral horizons to 1.56 - 1.62 g cm^{-3} for the more organic-rich horizons appeared to correspond with observed transitions in the sediment regime. Table 2.4 details the elemental and isotopic composition of organic matter in sediments.

Geophysics

In the recent past (10^0 - 10^2 years), yedoma-like permafrost thawed beneath our two interior Alaska study lakes by heat transferred from surface waters, a process of thermokarst lake development and expansion which has been described by Tomirdiaro et al. (1969) and recently modeled by West & Plug (2008). Resistivity data collected from three north-south trending transects intersecting our lakes revealed the presence of a >70 m deep talik beneath Killarney, a 40-50 m deep talik beneath Goldstream's western end, and a 20-30 m deep talik beneath Goldstream's eastern end (Figure 2.13). Very low

resistivity of materials 50-70 m beneath Killarney were observed, suggesting wet, thawed substrates at those depths. Resistivity data collected using 2 m electrode spacing gave greater surface resolution and showed encroachment of emergent vegetation and refreezing taberal sediments on Goldstream's north shore and Killarney's eastern shore (Figure 2.14). These geophysical data are consistent with observed shifts in shoreline. Refreezing of sediments is occurring in areas where the lake was present in 1949, but which are now exposed to freezing winter conditions due to partial lake drainage during recent decades (Figure 2.15).

Limnology

We measured lake water temperature, pH, salinity, conductivity, and turbidity bi-weekly from an inflatable boat in the center of the lakes during the open water season in 2008 using a Hydrolab Quanta 5. Killarney Lake, due to its lower-elevation, protected location and shorter fetch had a slightly cooler temperature regime and maintained a steeper thermocline throughout the summer than did Goldstream Lake (Appendix Figure A.2). Goldstream is longitudinally oriented in the direction of prevailing winds and therefore well mixed. Maximum recorded summer surface water temperatures for Killarney and Goldstream were 18.4°C on June 16, 2008 and 19.6°C on July 10, 2008, respectively. Maximum lake bottom temperatures were 4.3°C and 10.7°C (both occurring on June 4). Mean annual temperatures measured at 0.1 m were 13.5°C and 15.5°C for June 4 - September 11. Both lakes had similar average pH values of 8.0 for Goldstream and 7.9 for Killarney, and similar average redox potentials at the lake surface of 381 mV for Goldstream and 353 mV for Killarney. Goldstream had higher average conductivity (770 uS) and lower dissolved oxygen concentrations (5.33 mg/L) than Killarney (cond: 350 uS, DO: 7.61 mg/L) (Appendix Tables A.2 & A.3).

2.4 Discussion

Temperature and production pathway

Production of CH₄ via CO₂ reduction has been observed to dominate over production by acetate fermentation at cooler temperatures (0-4°C) in northern peatland soils (Metje and Frenzel 2007). Year-round sediment temperatures recorded using Hobo data loggers at Goldstream by Vas (2010) were 2-10°C at 0.1 m below the sediment surface and 0-1°C at 1 m below the sediment surface. Killarney sediments temperatures were up to 4°C cooler than Goldstream's during our sampling (1-6°C at 0.1 m depth, Vas 2010). Low sediment temperatures likely facilitated the dominance of CO₂-reducing methanogens in both lakes, and potentially more so in Killarney Lake. Goldstream's slightly warmer temperature regime may have allowed a mixture of CH₄ formation pathways to proceed. Walter et al. (2008) hypothesized that CH₄, emitted through sediment bubble tubes from high-flux seeps, is produced in a larger volume of sediments at depth. Gas-phase CH₄ migrates from microsites into continuously larger bubble tubes eventually exiting as a strong bubble stream (up to 25 L gas d⁻¹) at the sediment-water interface. The cooler temperatures of deep sediments in which high-flux seep CH₄ is produced could explain the positive relationship observed between α_c and flux rate (Figure 2.10). CO₂ reduction dominated high rates of methane production in colder, deeper sediments while acetate fermentation gained in importance in warmer, shallower sediments where less gas was produced.

Bubble gas composition variation

Bubbles emitted from Killarney had lower CH₄ concentrations than those emitted from Goldstream, despite relatively similar bubbling rates. The use of average measured bubble CH₄ concentrations from 85 Siberian and Alaskan lakes to scale up from surveyed bubble clusters would yield artificially high estimates of CH₄ emission from Killarney Lake (Figure 2.7). Different bubble CH₄ concentrations may be due to differences in diffusion rates and/or bubble sizes according to sediment texture. Previous studies demonstrated that atmospheric gases are transported to the rooting zone by emergent

macrophytes and incorporated into bubbling (Chanton et al. 1989, 1995). Water lily (*Nuphar spp.*) is present in Goldstream. However, the most widespread macrophyte species in both lakes (*Ceratophyllum demersum*) is both submerged and rootless, so it is unlikely that this is the dominant explanation for observed differences in CH₄/N₂ in bubbles emitted from Goldstream and Killarney. It is also possible that the less-dense, organic-rich sediments of Killarney Lake facilitated more rapid diffusion of atmospheric N₂ into sediments, resulting in lower sediment CH₄/N₂ ratios, compared to the dense mineral sediments of Goldstream, through which N₂ diffused more slowly. The plausibility of this explanation is challenged, however, by the comparison of low N₂ diffusion rates through sediment ($1.2 \times 10^{-9} \text{ mol N}_2 \text{ cm}^{-2} \text{ s}^{-1}$) to experimental CH₄ production rates supported by our mineral lake sediments ($1.1 \times 10^{-4} \text{ mol CH}_4 \text{ cm}^{-3} \text{ s}^{-1}$). A third possible explanation is that the loose textured, low density ($1.58 \pm 0.06 \text{ g cm}^{-3}$), organic-rich sections of lake sediments of Killarney acted as a sieve to separate bubbles into smaller sizes as they rose through sediments and into the water column, while the more dense ($1.92 \pm 0.08 \text{ g cm}^{-3}$) mineral sediments of Goldstream Lake focused bubbles into well-developed bubble tubes, from which larger bubbles were released. The funneling of bubble streams through bubble tubes may be a more important mechanism for CH₄ escape from lakes with dense mineral sediments than from lakes with significant, loose, peaty sediment layers. The low surface to volume ratio of small bubbles in Killarney would then have allowed proportionally more exchange with dissolved atmospheric gases during transit through the water column. There would be less exchange across the lower surface area to volume ratio of large bubbles released through bubble tubes, and hence, if traveling the same distance through the water column, these bubbles should reach the surface with higher CH₄/N₂ ratios.

Varadharajan (2009) first proposed bubble size as an explanation for bubble gas variation in a 20 m deep temperate lake, and tested her hypothesis using Greinert & McGinnis' single bubble dissolution model (SiBu-GUI) (2009). Here we used the same model, inputting measured parameters unique to our shallower (2 m deep) study lakes, to test the plausibility of this explanation for observed differences in bubble composition. Despite

the 10-fold difference in lake water depth between the temperate lake and our shallow interior lakes, we found significant differences in CH₄ concentrations (53-98%) projected for bubbles ranging from 1-10 mm in diameter through 2 m of water at 0°C (Table 2.6). Increasing the temperature parameter in the SiBu model to 20°C (representative of maximum summer lake water temperatures) yielded slightly higher bubble CH₄ projections because of the lower solubility of gases at higher temperatures. This effect of temperature was not reflected in our field data. Though actual bubble sizes in our lakes are unknown, the “upside down avalanche” model for CH₄ bubbling in wetlands predicts release of large bubbles when small bubbles are trapped and coalesce beneath hypothetical impediments in the medium (Coulthard et al. 2009). Varying the size, density and disposition of these obstacles simulates the pore structure of peat in the model (Coulthard et al. 2009). If Goldstream’s dense sediment structure acts as such an impediment at large, theories regarding episodic bubble releases facilitated by the formation of bubble tubes may corroborate Coulthard’s model results. Following this hypothesis, gas released artificially from Killarney sediments via stirring had a much higher CH₄ content (72.4%) than any natural bubbling we sampled from Killarney. By disturbing the sediment matrix, it is possible that we prompted release of larger bubbles, which did not experience as much dissolved gas exchange, and therefore contained more CH₄. Alternately, oxidation of CH₄ in bubbles remaining in the sediment for longer periods of time prior to release via natural bubbling could explain this observation. However, $\delta^{13}\text{C}$ values of bubbling from Killarney were on average very low ($-82.2 \pm 3.7\text{‰}$), suggesting that little oxidation (which would enrich remaining bubble CH₄) occurred.

In summary, using lake-ice bubble survey methods to upscale bubbling of small size produced by loosely compacted, organic sediments may give false impressions of high CH₄ emissions if bubble contents are not measured. Compared to 75 Alaskan lakes surveyed by our group, Killarney Lake is an outlier with respect to its bubble CH₄ concentrations. The thick package of Holocene-aged sediment containing low density organic layers found in Killarney’s lake bottom may set it apart from other interior

Alaskan thermokarst lakes. Because these sediments were fluvially deposited, connectivity of a lake to surface waters via an inlet stream draining a large watershed may be a potential indicator of low bubble CH_4 concentrations. Extremely old or productive lakes may also have enough accumulated organic sediment to yield bubbling of similar size and content.

Whole-lake CH_4 production

Though similar in their location, size, genesis, and rates of gas bubbling, Killarney and Goldstream lakes exhibited very different rates of CH_4 ebullition emission, which likely resulted from differences in OM substrate quantity and quality between the two lakes. OM of varying structural complexity and integrity is deposited to lake bottoms and incorporated into sediments. Some recalcitrant compounds such as lignin and cellulose remain intact or break down very slowly under cold lake-bottom conditions. Other, more labile compounds, such as carbohydrates and amino acids, break down quickly via hydrolysis and fermentation reactions facilitated by microbes, or are taken up directly by microbes and plants. Because precursors to methanogenesis are simple C compounds (CO_2 and acetate) almost all organic C reaching sediments must undergo microbial processing prior to being converted to CH_4 . The bioavailability of OM that is easily transformed to methanogenic precursors may thus contribute to the CH_4 production potential of lakes. Root exudates (sugars) have been shown to support high rates of CH_4 production in modern terrestrial ecosystems (Minoda and Kimura 1994, Chanton et al. 1995, Dannenberg and Conrad 1999, King et al. 2002). Incubation studies of wetland soils also found that addition of indirect (leaf leachate and glucose) and direct (acetate, CO_2 , H_2) methanogenic precursors increased CH_4 production (Bachoon & Jones 1992, Amaral & Knowles 1994, Valentine et al. 2004). These studies present a compelling case for the importance of OM quality as a factor controlling CH_4 production.

Interior Alaskan yedoma-like permafrost is comparable to Siberian yedoma because of its similarity in character and origin. Long-term aerobic and anaerobic incubations of thawed yedoma have demonstrated the high reactivity of organic C contained in permafrost,

which supported production of 1.2-4.2 mg CO₂ g C⁻¹ d⁻¹ at 10-20°C and 0.01 mg CH₄ g C⁻¹ d⁻¹ at 3.5°C (Zimov et al. 1997, 2006a). Dutta et al. (2006) found that during aerobic incubation, the labile fraction of yedoma soil organic C (mainly DOC) was respired within 2-3 months. Based upon rates of respiration following this initial pulse, the authors predicted depletion of the remainder of organic C (with the exception of the “inert” C pool = 0.04% of the total pool) would occur within the next four decades (Dutta et al. 2006). Similar results were obtained by Zimov et al. (1997, 2006a) in a long term aerobic incubation study where high rates of respiration were sustained for 20-30 days, and followed by a significant decrease in respiration to a lower baseline rate that was sustained for 6 summer seasons, and in an anaerobic incubation where CH₄ production rates dropped precipitously after ~18 months. Finally, permafrost thawed *in situ* for 8 years prior to incubation had an organic C content 39% lower than that of adjacent permafrost, and its respiration rate was 40% lower than that of recently thawed yedoma (Zimov et al. 2006a). These results imply that loess permafrost contains organic C that is highly reactive, but rapidly exhausted. The generation of fairly large amounts of CH₄ by anaerobic incubated yedoma-like taberal lake sediments (0.07 mg CH₄ g TC⁻¹ d⁻¹), thawed Alaskan yedoma-like permafrost (0.05 mg CH₄ g TC⁻¹ d⁻¹), and thawed Siberian yedoma (0.01 mg CH₄ g C⁻¹ d⁻¹, Zimov et al. 1997) suggests that the availability of highly reactive, recently thawed permafrost OM, may be an important control over rates of CH₄ production and bubbling in Alaskan thermokarst lakes.

Holocene-aged allochthonous and autochthonous OM may also contribute to CH₄ production and bubbling in Alaskan lakes, but may be limited in quantity. Incubated modern organic lake sediments yielded more CH₄ than did taberal sediments. However, the limited quantity of modern OM in our study lake bottoms appears to constrain the amount of CH₄ produced from this source. Given the production potential (0.52 mg CH₄ g TC⁻¹ d⁻¹), average density (1.5 g cm⁻³) and thickness (3 cm) of Goldstream gyttja, this modern OM source could yield only ~19 mg CH₄ m⁻² day⁻¹, 10.5% of the CH₄ that we estimated bubbles from Goldstream on a per meter basis (183 mg CH₄ m⁻² day⁻¹). Thus,

despite its high quality and bioavailability, modern organic sediment cannot be responsible for the bulk of CH₄ production in Goldstream. Though material from Killarney's trash layer produced CH₄ at half the rate (0.24 mg CH₄ g TC⁻¹ d⁻¹) of Goldstream gyttja, the larger quantity of Holocene-aged OM distributed throughout the surface 130 cm of Killarney lake sediments could play a more important role in overall CH₄ production from the lake, and could contribute up to 32 mg CH₄ m⁻² day⁻¹, or 27% of observed emissions.

Radiocarbon data of ¹⁴C_{CH₄} in bubbles were consistent with the incubation-derived estimate of CH₄ production from modern sediments. Variation in ¹⁴C ages (515-30,800 y.b.p.) among seeps in Goldstream suggested mixing of modern and late-Pleistocene OM sources. Radiocarbon ages of CH₄ bubbling from Killarney were intermediate and less variable (8,290-12,950 y.b.p.), and also suggested a mixture of C sources. Methane of a younger radiocarbon age produced and emitted from Killarney suggests a lesser contribution permafrost C and larger contribution of Holocene-aged C to whole lake CH₄ release than in Goldstream Lake. Using a mixing model approach (equations 2.2 & 2.3) and assuming redeposited loess permafrost ages of 12-30 ka, we calculated that 87-100% of CH₄ emitted from near Goldstream's thermokarst margin was generated from thawed Pleistocene-aged permafrost OM. This is consistent with the laboratory incubation-derived estimate of 10% CH₄ production from modern lake sediments. For lower-flux seeps and seeps further from the thermokarst margin, only 11-81% of CH₄-C came from permafrost sources. Killarney lake seep CH₄ was generated from 83-100% 12 ka permafrost C, or 62-91% 30 ka permafrost C (mean = 85%). These results also corresponded well with the amount of CH₄ we estimated was produced from Holocene-aged OM sources (27%), which fueled the balance of CH₄ production for most seeps (Figure 2.16).

In Goldstream Valley, redeposited loess varies from 10-30 m thick and is underlain by schistose gravel or bedrock (Péwé 1975). Killarney's water depth (2.2 m), modern sediment package thickness (1.3 m) and bluff height (3m) together suggest 6.5 m of

ground subsidence from the original surface elevation. Assuming an average excess ice content of 30% for loess permafrost (Jorgenson et al. 2001), we calculate that the total thickness of the loess unit beneath Killarney could be up to 22 m. That Killarney is an older lake is suggested by the 290 ± 25 y.b.p. radiocarbon age of a spruce needle from the trash layer. Geophysical data suggest that Killarney's talik extends well below 22 m and that over 290 years the talik has thawed through the loess unit beneath the lake (Figure 2.17). Thus, a potential explanation for the lesser contribution of yedoma-like permafrost OM to Killarney's CH₄ budget is that organic C formerly contained in this unit has been significantly depleted over the time it has been thawed. This implies that methanogens may use relatively more Holocene-aged OM contained Killarney lake sediments, but that due to the limited quantity of this C source, potentially low quality of the autochthonous C fraction, and the depletion the labile permafrost C pool in taberal sediments, Killarney can support only moderately high rates of CH₄ production and bubbling.

In contrast, our results suggest that thawed loess permafrost is a more dominant source of C to methanogens in Goldstream Lake, and that the greater availability of this C source supports higher rates of CH₄ production and bubbling in Goldstream than in Killarney. Geophysical data collected from Goldstream suggested asymmetric talik depths of 30-60 m beneath the west end of the lake and 20-50 m beneath the east end. Edge effects and the lake's proximity to Ballaine Road prevented us from measuring resistivity along transects nearer or perpendicular to the thermokarst margin, but we strongly suspect that the talik is shallower near this margin for two reasons: 1) during our lake coring efforts <5 m from this margin, we encountered impermeable material 1 m below the sediment surface at three different attempted coring locations 1 m or more apart; it is possible that this was permafrost; 2) aerial photography and satellite imagery suggested significant lake expansion ($\sim 1 \text{ m y}^{-1}$) along this margin over the last 35 years, implying that the talik has had less time to develop beneath this portion of the lake. Vas (2010) determined from local Department of Transportation borehole data that the loess unit beneath Goldstream is approximately 12-19 m thick. Goldstream is also thought to be a younger lake (<100 years old). From these observations, we conclude that Goldstream's talik is less well-

developed than Killarney's due to the shorter amount of time over which thaw has occurred, and that the talik is shallowest near the thermokarst margin – having not yet thawed totally through the loess unit beneath the lake (Figure 2.18). If this is the case, then labile yedoma-like permafrost C should be present in largest quantity near Goldstream's active thermokarst margin, where nearly all bubbling occurs.

In the lake center, where permafrost has been thawed for longer than 50 years (Figure 2.18) and where there is very little modern OM present, CH₄ emissions were 5-times lower; and CH₄ ages suggested incorporation of only 11-81% old permafrost C. One possible explanation for this trend is that taberal sediments beneath the center and far end of the lake have been completely thawed for a longer period of time over which their labile fraction has potentially become depleted (Dutta et al. 2006), resulting in both less seep bubbling, and bubbling of CH₄ generated from proportionally more modern C, further from the thermokarst margin. On the whole, our data suggest that progressing thaw has recently made available labile permafrost C near Goldstream's thermokarst margin, and that this C fuels more CH₄ production than does modern surface lake sediment in Goldstream Lake.

2.5 Conclusion

From anaerobic laboratory incubations and observations of ebullition dynamics, radiocarbon ages, and isotopic and elemental composition of bubbling from two thermokarst lakes differing in their age and sediment structure, we conclude that organic matter availability from recently thawed permafrost is an important control over the CH₄ production capacity of lakes. Accumulation of organic-rich lake sediments (3 cm and 130 cm) overlying thawed permafrost provided limited (10% and 27%) substrate for methanogenesis in Goldstream and Killarney lakes, respectively, reflecting the lower abundance and bioavailability of allochthonous/autochthonous organic matter. The presence of low-density organic-rich layers also appeared to affect bubble size and diffusion rates of atmospheric gases into bubbles rising through the water column,

thereby influencing bubble gas mixing ratios. These results suggest that variability in CH₄ production and ebullition observed within and between the lakes can be explained by differences in organic matter quality, quantity and sediment density. Measurement or knowledge of these parameters could improve the accuracy of upscaling CH₄ emission estimates for northern lakes.

Acknowledgements

Thanks to: Mat Wooller and Nancy Bigelow who provided lake coring equipment and assisted, along with Mary Edwards, Ben Gagliotti and Sean Brennan, with lake sediment coring and interpretation; Laura Oxtoby, Louise Farquarson and Katey Walter Anthony who assisted with lake core analysis at the National Lacustrine Core Repository; Katey Walter Anthony, Dragos Vas, Laurel McFadden, Laura Oxtoby and Marie-Laure Geai who helped collect ice-bubble survey data; Melissa Smith and Brian Sweeney who helped with gas sample collection; Bill Lee, Edda Mutter and Laurel McFadden who helped collect resistivity data and Bill Schnabel and Jens Monk who loaned electrical resistivity equipment.

References

- Amaral JA, Knowles R (1994) Methane metabolism in a temperate swamp. *Appl Environ Microbiol* 60:3945-3951.
- Bachoon D, Jones RD (1992) Potential rates of methanogenesis in sawgrass marshes with peat and marl soils in the Everglades. *Soil Biol Biochem* 24:21-27.
- Barber LE, Ensign JC (1979) Methane formation and release in a small Wisconsin lake. *Geomicrobiol J* 1:341-354.
- Bartlett KB, Crill PM, Sebacher DI, Harriss RC, Wilson JO, Melack JM (1988) Methane flux from the central Amazonian floodplain. *J Geophys Res* 93:1571-1582.
- Bastviken D, Cole J, Pace M, Tranvik L (2004) Methane emissions from lakes: dependence of lake characteristics, two regional assessments, and a global estimate. *Global Biogeochem Cycles* 18 DOI 10.1029/2004GB002238.
- Bray MT, French HM, Shur Y (2006) Further cryostratigraphy observations in the CRREL permafrost tunnel, Fox, Alaska. *Permafrost Periglac* 17:233-243.
- Casper P, Maberly SC, Hall GH, Finlay BJ (2000) Fluxes of methane and carbon dioxide from a small productive lake to the atmosphere. *Biogeochem* 49:1-19.
- Chanton JP, Martens CS, Kelley CA (1989) Gas transport from methane-saturated, tidal freshwater and wetland sediments. *Limnol Oceanog* 34:807-819.
- Chanton JP, Bauer JE, Glaser PA, Siegel DI, Kelley CA, Tyler SC, Romanoicz EH, Lazarus A (1995) Radiocarbon evidence for the substrates supporting methane formation within northern Minnesota peatlands. *Geochim Cosmochim Acta* 59:3663-3668.
- Chanton JP (2005) The effect of gas transport on the isotope signature of methane in wetlands. *Org Geochem* 36:753-768.
- Conrad R (2005) Quantification of methanogenic pathways using stable carbon isotopic signatures: a review and a proposal. *Org Geochem* 36:739-752.
- Coulthard TJ, Baird AJ, Ramirez J, Waddington JM (2009) Methane dynamics in peat: importance of shallow peats and a novel reduced-complexity approach for modeling ebullition. *Geoph Monog Series* 184:173-187.
- Dannenberg S, Conrad R (1999) Effect of rice plants on methane production and rhizospheric metabolism in paddy soil. *Biogeochem* 45:53-71.

Duc NT, Crill P, Bastviekn D. Implication of temperature and lake characteristics on methane formation and oxidation in lake sediments. *Biogeochem* (in review).

Dutta K, Schuur EAG, Neff JC, Zimov SA (2006) Potential carbon release from permafrost soils of northeastern Siberia. *Global Change Biol* 12:2336–2351.

Fortier R, LeBlanc A, Allard M, Buteau S, Calmels F (2008) Internal structure and conditions of permafrost mounds at Umiujaq in Nunavik, Canada, inferred from field investigation and electrical resistivity tomography. *Can J Earth Sci* 45:367-387.

Greinert J, McGinnis DF (2009) Single bubble dissolution model: the graphical user interface SiBu-GUI. *Environ Mod & Software* DOI 10.1016/j.envsoft.2008.12.011.

Hamilton TD, Craig JL, Sellmann PV (1988) The Fox permafrost tunnel: a late Quaternary geologic record in central Alaska. *GSA Bulletin* 100:948-969.

Hoekstra P, Sellman PV, Delaney AJ (1973) Airborne resistivity mapping of permafrost near Fairbanks, Alaska. *Cold Regions Research and Engineering Laboratory Report* 324. 51 pp.

Hornibrook ERC, Longstaffe FJ, Fyfe WS (1997) Spatial distribution of microbial methane production pathways in temperate zone wetland soils: stable carbon and hydrogen isotope evidence. *Geochimica Cosmochim Acta* 61:745-753.

Hornibrook ERC, Longstaffe FJ, Fyfe WS (2000a) Evolution of stable carbon isotope compositions for methane and carbon dioxide in freshwater wetlands and other anaerobic environments. *Geochimica Cosmochim Acta* 64:1013-1027.

Hornibrook ERC, Longstaffe FJ, Fyfe WS (2000b) Factors influencing stable isotope ratios in CH₄ and CO₂ within subenvironments of freshwater wetlands: implications for delta-signatures of emissions. *Isot Environ Healt S* 36:151-176.

Huttunen JT, Alm J, Saarigarvi E, Lappalainen KM, Silvola J, Martikainen PJ (2003a) Contribution of winter to the annual CH₄ emission from a eutrophied boreal lake. *Chemosphere* 50:247-250.

Huttunen JT, Alm J, Liikanen A, Juutinen S, Larmola T, Hammar T, Silvola J, Martikainen PJ (2003b) Fluxes of methane, carbon dioxide and nitrous oxide in boreal lakes and potential anthropogenic effects on the aquatic greenhouse gas emissions. *Chemosphere* 52:609-621.

Jorgenson MT, Racine CH, Walters JC, Osterkamp TE (2001) Permafrost degradation and ecological changes associated with a warming climate in central Alaska. *Clim Change* 48:551-579.

Juutinen S, Alm J, Larmola T, Huttenen JT, Morero M, Martikainen PJ, Silvola J (2003) Major implication of the littoral zone for methane release from boreal lakes. *Global Biogeochem Cycles* 17 DOI 10.1029/2003GB002105.

Keller M, Stallard RF (1994) Methane emission by bubbling from Gatun Lake, Panama. *J Geophys Res* 99:8307-8319.

King JY, Reeburgh WS, Thieler KK, Kling GW, Loya WM, Johnson LC, Nadelhoffer KJ (2002) Pulse-labeling studies of cycling in Arctic tundra ecosystems: The contribution of photosynthates to methane emission. *Global Biogeochem Cycles* 16:1062-1070.

Mattson MD, Likens GE (1990) Air pressure and methane fluxes. *Nature* 347:718-719.

Metje M, Frenzel P (2007). Methanogenesis and methanogenic pathways in a peat from subarctic permafrost. *Environ Microbiol* 9:954-964.

Meyer H, Dereviagin AY, Siegert C, Hubberten HW (2002) Paleoclimate studies on Bykovsky Peninsula, North Siberia – hydrogen and oxygen isotopes in ground ice. *Polarforschung* 70:37-51.

Meyer H, Yoshikawa K, Schirrmeister L, Andreev A (2008) The Vault Creek Tunnel (Fairbanks Region, Alaska): A late Quaternary palaeoenvironmental permafrost record. Ninth International Conference on Permafrost, Fairbanks, Alaska. 1191-1196.

Minoda T, Kimura M (1994) Contribution of photosynthesized carbon to the methane emitted from paddy fields. *Geophys Res Lett* 21:2007-2010.

Muhs DR, Ager TA, Bettis EA III, McGeehin J, Been JM, Beget JE, Pavich MJ, Stafford TM Jr, Stevens DSP (2003) Stratigraphy and palaeoclimatic significance of Late Quaternary loess-palaeosol sequences of the last interflacial-glacial cycle in central Alaska. *Quat Sci Rev* 22:1947-1986.

Muhs DR, Budahn JR (2006) Geochemical evidence for the origin of late Quaternary loess in central Alaska. *Can J Earth Sci* 43:323-337.

Péwé TL (1952) Geomorphology of the Fairbanks area, Alaska. Dissertation, Stanford University

Péwé TL (1975) Quaternary Geology of Alaska. United States Government Printing Office, Washington.

- Poissant L, Constant P, Pilote M, Canario J, O'Driscoll N, Ridal J, Lean D (2007) The ebullition of hydrogen, carbon monoxide, methane, carbon dioxide and total gaseous mercury from the Cornwall Area of Concern. *Sci Total Environ* 381:256-262.
- Schirrmeister L, Siegert C, Kuznetsova T, Kuzmina S, Andreev A, Kienast F, Meyer H, Bobrov A (2002) Paleoenvironmental and paleoclimatic records from permafrost deposits in the Arctic region of Northern Siberia. *Quaternary Int* 89:97-118.
- Sellmann PV (1967) Geology of the USA. CRREL permafrost tunnel, Fairbanks, Alaska. Technical Report 199, US Army CRREL. Hanover, New Hampshire, 22pp.
- Shur Y, French HM, Bray MT, Anderson DA (2004) Syngenetic permafrost growth: cryostratigraphic observations from the CRREL tunnel near Fairbanks, Alaska. *Permafrost Periglac* 15:339-347.
- Smith LK, Lewis WM Jr (1992) Seasonality of methane emissions from five lakes and associated wetlands of the Colorado Rockies. *Global Biogeochem Cycles* 6:323-338.
- Stayer RF, Tiedje JM (1978) In situ methane production in a small hypereutrophic, hard-water lake: loss of methane from sediments by vertical diffusion and ebullition. *Limnol Oceanogr* 23:2101-1206.
- Stuiver MM, Polach H (1977) Reporting of ^{14}C data. *Radiocarbon* 19:355-363
- Tarnocai C, Canadell JG, Schuur EAG, Kuhry P, Mazhitova G, Zimov S (2009) Soil organic carbon pools in the northern circumpolar permafrost region. *Global Biogeochem Cycles* 23. DOI 10.1029/2008GB003327.
- Tomirdiaro SV, Nishchanskii GM, Kirillov VA (1969) Sublacustrine talik zones and their delineation in sublacustrine practice. *Kolyma* 9:35-44.
- Turner H (2009) An investigation into the formation and evolution of two lakes in Fairbanks, AK. B.S. Sr. Honors Thesis, University of Southampton.
- Valentine DL, Chidthaisong A, Rice A, Reeburgh WS, Tyler SC (2004) Carbon and hydrogen isotope fractionation by moderately thermophilic methanogens. *Geochimica Cosmochim Acta* 68:1571-1590.
- Varadharajan C (2009) Magnitude and spatio-temporal variability of methane emissions from a eutrophic freshwater lake. Dissertation, Massachusetts Institute of Technology.
- Vas DA (2010) Methane seep dynamics in an interior Alaska thermokarst lake using high-temporal resolution automated bubble traps. M.Sc. Thesis. University of Alaska Fairbanks.

Walter KM, Zimov SA, Chanton JP, Verbyla D, Chapin FS III (2006) Methane bubbling from siberian thaw lakes as a positive feedback to climate warming. *Nature* 443:71-75.

Walter KM, Chanton JP, Chapin FS III, Schuur AG, Zimov SA (2008) Methane production and bubble emissions from arctic lakes: isotopic implications for source pathways and ages. *J Geophys Res* 113 DOI 10.1029/2007JG000569.

Walter Anthony KM, Chapin FS III, Zimov SA, Zhuang Q (2010) Estimating methane emissions from northern lakes using ice-bubble surveys. *Limnol Oceanogr* (in review).

West JJ, Plug LJ (2008) Time-dependant morphology of thaw lakes and taliks in deep and shallow ground ice. *J Geophys Res* 113 DOI 10.1029/2007JG000569.

Whiticar MJ, Faber E, Schoell M (1986) Biogenic methane formation in marine and freshwater environments: CO₂ reduction vs. acetate fermentation – isotopic evidence. *Geochimica Cosmochim Acta* 50:693-709.

Whiticar MJ (1999) Carbon and hydrogen isotope systematic of bacterial formation and oxidation of CH₄. *Chem Geol* 161:291-314.

Wuebbles DJ, Hayhoe K (2002) Atmospheric methane and global change. *Earth Sci Rev* 57: 177–210.

Zimov SA (2005) Pleistocene Park: return of the mammoth's ecosystem. *Science* 308:796-798.

Zimov SA, Voropaev YV, Semiletov IP, Davidov SP, Prosiannikov SF, Chapin FS III, Chapin MC, Trumbore S, Tyler S (1997) North Siberian lakes: a methane source fueled by Pleistocene carbon. *Science* 277 DOI 10.1126/science.277.5327.800.

Zimov SA, Voropaev YV, Davydov SP, Zimova GM, Davydova AI, Chapin FS III, Chapin MC (2001) Flux of methane from north Siberian aquatic systems: influence on atmospheric methane. In: Paepe R, Melnikov V (ed.) *Permafrost response on economic development, environmental security and natural resources*. Kluwer Academic Publishers, Netherlands.

Zimov SA, Davydov SP, Zimova GM, Davydova AI, Schuur EAG, Dutta K, Chapin FS III (2006a) Permafrost carbon: stock and decomposability of a globally significant carbon pool. *Geophys Res Lett* 33 DOI 10.1029/2006GL027484.

Zimov, SA, Schuur, EAG, Chapin FS III (2006b) Climate change: permafrost and the global carbon budget. *Science* 312 DOI 10.1126/science.11289.

Figures

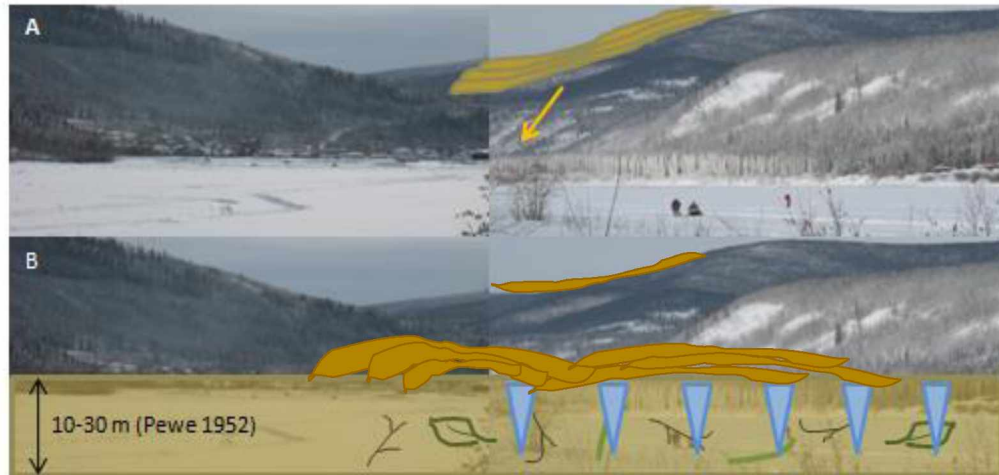


Figure 2.1 During the Last Glacial Maximum, aeolian silt accumulated on hillsides in arid interior Alaska (Péwé 1952, Muhs et al. 2003). Colluvial forces and frost action gradually eroded loess down slope, partially redepositing it to valley bottoms (Péwé 1952) (A). This process incorporated graminoid roots and litter from the steppe environment as permafrost formed syngenetically (B).

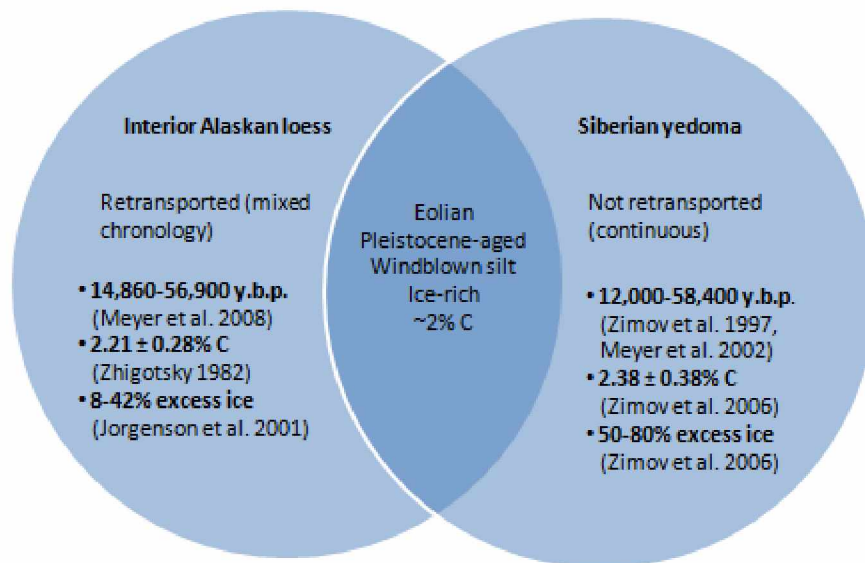


Figure 2.2: Similarities and differences between valley-bottom Alaskan Pleistocene-aged loess permafrost and Siberian yedoma

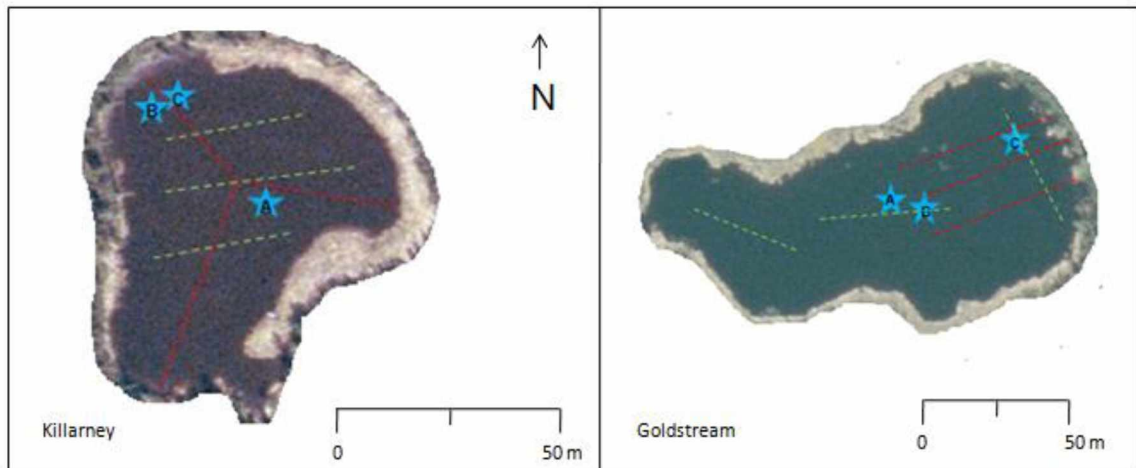


Figure 2.3: Approximate coring locations (A, B, C) and approximate transect locations for lake ice bubble surveys conducted in 2007 (green) and 2009 (red) for each lake.

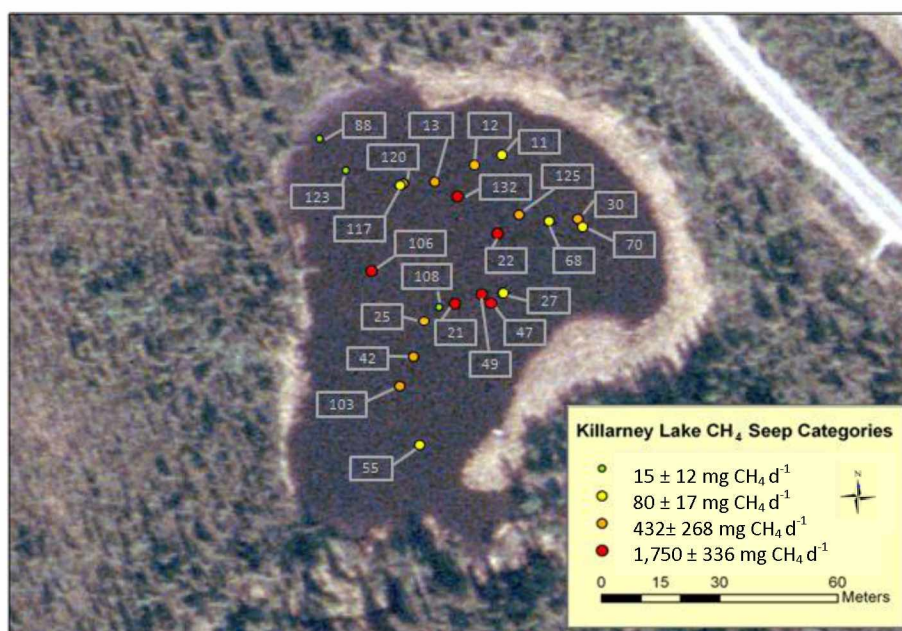


Figure 2.4a: Seep locations colored by flux in Killarney Lake. Boxed numbers give seep IDs.

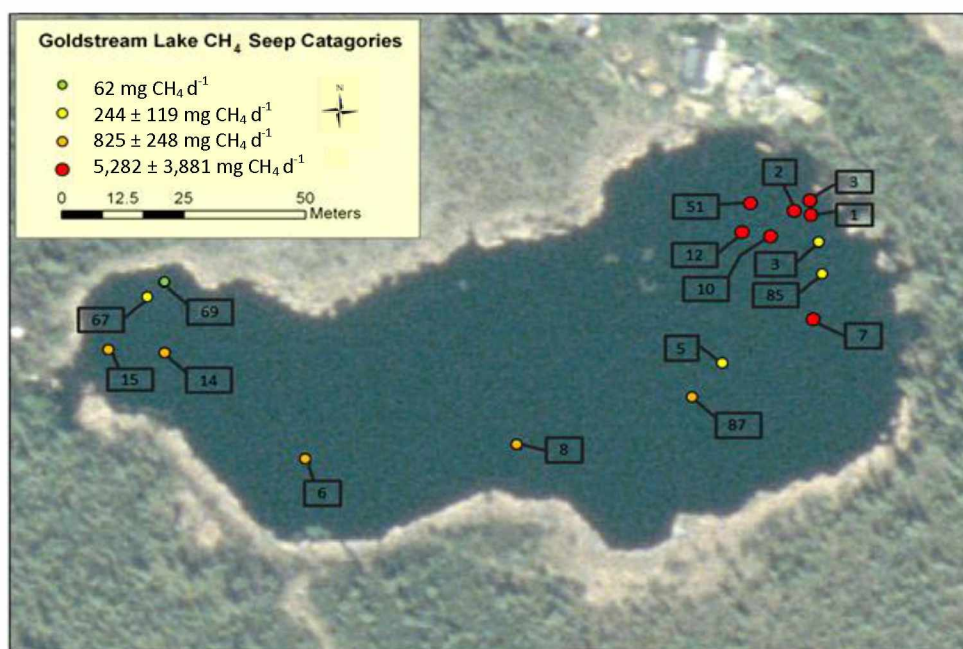


Figure 2.4b: Seep locations colored by flux in Goldstream Lake. Boxed numbers give seep IDs.

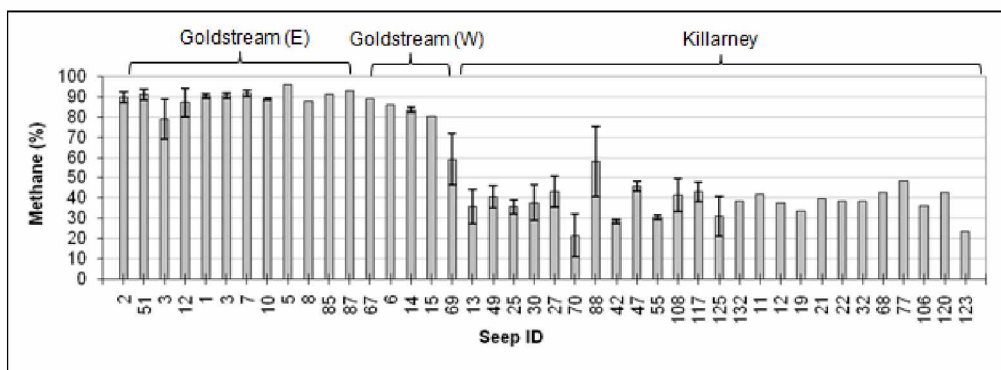


Figure 2.5: Average CH_4 concentrations for all ebullition point seeps studied in Killarney and Goldstream Lakes. Error bars, where present, represent variation in CH_4 concentration over multiple sampling dates. CH_4 concentrations of bubbles emitted from Goldstream Lake are over 50% higher on average than bubbles emitted from Killarney

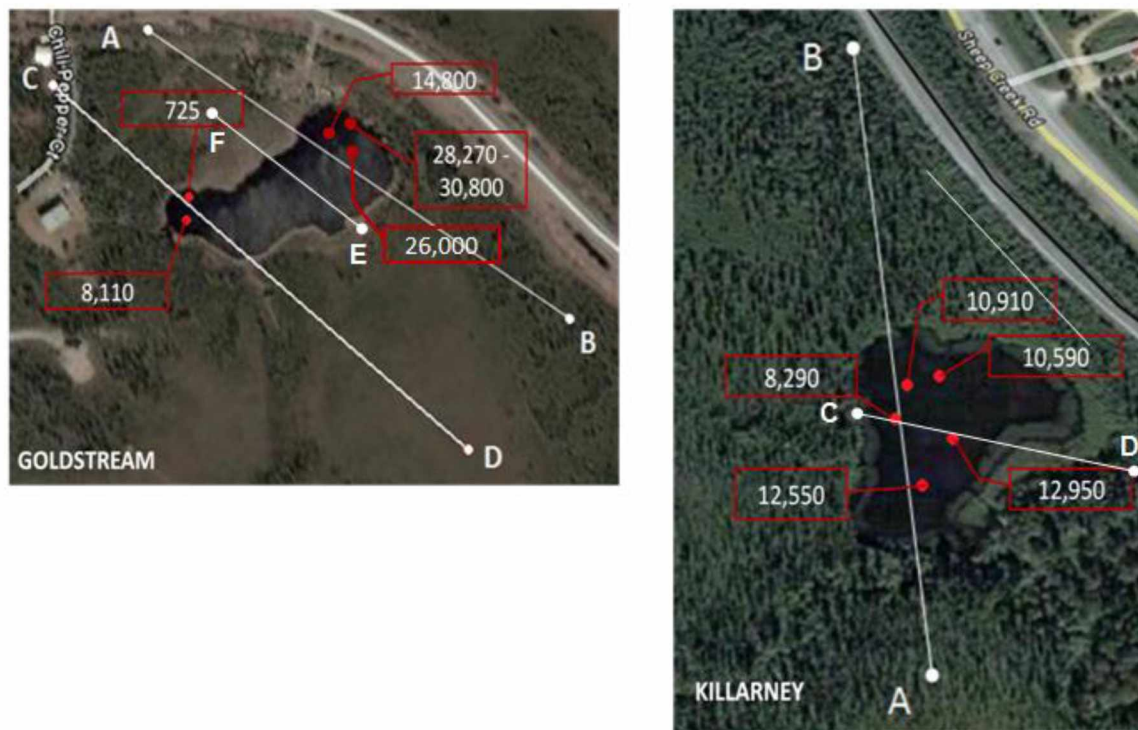


Figure 2.6: Study lake $^{14}\text{C-CH}_4$ radiocarbon ages of bubbling and resistivity transect lines. $^{14}\text{C-CH}_4$ ages indicate incorporation of old permafrost C near the eastern thermokarst margin in Goldstream, and more modern C near the opposite margin. Killarney emitted CH_4 composed of a mixture of modern and old C.

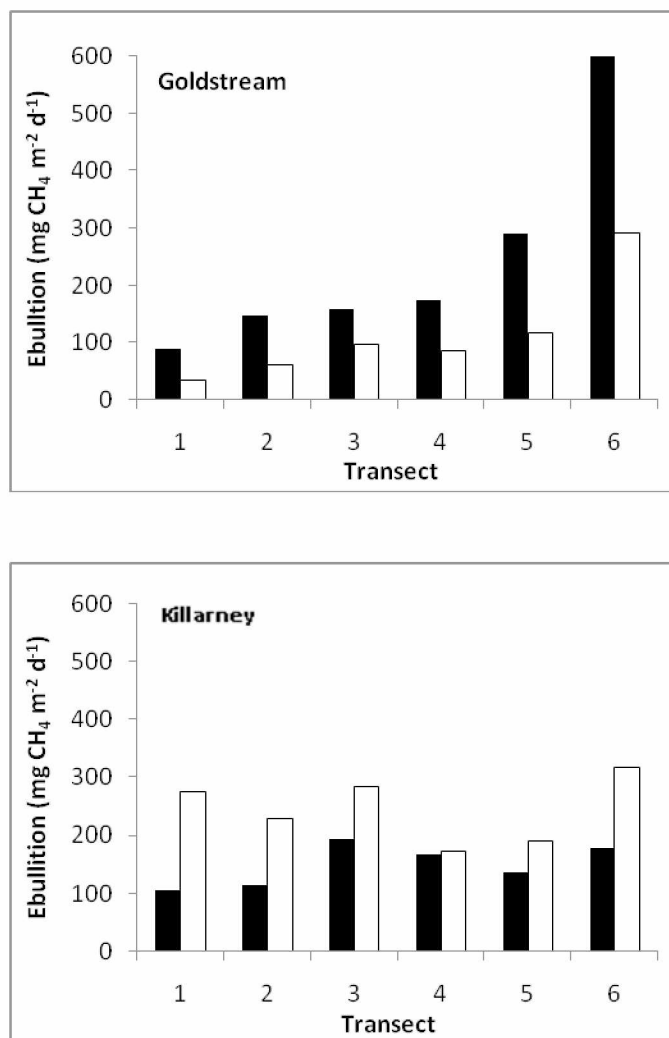


Figure 2.7: The result of 1) upscaling lake ice bubble survey results using average bubble CH_4 concentrations and flux rates for thermokarst seeps based on Walter Anthony et al. (in review) (open bars); and 2) upscaling lake ice bubble survey results using bubble flux and CH_4 concentrations specific to our study lakes, (solid bars).

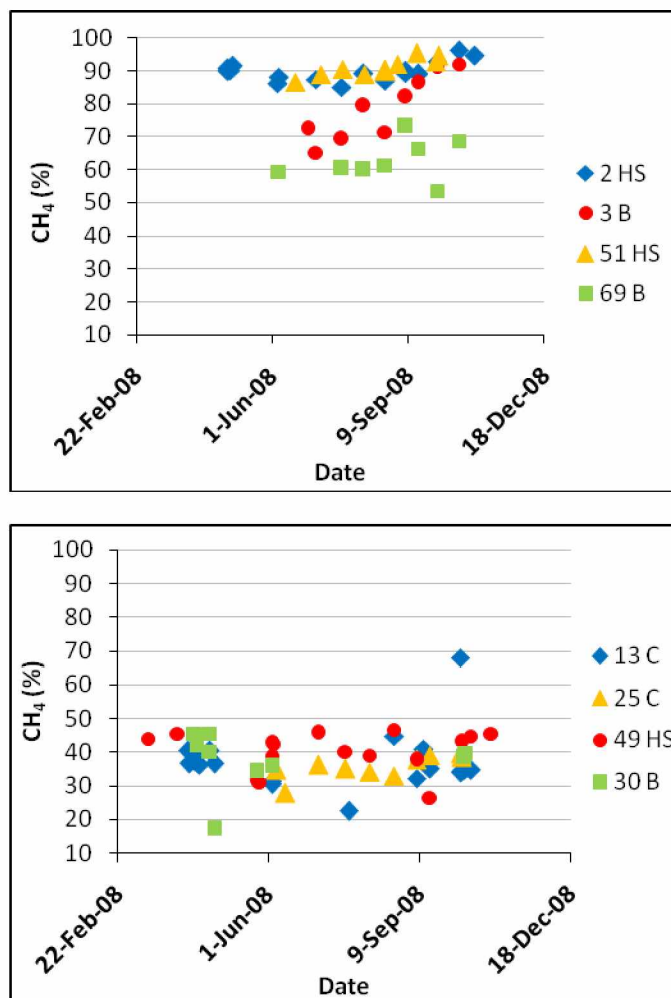


Figure 2.8: Changes in bubble CH₄ concentration of discreet seeps in Goldstream Lake (left) and Killarney Lake (right) over time. More variation is apparent amongst lower flux seeps in Goldstream (3B, 69B). Seeps in Killarney Lake appear to display more variation over time than do seeps in Goldstream Lake.

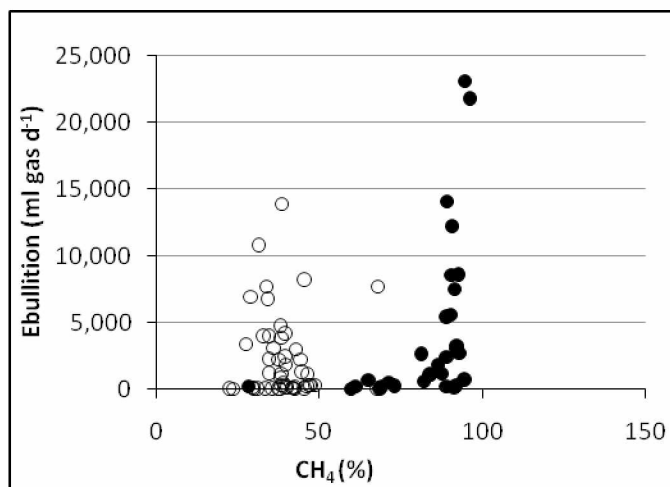


Figure 2.9: Bimodal graph of bubble flux rate vs. CH₄ concentration. Open circles = Killarney, closed circles = Goldstream. Each point represents a separate sampling event.

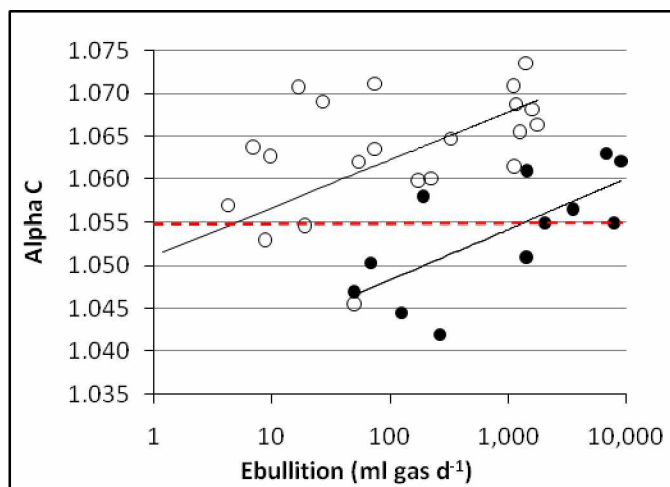


Figure 2.10: High-emission ebullition seeps were dominated by CO₂ reduction. Closed circles = Goldstream, $y = 0.0026 \ln(x) + 1.037$, $R^2 = 0.50$; open circles = Killarney, $y = 0.0024 \ln(x) + 1.051$, $R^2 = 0.35$. Alpha C values above the dashed red line indicate CO₂ reduction; and below the red line, acetate fermentation.

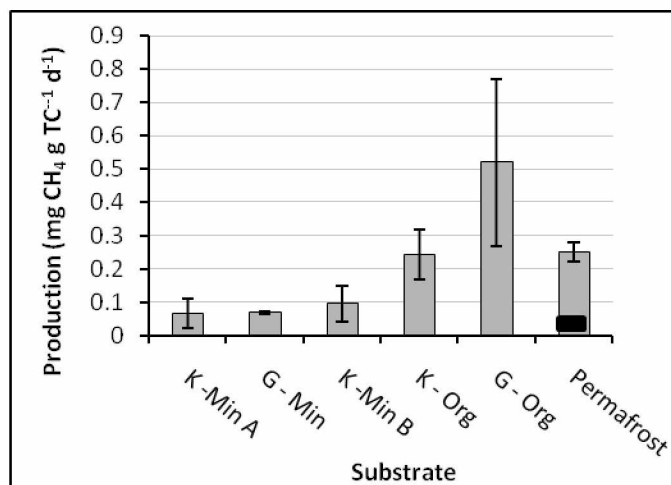


Figure 2.11: Production potentials of anaerobically incubated lake sediments sections and loess permafrost over 39 week at 4°C (permafrost, 21-23°C). The black bar gives the production potential of thawed permafrost at 4°C based on correction by a Q_{10} value of 2.7 (Duc et al. in review). Error bars show standard deviations.

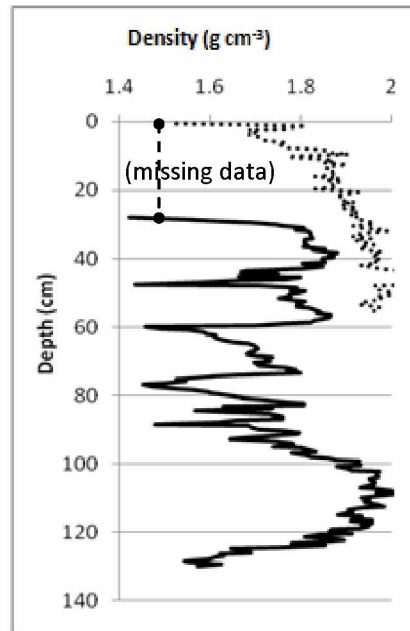


Figure 2.12: Down-core gamma density (g cm^{-3}) of Killarney Core B (solid) and Goldstream Core A (dotted) lake sediments. Data from the top 27 cm of the Killarney core were unreliable. Killarney Lake sediments were more variable and of lower density overall.

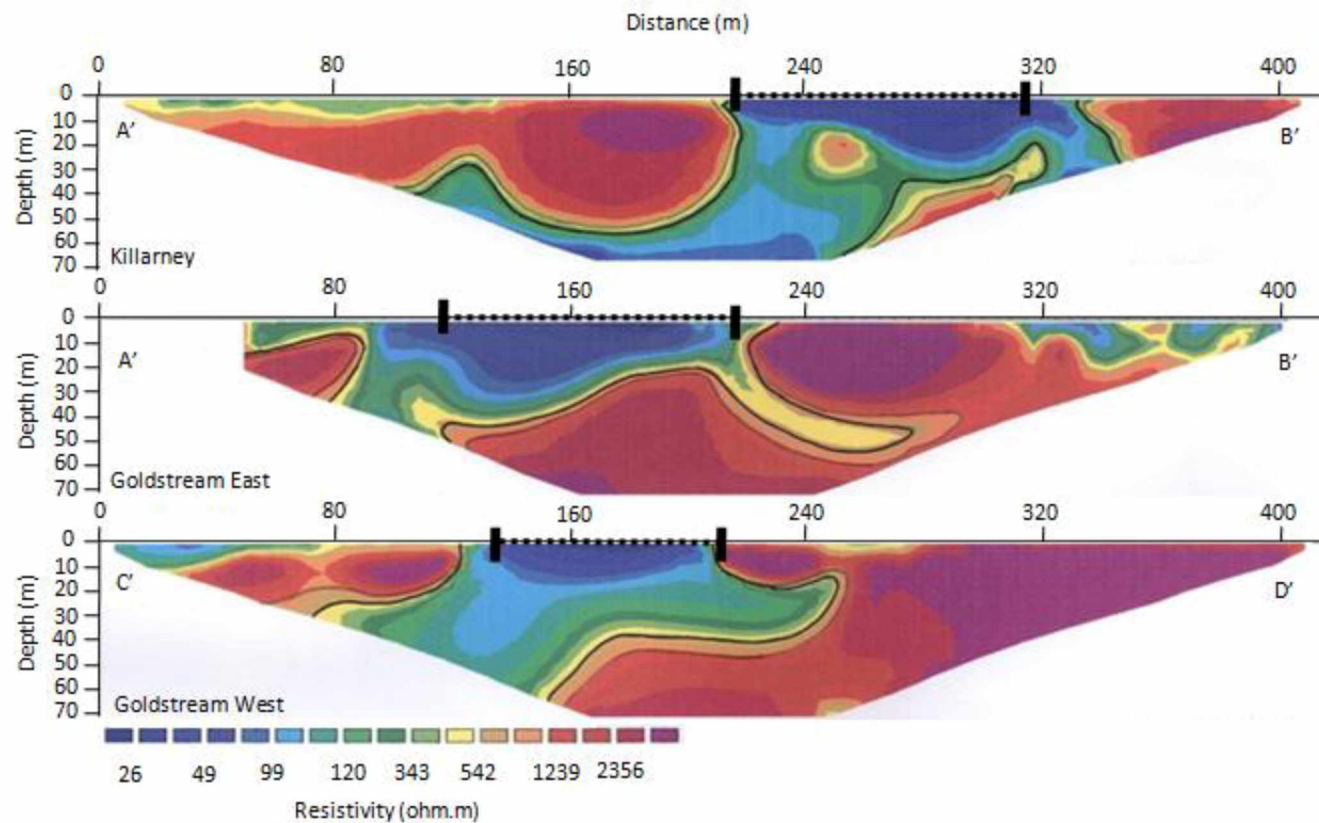


Figure 2.13: Deep resistivity data collected using 5 m electrode spacing. Yellow through blue values show materials containing liquid water, which suggested thawed sediments. Red-orange values suggest frozen (ice-containing) horizons. Probable talik extents are drawn in black and are 20-50 m for Goldstream's eastern end, 30-60 m for Goldstream's western end and >70 m for Killarney. Gray lines represent our range of uncertainty. Dashed black lines represent the lake surfaces.

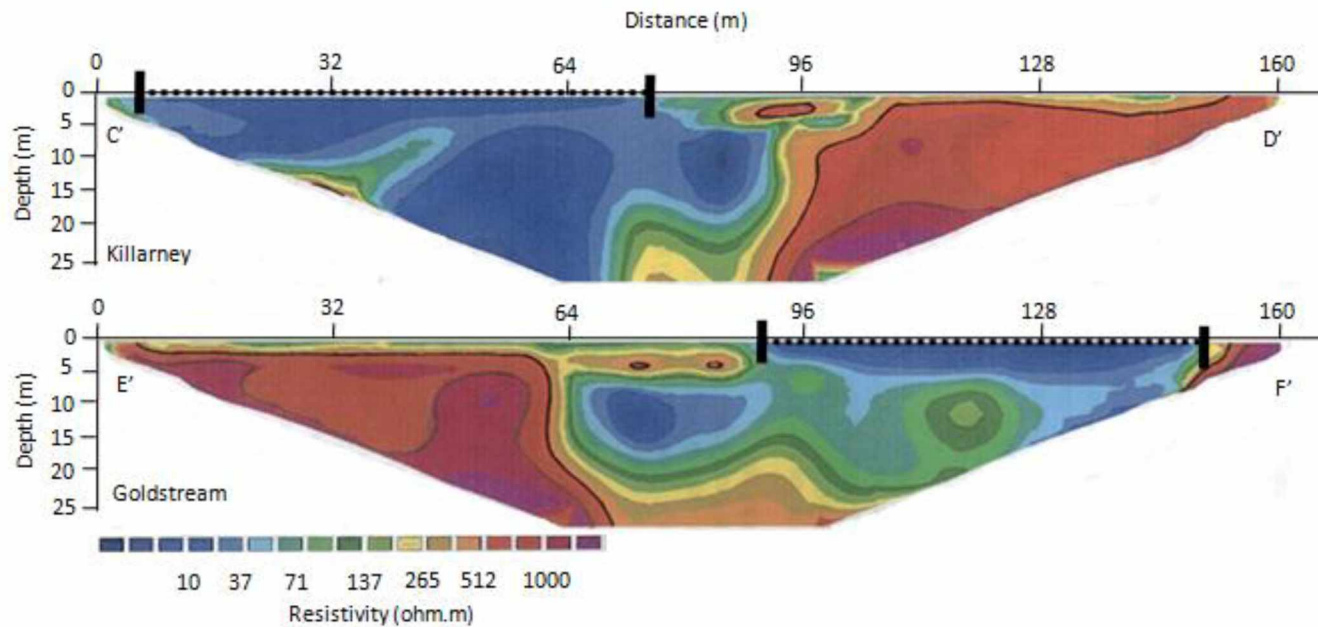


Figure 2.14: Shallow resistivity data collected using 2 m electrode spacing. Yellow through Blue values show materials containing liquid water, which suggested thawed sediments. Red-Orange values suggest frozen (ice-containing) horizons. Figure shows encroachment of floating mats and refreeze of taberal sediments along the northern margin of Goldstream Lake and eastern margin of Killarney Lake. Lake change along these margins can also be seen in repeat aerial photographs and satellite imagery. Probable talik extents are drawn in black. Dashed black lines represent the lake surfaces.



Figure 2.15: Goldstream Lake's 1949 margin shown here as digitized aerial photography (blue) provides evidence of significant lake expansion along the eastern thermokarst margin, as well as encroachment of the northern margin when compared to the lake's current margin (green). 2007 lake perimeter by Melanie Engram from 2007 Fairbanks digital orthorectified quarter-quadrangles, distributed by Geographic Information System of Alaska (GINA). 1949 lake perimeter by Benjamin Jones from 1949 U.S. Airforce aerial photography single frame, Project MO8170.

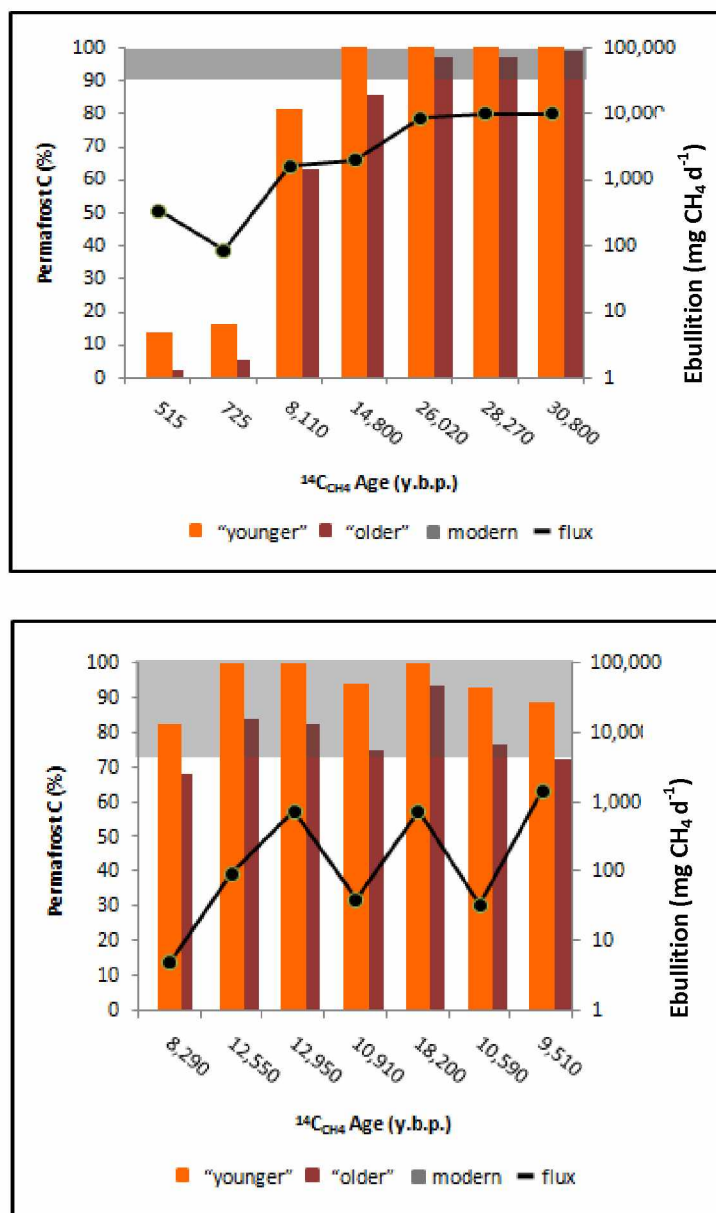


Figure 2.16: Range of potential permafrost C contributions to specific seep bubbling in Goldstream Lake (top), and Killarney Lake (bottom) determined from mixing model calculations using measured radiocarbon ages of seep CH_4 and younger permafrost OM (12 ka) and older permafrost OM (30 ka). Gray boxes show the amount of CH_4 that could be produced from modern C sources based on anaerobic incubation results and total carbon quantities within the lakes, assuming that the organic fraction dominates the total carbon pool.

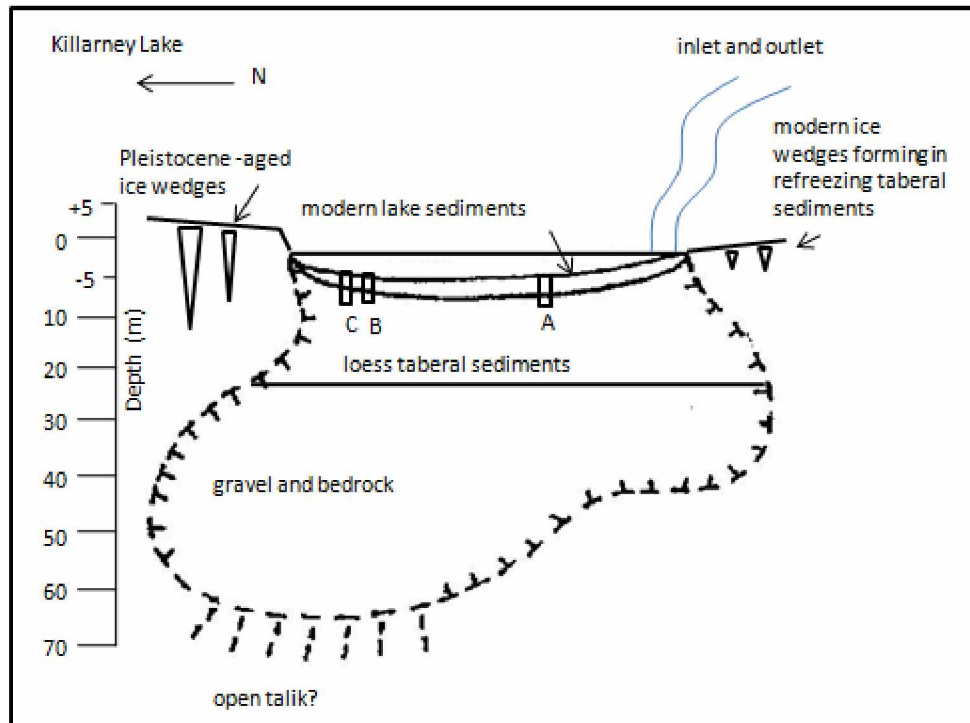


Figure 2.17: Schematic of Killarney Lake and its talik drawn roughly to scale. A, B, and C demarcate coring locations. Loess unit thickness was calculated from subsidence estimates (based on bluff height, water depth and modern sediment thickness) and an assumed excess ice content of 30% for redeposited loess permafrost.

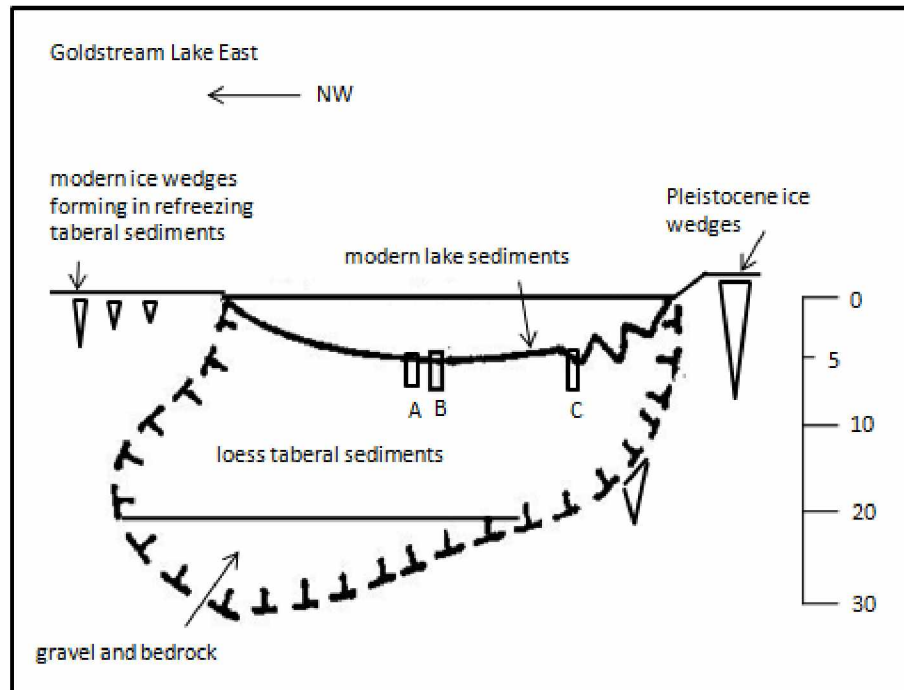


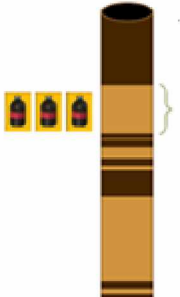



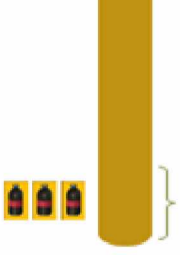

Figure 2.18: Schematic of the eastern end of Goldstream Lake and its talik drawn roughly to scale. A, B and C demarcate coring locations. Loess unit thickness was determined from local borehole data (Vas et al. in prep).

Tables

Table 2.1: Summary of past studies measuring CH₄ concentrations in bubbling from aquatic environments. n = number of sampling sites, CH₄ (%) expressed as mean ± std.

<i>Source</i>	<i>Object</i>	<i>n</i>	<i>CH₄ (%)</i>	<i>Range CH₄ (%)</i>
Stayer & Tiedje 1978	Lake Wintergreen, Michigan	-	-	73 - 107
Barber & Ensign 1979	Lake Wingra (eutrophic)	-	-	4-56
Bartlett et al. 1988	Amazon floodplain lakes	-	-	58 - 72
Chanton et al. 1989	Temperate estuaries (non-vegetated)	11	69.3 ± 12.9	46 - 89.7
Chanton et al. 1989	Temperate estuaries (vegetated)	3	26.8 ± 14.2	12.6 - 40.9
Mattson & Likens 1990	Mirror Lake, UK	-	-	70
Keller & Stallard 1994	Tropical man-made lake	-	-	66 - 77
Casper et al. 2000	Priest Pot Lake, UK	7	66	43.7 - 88.1
Zimov 2001	Siberian thermokarst lakes	-	-	>80
Poissant et al. 2007	Temperate estuary	2	26.8 ± 5.7	22.7 - 30.8
Varadharajan 2009	Upper Mystic Lake (2007)	11	54 ± 17	22 - 74
Varadharajan 2009	Upper Mystic Lake (2008)	13	63 ± 10	38 - 81
Walter et al. 2008	Siberian & Alaskan thermokarst lakes	55	82 ± 10	67-94

Table 2.2: Anaerobic incubation substrate characteristics and methane production potentials expressed as mean \pm std on the basis of total carbon (TC) content and dry weight (DW).

	Depth from surface (cm)	Unit description	TC (%)	C:N	Production Potential	
					mg CH ₄ g TC ⁻¹ d ⁻¹	mg CH ₄ g DW ⁻¹ yr ⁻¹
Killarney						
	55-65	Mineral (fluvial)	1.22	10.6	0.07 \pm 0.04	0.29 \pm 0.20
	123-134	Organic (trash layer)	9.27	11.3	0.24 \pm 0.08	8.28 \pm 2.56
	168-185	Mineral (taberal)	0.71	8.2	0.09 \pm 0.05	0.25 \pm 0.14
Goldstream						
	0-3	Organic (gyttja)	19.12	20.3	0.52 \pm 0.25	38.39 \pm 18.5
	50-60	Mineral (taberal)	1.47	13.1	0.07 \pm 0.00	0.17 \pm 0.01
Rosie Creek						
	**	Mineral (permafrost)	3.47	11.51	0.25 \pm 0.03 (0.05 \pm 0.01)*	3.18 \pm 0.31

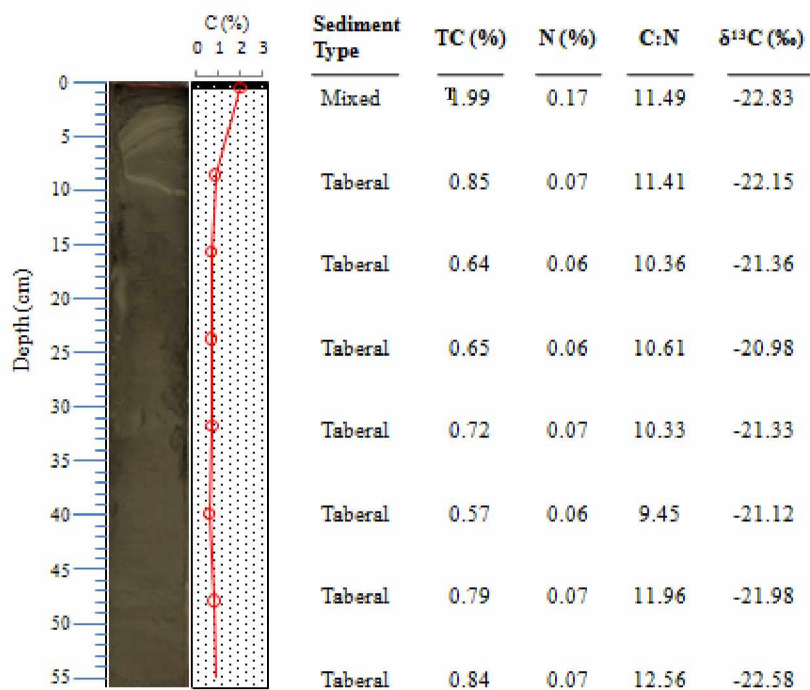
*Q¹⁰-corrected production potential based on Q¹⁰ = 2.7 (determined experimentally for lake sediments by Duc et al. in review)

**Permafrost collected by K. Yoshikawa, exact depth of collection unknown.

Table 2.3: Elemental and isotopic composition of lake bubbles emitted from Killarney Lake and Goldstream Lake expressed as mean \pm std. O_2 values are not corrected for potential coelution with Ar.

<i>Sampling location</i>	$\delta^{13}C_{CH_4}$ (‰)	$\delta^{13}C_{CO_2}$ (‰)	δD_{CH_4} (‰)	CO_2 (%)	CH_4 (%)	O_2 (%)	N_2 (%)
Killarney (n=26)	-82.2 \pm 3.7	-26.2 \pm 8.2	-306 \pm 13	0.92 \pm 0.68	39.85 \pm 11.8	3.49 \pm 2.58	57.24 \pm 11.84
Goldstream (n=17)	-67.7 \pm 5.7	-16.1 \pm 2.1	-333 \pm 19	0.49 \pm 0.16	86.38 \pm 8.29	2.01 \pm 1.71	13.57 \pm 6.66
Non-thermokarst shore (n=6)	-67.9 \pm 6.2	-17.4 \pm 3.5	-322 \pm 23	0.45 \pm 0.17	79.5 \pm 11.9	2.92 \pm 2.65	19.71 \pm 8.19
Thermokarst shore (n=11)	-68.7 \pm 5.8	-18.3 \pm 4.2	-336 \pm 16	0.52 \pm 0.16	89.2 \pm 4.3	1.36 \pm 1.09	10.42 \pm 3.99

Table 2.4a: Sediment core photo, interpretation, and subsample %TC (total carbon), %N, C:N and ^{13}C isotope values for Goldstream Core A (LacCore ID: FAI-GB09-4A-1N-1). Key for Tables 2.4a-f follows.



Key

★	^{14}C radiocarbon age
○	C/N and $\delta^{13}\text{C}$, bulk density
◇	C/N and $\delta^{13}\text{C}$, δD pore water
◆	C/N and $\delta^{13}\text{C}$
■	modern gyttja
▨	organic with few thin (1 mm) mineral laminations
▧	mineral with frequent thick (5-10 mm) organic laminations
▩	mineral with frequent thin (1 mm) organic laminations, sometimes indistinct
▪	gyttja with well-preserved coarse organic debris
▫	mineral with indistinct organic laminations or some organic content
▬	silt with distinct organic components (fine roots, detritus) mixed in
▭	homogeneous silt
▮	lacustrine peat, mostly <i>Chapanocladum</i> moss

Table 2.4b: Interpretation, and subsample %TC (total carbon), %N, C:N and ^{13}C isotope values for Goldstream Core B.

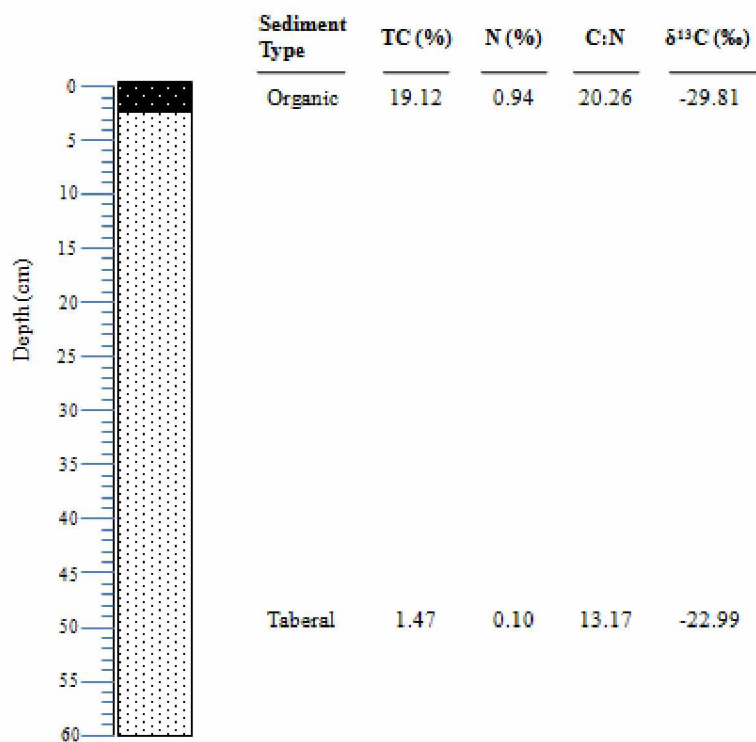


Table 2.4c: Interpretation and subsample %TC (total carbon), %N, C:N and ^{13}C isotope values for Goldstream Core C.

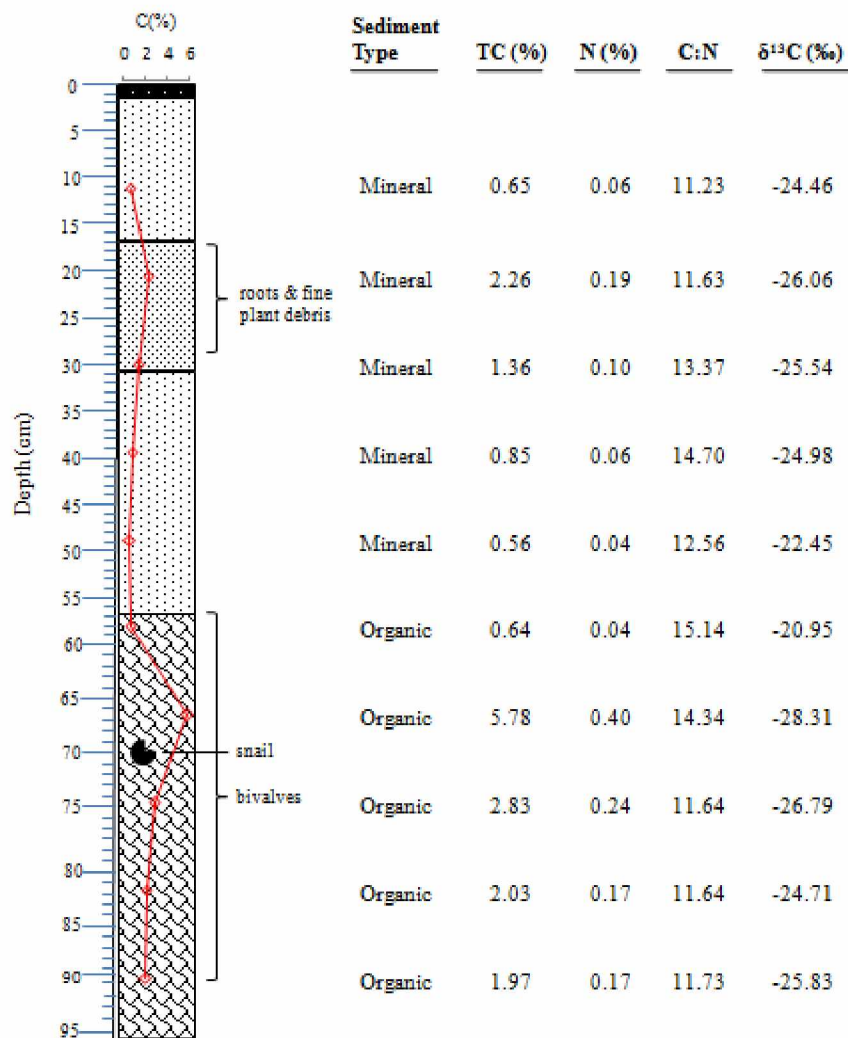


Table 2.4d: Interpretation, and subsample %TC (total carbon), %N, C:N and ^{13}C isotope values for Killarney Core A.

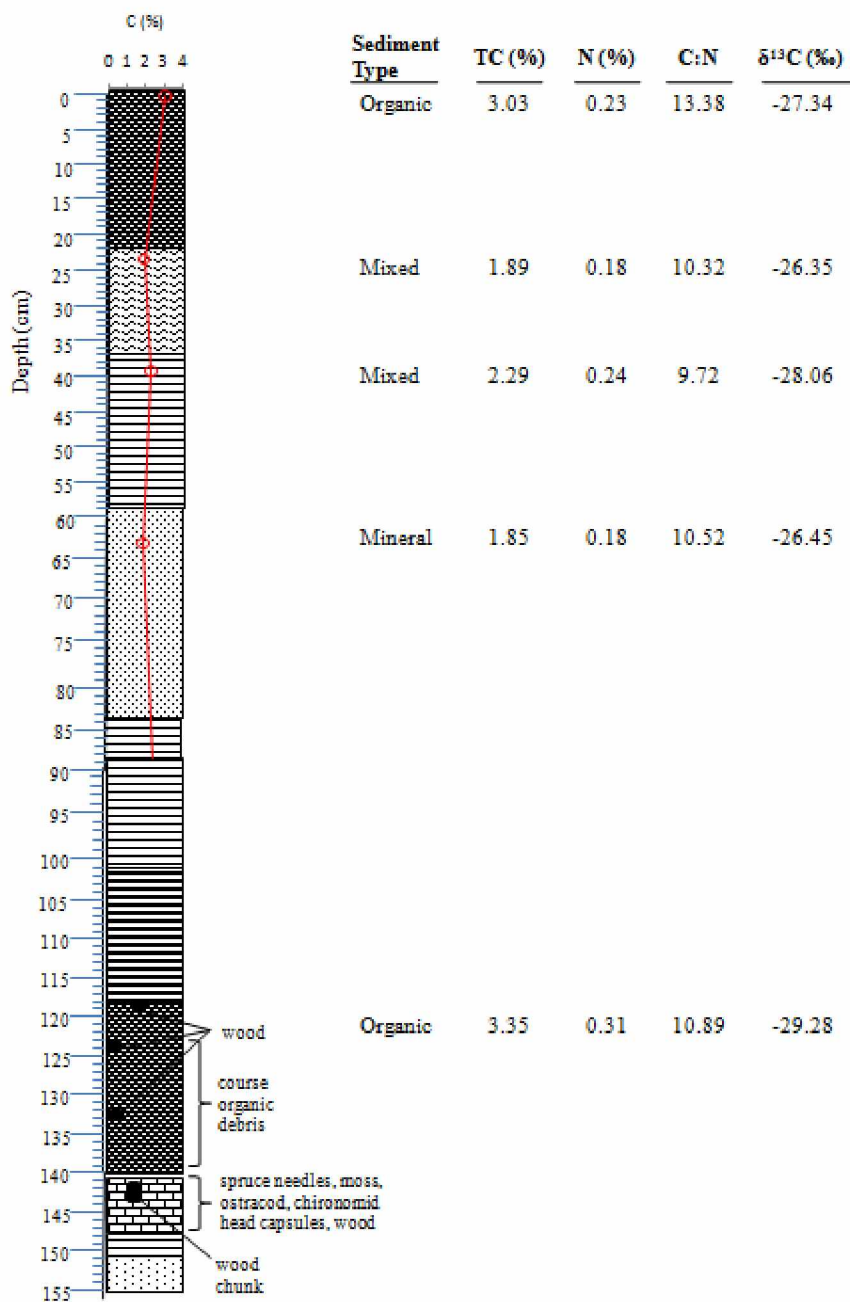


Table 2.4e: Sediment core photo, interpretation, and subsample %TC (total carbon), %N, C:N and ^{13}C isotope values for Killarney Core B (LacCore ID's: FAI-KILL09-1A-1N-1 and FAI-KILL09-1A-1N-2)

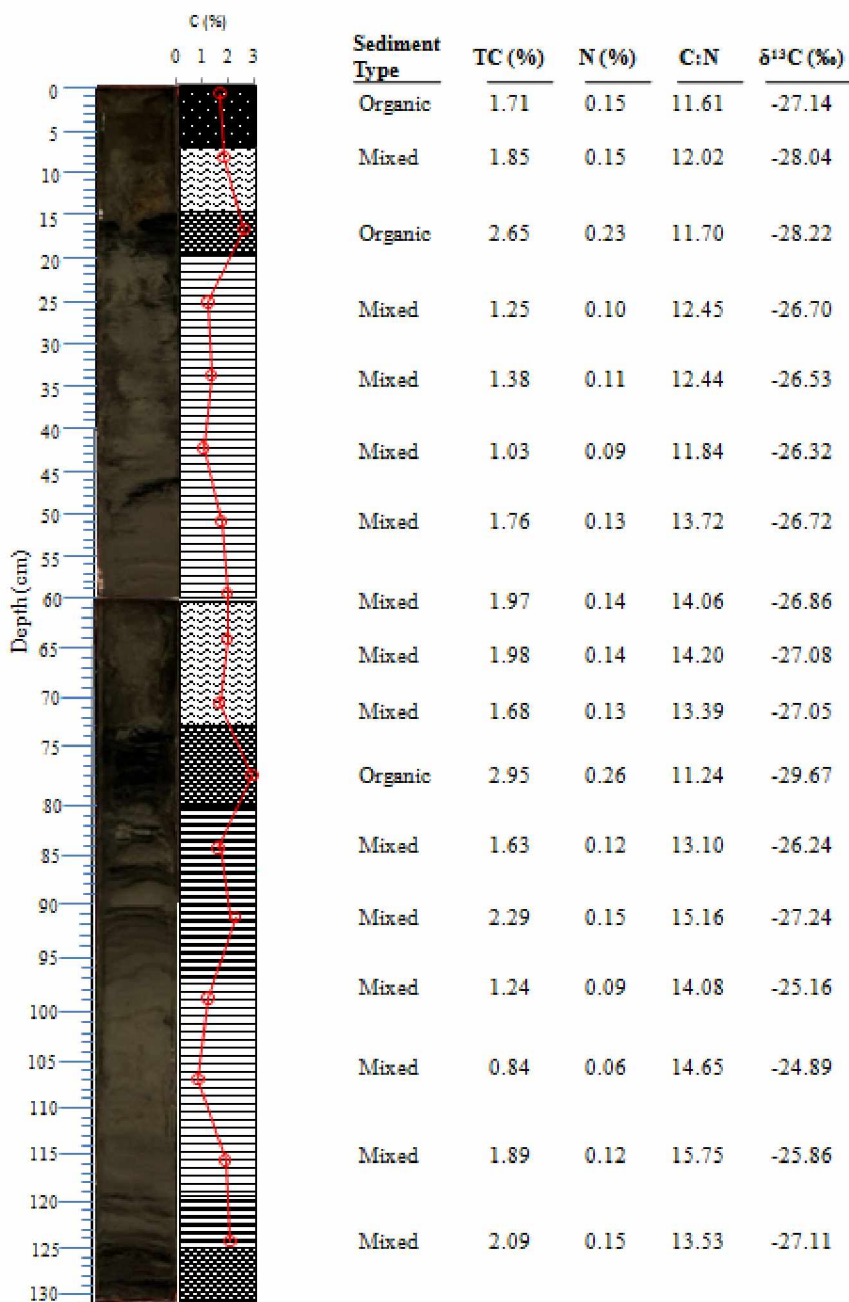


Table 2.4f: Interpretation of Killarney sediment Core C. The only subsamples analyzed from this core were from incubated sediment sections. Data are shown in Table 2.2.

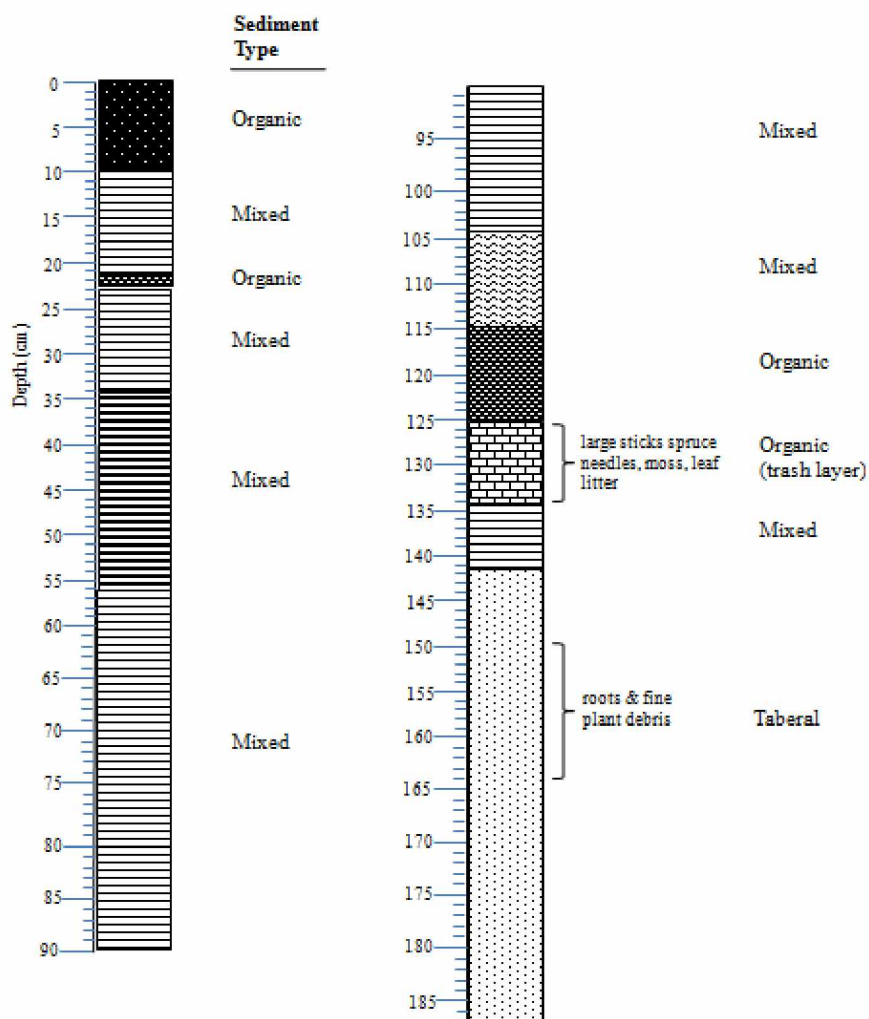


Table 2.5: Permafrost and sediment isotopic and elemental composition shown as the average of all samples taken from each object reported as mean \pm std. TC(%) = total C for all core objects. OC(%) = organic C for all permafrost objects

<i>Lake</i>	<i>Object</i>	<i>n</i>	<i>TC or OC (%)</i>	<i>N (%)</i>	<i>C:N</i>	$\delta^{13}\text{C} (\text{‰})$	$\delta^{15}\text{N} (\text{‰})$
Killarney	Core A	5	2.48 \pm 0.68	0.23 \pm 0.05	11.0	-27.5 \pm 1.2	3.1 \pm 0.8
Killarney	Core B	13	1.86 \pm 0.54	0.15 \pm 0.05	12.8	-27.3 \pm 0.9	3.0 \pm 0.4
Killarney	Core C	3	3.74 \pm 4.80	0.34 \pm 0.42	10.0	-26.6 \pm 1.8	1.4 \pm 1.1
Goldstream	Core B	8	0.88 \pm 0.46	0.08 \pm 0.04	10.6	-21.8 \pm 0.7	3.1 \pm 0.8
Goldstream	Core C	10	1.89 \pm 1.58	0.15 \pm 0.11	12.8	-25.0 \pm 2.1	3.1 \pm 0.4
Goldstream	Permafrost	1	0.56	0.04	14.0	-25.9	4.0
Killarney	Permafrost	1	2.48	0.13	19.5	-26.0	2.3
Rosie Creek	Permafrost	1	3.47	0.30	11.51	-26.7	-

Table 2.6: Predicted bubble gas composition for bubbles of different sizes at 0 and 20°C using the SiBu-GUI model (Greinert & McGinnis 2009).

<i>Diameter (mm)</i>	0°C			20°C		
	<i>CH₄ (%)</i>	<i>N₂ (%)</i>	<i>O₂ (%)</i>	<i>CH₄ (%)</i>	<i>N₂ (%)</i>	<i>O₂ (%)</i>
1	53.0	37.8	8.4	56.2	29.7	13.5
2	84.3	12.2	3.3	83.3	10.8	5.7
4	93.3	5.1	1.5	92.2	5.0	2.7
10	97.9	1.6	0.5	97.5	1.6	0.9

Chapter 3: Implications of δD_{CH_4} from Alaskan thermokarst lakes for past and present atmospheric CH_4 budgets²

Abstract

Thermokarst lakes are thought to have been a major source of atmospheric methane (CH_4) during the early Holocene, when the climate was warmer and wetter than today (Walter et al. 2007a). Future warming in the Arctic may once again accelerate the thermokarst lake cycle, leading to enhanced CH_4 emissions as the large amount of C contained in permafrost (1466 Gt) is processed by microbes upon thaw (Walter et al. 2007b, Tarnocai et al. 2009). The low δD signature of CH_4 from Siberian thermokarst lakes was shown to be consistent with ice core records of δD_{CH_4} depletion when northern sources of atmospheric CH_4 increased rapidly 11-9 ka (Walter et al. 2007a, Sowers 2009). We show here that methanogens in close proximity to thermokarst activity in interior Alaska also utilized pore water derived from melted permafrost ice as a hydrogen source, and that the δD of evolved CH_4 reflected the δD of ancient precipitation that was incorporated into permafrost during ice wedge formation. δD_{CH_4} values from Alaskan thermokarst lakes were found to be less-depleted than δD_{CH_4} values from Siberian lakes because of differences in palaeoclimate between the two locations. Thus, contributions of thermokarst lakes to past atmospheric CH_4 concentrations based upon comparison of Siberian δD_{CH_4} values to palaeoisotopic records were likely higher than previously thought. δD_{CH_4} , $\delta^{13}C_{CH_4}$, and $\delta^{14}C_{CH_4}$ isotopic values of contemporary interior Alaska thermokarst lake CH_4 emissions reported in this study differ from other bacterial CH_4 sources (e.g. northern wetlands and Siberian lakes). This knowledge can improve estimates of thermokarst lakes contributions to the global atmospheric CH_4 budget of the past and present.

3.1 Introduction

Thermokarst lakes are thought to have been a major source of atmospheric methane

² Brosius LS, Walter Anthony KM. In preparation for publication in Biogeoscience.

during the early Holocene (Walter et al. 2007a), when western Arctic climate was warmer and wetter than today (Kaufman et al. 2004). Future warming in the Arctic may once again accelerate the thermokarst lake cycle, leading to enhanced CH₄ emissions as the large amount of C contained in permafrost (1466 Gt, Tarnocai et al. 2009) is processed by microbes upon thaw (Walter et al. 2007b). Researchers posit that amplification of thermokarst lake CH₄ emissions via lake formation and expansion may have contributed to a rise in atmospheric methane concentration (AMC) during the Younger Dryas-Preboreal transition (YD-PB) 9,000-12,000 years ago (Walter et al. 2007a). This theory is based on contemporary observations of thermokarst lake ebullition dynamics, incubations of permafrost organic matter (OM), and paleoecological reconstructions of thermokarst lake extent during the late Pleistocene (Walter et al. 2007a).

By constraining the isotopic composition of contemporary CH₄ emissions from northern lakes and understanding the processes that control these isotope values, we can more accurately assess the feasibility of this argument. Comparison of δD , $\delta^{13}C$, and $\delta^{14}C$ values of palaeoatmospheric CH₄, extracted from Greenland ice cores (GISP & GISP2) and the Pakitsoq ice exposure (Schaefer et al. 2006, Sowers 2006, 2009, Petrenko et al. 2009), with contemporary thermokarst lake bubble isotope values could clarify the role of thermokarst lake CH₄ in climate shifts during the YD-PB and during earlier deglaciations. Walter et al. (2007a) hypothesized that the low δD signature of CH₄ from Siberian thermokarst lakes was consistent with the ice core record of low δD_{CH_4} when northern sources of atmospheric CH₄ increased rapidly 11.6 thousand years ago (11.6 ka). However, Siberia was likely only one region in which thermokarst lakes formed and/or expanded and emitted CH₄ during this time. According to the Global Lakes and Wetland Database, 73% of the lakes northwards of 45.5N latitude occur in permafrost (Smith et al. 2007). While not all lakes within the permafrost zone are of thermokarst origin (Smith et al. 2007, Jorgenson & Shur 2007), it is very likely that thermokarst dynamics play an important role in many lake systems occurring in a wide variety of permafrost types and

climate regimes (Burn & Smith et al. 1990, Smith et al. 2007, Jorgenson & Shur 2007, Arp & Jones 2009). Thus, an interpretation of the palaeoisotopic record based upon the isotope values of CH₄ emitted only from Siberian lakes may be limited in scope and accuracy.

Isotopic analysis can be a useful tool for investigating controls over CH₄ production and cycling in lakes. Specifically, δD_{CH_4} can be used to identify H contributions to CH₄ production in cases where methanogens could gain protons from different water sources with different δD signatures. Methane produced by acetate-fermenting microbes gains three H atoms from acetate (transferred intact as a methyl group) and a single H from environmental water. In contrast, labeling experiments using deuterated H₂O demonstrated that CO₂-reducing methanogens derive all four H atoms from environmental water (Daniels et al. 1980). Other biochemical studies (Schworer et al. 1993, Schleucher et al. 1994, Klein et al. 1995) suggest that at least one H from H₂ may be added during CO₂ reduction, but δD of environmental water still dominates δD_{CH_4} signatures (Valentine et al. 2004, Chanton et al. 2006), possibly because of H₂O/H₂ equilibration prior to H addition (Valentine et al. 2004). Hence, evolved CH₄ should carry with it the signature of its source water, if CH₄ production occurs primarily by CO₂ reduction. With knowledge about the methanogenic pathway of CH₄ production in arctic lakes, it is possible to constrain contributions of different environmental water sources to seep methane production. In ice-rich permafrost regions, potential water sources include surface water, and melt of ancient ice in conjunction with permafrost thaw.

To understand the contribution of lakes to the global atmospheric CH₄ budget throughout the Holocene and during previous interglacials, we need to take into consideration the variability of δD values of permafrost melt water that may be incorporated into CH₄ emitted from lakes. δD values of ice wedges reflect the isotope values of winter and spring precipitation that fell during the time of ice wedge formation, which in turn reflect contemporaneous winter climate conditions (Mackay 1983, Meyer et al. 2002a, Meyer et

al. 2010) that likely varied by region due to differences in circulation patterns, continentality and temperature. Significant fractionation occurs as moisture-filled air masses move across continents. Fractionation results from the rain-out effect described by the Rayleigh-distillation model (Dansgaard 1964). Because of this effect, vapor reaching NE Siberia via the Westerlies today is δD -depleted. Conditions of extreme continentality when greater continental shelf area was exposed at a time of 120 m-lower sea level (Svedsen et al. 1999), and cold winter temperatures in Siberia during the late Pleistocene (Kokorowski et al. 2008) resulted in severely depleted permafrost ice: northern Siberia, -220 to -250‰ (Meyer et al. 2002a, Meyer et al. 2002b), northeast Siberia (Yakutia), -230‰ (Popp et al. 2006). Permafrost that formed under warmer, less continental conditions evidenced by palynological climate proxies in interior Alaska and NW Canada (Kokorowski et al. 2008) contains heavier water: -164 to -225‰, Dawson City, YT (Kotler & Burn 2000); -193 to -224‰, Barrow AK (Meyer et al. 2010); -180 to -210‰, Vault Creek, Fairbanks region, AK (Meyer et al. 2008).

Walter et al. (2008) found CH_4 bubbling from Siberian lakes to be significantly δD -depleted ($-392 \pm 8\text{‰}$, $n=40$), with minimum values as low as -420‰. They attributed these values to δD -depleted winter precipitation produced and incorporated into permafrost ice during syngenetic formation under extreme continental conditions during the late Pleistocene. Given the heavier δD values of North American Pleistocene-aged ice wedges we hypothesized that CH_4 produced in Alaskan thermokarst lakes may have a heavier δD signature than CH_4 produced in Siberian lakes. Only Siberian lakes were accounted for in Walter et al. 2007a. Here we suggest that thermokarst lakes that formed in other permafrost regions, outside of Siberian yedoma, may have contributed additionally to past AMC, since thermokarst lakes were present throughout Alaska, Canada and parts of Europe. The potential overlap in higher δD_{CH_4} values between non-Siberian thermokarst lakes and boreal wetlands may have prevented distinction between these two sources in past modeling efforts. We combine knowledge of the extent of thermokarst lake formation, magnitude of CH_4 release from lakes, and region-specific

δD_{CH_4} values from non-Siberian thermokarst lakes to estimate the increase in contribution of thawing permafrost to atmospheric methane during the early Holocene.

3.2 Methods

Study site

We observed a shallow thermokarst lake near Fairbanks, Alaska. Goldstream Lake (64.92°N, 147.85°W, elev. 177 m) (hereafter: Goldstream) is a typical thermokarst lake in interior Alaska (Chapter 1). It is 2.2 m deep and is located in Goldstream Valley, a region of discontinuous permafrost north of Fairbanks. Goldstream's longitudinal lake shores consist of wide (2-5 m), emergent grass and cattail (*Typha spp.*) bands. Large ground fissures (caused by freeze-thaw cycling), freshly eroded surfaces and inundated vegetation on the eastern lake margin indicate acute thermokarst activity eroding loess permafrost. On the lake bottom, an extremely thin (< 5 cm) modern organic sediment layer, composed mainly of locally dominant *Ceratophyllum demersum* detritus, overlaid a thick package of dense silt. This sediment was interpreted as thawed Pleistocene-aged retransported loess, commonly found in area valley bottoms (Péwé 1975), which was dated 14,860-56,900 years before present (y.b.p.) near Fairbanks (Péwé 1952) and 5,320-52,790 y.b.p. at Vault Creek, 35 km away (Meyer et al. 2008). Lake sediment dating by ^{210}Pb revealed a young age of less than 100 years for Goldstream Lake (Turner 2009, *Sr. honors thesis*).

Sample collection and analysis

We collected gas samples and made flux measurements on bubbling seeps using umbrella-style traps from Walter et al. (2006). Five seeps were sampled every 3-12 days from March through October 2008, while 1-3 samples were collected from 13 additional seeps in October 2008. We stored samples at 4°C in clear glass serum bottles sealed with butyl rubber stoppers and aluminum crimp caps until analysis. We determined the composition of each sample using a gas chromatograph (Shimadzu GC-2014) outfitted with both thermal conductance and flame ionization detectors (precision: <1%). We

measured gas phase $\delta^{13}\text{C}_{\text{CH}_4}$ and $\delta^{13}\text{C}_{\text{CO}_2}$ using a paired GC and Delta V IRMS at Florida State University; and measured $\delta\text{D}_{\text{CH}_4}$ at the National High Magnetic Field Laboratory in Tallahassee, FL using a similar setup (instrument precision: 3‰). We marked sampling locations using a Trimble GPS unit, then calculated the distance of each bubbling source from the eastern thermokarst margin using ArcMap software.

Using winter lake ice as a platform, we recovered three intact 0.55-0.95 m sediment cores in 5.5 cm diameter polycarbonate tubes from each lake using a piston hammer corer (Aquatic Instruments) (Chapter 2, Figure 2.1). We sampled pore water from two of the sediment cores at either 2 or 9 cm intervals by drilling holes in the core casings and inserting Rhizone pore water sippers attached to 60 mL syringes, which, set to pull a vacuum for 1.5 hr, yielded 8-19 ml samples. We sampled permafrost adjacent to the lake shores by chiseling frozen ground >10 cm below the bottom of the seasonal active layer at the bottom of soil pits when active layer depth was greatest (72 cm, late September 2008), then extracted permafrost water by letting airtight bags of permafrost thaw completely. We collected lake water samples by hand at the surface and at 2.0 m near the lake bottom using a Van Dorn bottle in July and October 2008. All water samples were transferred to 3 ml glass vials, capped shut with no headspace, and stored in a refrigerator prior to analysis for δD and $\delta^{18}\text{O}$. A CTC Analytics A200SE liquid autosampler injected 0.2 ul of each sample into an on-line pyrolysis thermochemical reactor elemental analyzer (Finnigan ThermoQuest TCEA) coupled to a continuous flow IRMS (Finnigan MAT Delta Plus XL) for isotopic analysis. Instrument precision was 1‰ for D and <0.3‰ for O.

Calculations

We used α_{C} calculations and Whiticar's proxy ($1.055 < \alpha_{\text{C}} < 1.090 = \text{CO}_2$ reduction, $1.040 < \alpha_{\text{C}} < 1.055 = \text{acetate fermentation}$, Whiticar 1999) (see Chapter 2 Methods) to determine the proportion of CH_4 produced in our study lake via each methanogenic pathway. Based on the production pathway we determined, we were able to identify the

proportion of H gained by methanogens from multiple water sources. Potential sources of water in thermokarst lake environments include modern surface water and permafrost melt water. Contributions of each were identified using a mixing model approach. We assumed that microbial consortia operate under non H-limited conditions, and that the corresponding average microbial fractionation factor (ϵ_h) associated with CO₂ reduction was -160‰ (Schoell 1980, Whiticar 1999, Valentine et al. 2004). The following equations were used to determine the fraction of H derived from lake (L) and permafrost (P) water sources:

$$\delta D_{CH_4} = f_L (\delta D_{Lake\ H_2O} - \epsilon_h) + f_P (\delta D_{Perm\ H_2O} - \epsilon_h) \quad (3.1)$$

$$1 = f_L + f_P \quad (3.2)$$

3.3 Results

Bubble isotopic and elemental composition

Average values of $\delta^{13}C_{CH_4}$, δD_{CH_4} and $\delta^{13}C_{CO_2}$ in bubbles were $-67.7 \pm 5.7\%$, $-333 \pm 19\%$, and $-16.1 \pm 2.1\%$, respectively (Chapter 2, Table 2.2). The isotopic composition of gases collected from the same seeps was not statistically different over time, although spatial patterns in isotopic composition did emerge. Seep δD_{CH_4} differed along a distance gradient away from the thermokarst shore. Seeps furthest away from the thermokarst shore had the relatively highest δD_{CH_4} values (Figure 3.1).

Water isotopes and H mixing model

Isotopic values of water sources were well constrained. δD and $\delta^{18}O$ analysis of surface and permafrost water (interstitial and segregated ice) revealed significant separation. Average δD values of permafrost water and lake water were -186% (n=1) and $-134 \pm 2\%$, (n=4), respectively (Table 3.1). The δD value of permafrost ice extracted from Goldstream's shore was similar to the values reported by Meyer et al. (2008) for Pleistocene-aged ice wedges (-190 to -210%) in the Vault Creek Tunnel, 35 km from our site. Lake surface water samples taken in June and October varied in δD by a maximum of 4% . Water sampled at the lake surface and from the hypolimnion at the end of June

when thermal stratification was near its maximum also showed little evaporative D-enrichment ($< 2\text{‰}$). δD variation of lake water over time and between different water depths was ten times less than the separation in δD of permafrost and lake water.

CO_2 reduction dominated CH_4 production in Goldstream Lake and has been found to dominate in low pH, ombrotrophic bogs elsewhere in Alaska (Duddleston et al. 2002, Rooney-Varga et al. 2007), and in Siberian and other Alaskan lakes (Walter et al. 2008). Chanton et al. (2006), however, noted a mixture of production pathways in a variety of Alaskan wetlands spanning a latitudinal gradient. α_{C} calculations in this study showed that 88% by volume of CH_4 emitted from Goldstream was produced via CO_2 reduction. For this reason, we were able to utilize equations 3.1 and 3.2 to determine mixing ratios of H from two potential sources: permafrost water and lake water.

Our mixing model results showed that permafrost melt water was a significant source of H to methanogens in Goldstream Lake. We discovered that within 5 m of Goldstream's eastern thermokarst margin, methanogens derived 100% of their H from permafrost. With distance from shore, the contribution of permafrost melt water to methanogenesis declined. 10-30 m away from the margin, permafrost melt water contributed 52-88% of H atoms to seep CH_4 . Only 24-52% of seep CH_4 -H came from permafrost 40-80 m away from shore, and most seeps located along the margin opposite the thermokarst shore (100-150 m away) emitted only CH_4 containing H derived from lake water (Figure 3.2). These results imply that the melting of permafrost ice beneath and around lake margins supplies hydrogen to methanogens. This was especially evident near the thermokarst margin of Goldstream where progressing thaw (50 y.b.p.- present) has liberated permafrost water that was incorporated with high efficiency into CH_4 . The availability of permafrost melt water as an H source to methanogens near the thermokarst margin was also evidenced by the δD values of pore water samples we extracted from sediment cores. Pore water contained in a core we took from near the thermokarst margin (Core C) was more δD -depleted (mean \pm std, $-152 \pm 4\text{‰}$, $n=10$) than pore water extracted from a lake center core ($-142 \pm 1\text{‰}$, $n=12$, Core A, Table 3.1), suggesting that more permafrost melt

water was incorporated into sediment pore waters near the thermokarst margin than in the lake center.

3.4 Discussion

Prior studies have suggested that thermokarst lake CH₄ played an important role in YD-PB AMC shifts (Walter et al. 2007a). $\delta^{13}\text{C}_{\text{CH}_4}$, $\delta\text{D}_{\text{CH}_4}$ and $\delta^{14}\text{C}_{\text{CH}_4}$ isotope data are consistent with this argument. Results from Sowers (2009) show a mean decrease in $\delta^{13}\text{C}$ of 1.9 ‰ and a slight decrease in δD (~3‰) of northern hemisphere CH₄ between 10.5 ka and 4 ka. Possible explanations put forth by the author were: 1) an increase in arctic lake and wetland emissions; 2) a gradual increase in C₃/C₄ plant ratios where CH₄ is produced and emitted; or 3) a proportional increase in dominance of the CO₂-reduction pathway. However, the predicted decline in δD for the first scenario is too great given measured $\delta\text{D}_{\text{CH}_4}$ values from Siberian thermokarst lakes (Sowers 2009). While this assessment is sound, we suggest that CH₄ emitted from Alaskan lakes is not as D-depleted as CH₄ bubbling from Siberian lakes, and that both past and present water sources influence the $\delta\text{D}_{\text{CH}_4}$ of bubbling. $\delta\text{D}_{\text{CH}_4}$ values of bubbling from seven Alaskan lakes sampled in 2001, (Walter et al. 2008) and from our interior study lake together averaged $-325 \pm 28\text{‰}$. These data, when combined with isotopic data from Siberian thermokarst lake CH₄ bubbling, match palaeoisotopic records more closely and suggest that thermokarst lakes may have been an even greater source of atmospheric methane during the YD-PB than previously suggested.

Finally, constraining isotopic values of CH₄ bubbling from thermokarst lakes is important for identifying sources to present day AMC and for assessing the vulnerability of these sources to change with projected climate warming. Methane generated from biomass burning, natural gas and coal is distinctly different in its isotopic signature ($\delta^{13}\text{C}$, 24.6 to -44.0 ‰; δD , -140 to -225‰). Marine hydrate CH₄ is also set widely apart from other sources by a combination of $\delta^{13}\text{C}$ depletion (-62.5‰) and δD enrichment (-190‰) (Whiticar & Schaefer 2007). The isotopic values of a variety of other bacterial sources,

such as wetlands, rice paddies, termites and lakes, fall within a similar range, making distinction of individual sources difficult. However, we show here that interior Alaskan thermokarst lake CH₄ emissions differ isotopically from: Alaskan wetland sources, which have younger ¹⁴C ages and similar δD and δ¹³C values (Chanton et al. 2006); from Siberian thermokarst lakes, which are more δD-depleted and have similar ¹⁴C ages and δ¹³C ranges (Walter et al. 2008); and from temperate and tropical systems which have younger ¹⁴C ages, more enriched δD values and similar δ¹³C values (Whiticar & Schaefer 2007) (Figure 3.3). Given the range of isotopic values of potential AMC sources, knowledge of δD_{CH₄}, δ¹³C_{CH₄} and δ¹⁴C_{CH₄} values from Alaskan thermokarst lakes may improve modeling efforts to identify drivers of past and present climate.

3.5 Conclusion

δD_{CH₄}, δ¹³C_{CH₄}, and δ¹⁴C_{CH₄} isotopic values of typical interior Alaska thermokarst lake CH₄ emissions reported in this study are different from the isotopic values of northern wetland and Siberian thermokarst lake emissions, and can help constrain contributions of thermokarst lakes to the global atmospheric CH₄ budget of the past and present.

Methanogens in close proximity to thermokarst activity utilize pore water derived from melted permafrost ice as a hydrogen source and reflect regionally varying δD values of precipitation incorporated into permafrost at the time of its formation. δD_{CH₄} values from Alaskan thermokarst lakes are less-depleted than δD_{CH₄} values from Siberian lakes because of differences in palaeoclimate between the two locations. Thus, prior estimates of thermokarst lake contributions to past AMC based upon comparison of Siberian δD_{CH₄} values to palaeoisotopic records were likely too low. The results of this study suggest that contributions from thermokarst lakes around the Arctic could have been greater to atmospheric methane throughout the Holocene than has been previously reported.

Acknowledgements

Thanks to Jeff Chanton and Claire Langford at Florida State University for their assistance with δD isotopic analysis of CH₄.

References

- Arp CD, Jones BM (2009) Geography of Alaska lake districts: Identification, description, and analysis of lake-rich regions of a diverse and dynamic state. U.S. Geological Survey Scientific Investigations Report 2008–5215. 40 pp.
- Beckmann M, Llyod D (2001) Mass spectrometric monitoring of gases (CO₂, CH₄, O₂) in a mesotrophic peat core from Kopparas Mire, Sweden. *Global Change Biol* 7:171-180.
- Burn CR, Smith MW (1990) Development of thermokarst lakes during the Holocene at sites near Mayo, Yukon territory. *Permafrost Periglac* 1:161-175.
- Chanton JP, Fields D, Hines ME (2006) Controls on the hydrogen isotopic composition of biogenic methane from high-latitude terrestrial wetlands. *J Geophys Res* 111 DOI 10.1029/2005JG000134.
- Daniels L, Fulton G, Spencer RW, Orme-Johnson WH (1980) Origin of hydrogen in methane produced by *Methanobacterium thermoautotrophicum*. *J Bacteriol* 141:694-698.
- Dansgaard W (1964) Stable isotopes in precipitation. *Tellus* 16:436-468.
- Duddleston KN, Kinney MA, Keine RP, Hines ME (2002) Anaerobic microbial biogeochemistry on a northern bog: acetate as a dominant metabolic end product. *Global Biogeochem* 16. DOI 10.1029/201GB001402.
- Jorgenson MT, Shur Y (2007) Evolution of lakes and basins in northern Alaska and discussion of the thaw lake cycle. *J Geophys Res* 112 DOI 10.1029/2006JF000531
- Kaufman DS, Ager TA, Anderson NJ, Anderson PM, Andrews JT, Bartlein PJ, Brubaker LB, Coats LL, Cwynar LC, Duvall ML, Dyke AS, Edwards ME, Eisner WR, Gajewski K, Geirsdottir A, Hu FS, Jennings AE, Kaplan MR, Kerwin MW, Lozhkin AV, MacDonald GM, Miller GH, Mock CJ, Oswald WW, Otto-Bliesner BL, Porinchu DF, Ruhland K, Smol JP, Steig EJ, Wolfe BB (2004) Holocene thermal maximum in the western Arctic (0° to 180°W). *Quat Sci Rev* 23:529–560.
- Klein AR, Fernandez VM, Thauer RK (1995) H₂-forming N⁵, N¹⁰-methylenetetrahydromethanopterin dehydrogenase: Mechanism of H₂ formation analyzed using hydrogen isotopes. *FEMS Lett* 368:203-206.
- Kokorowski HD, Anderson PM, Mock CJ, Lozhkin AV (2008) A re-evaluation and spatial analysis of evidence for a Younger Dryas climatic reversal in Beringia. *Quat Sci Rev* 27:1710–1722.

Kotler E, Burn CR (2000) Cryostratigraphy of the Klondike “muck” deposits west-central Yukon Territory. *Can J Earth Sci* 37:849-861.

Mackay JR (1983) Oxygen isotopic variation in permafrost, Tuktoyaktuk peninsula area, Northwest Territories. *Pap. Geol Surv Can.* 18:67-74.

Meyer H, Dereviagin AY, Siegert C, Hubberten HW (2002a) Paleoclimate studies on Bykovsky Peninsula, North Siberia – hydrogen and oxygen isotopes in ground ice. *Polarforschung* 70:37-51.

Meyer H, Dereviagin A, Siegert C, Schirrmeister L, Hubberten HW (2002b) Palaeoclimate reconstruction of Big Lyakhavsky Island, North Siberia – hydrogen and oxygen isotopes in ice wedges. *Permafrost Periglac* 13:91-105.

Meyer H, Yoshikawa K, Schirrmeister L, Andreev A (2008) The Vault Creek Tunnel (Fairbanks Region, Alaska): A late Quaternary palaeoenvironmental permafrost record. Ninth International Conference on Permafrost, Fairbanks, Alaska. 1191-1196.

Meyer H, Schirrmeister L, Yoshikawa K, Opel T, Wetterich S, Hubberten HW, Brown J (2010) Permafrost evidence for severe winter cooling during the Younger Dryas in northern Alaska. *Geophys Res Let* 37 DOI 10.1029/2009GL041013.

Petrenko VV, Smith AM, Brook EJ, Lowe D, Riedel K, Brailsford G, Hua Q, Schaefer H, Reeh N, Weiss RF, Etheridge D, Severinghaus JP (2009) $^{14}\text{CH}_4$ measurements in Greenland ice: investigating last glacial termination CH_4 sources. *Science* 324:506-508.

Péwé TL (1952) Geomorphology of the Fairbanks area, Alaska. Dissertation, Stanford University

Péwé TL (1975) Quaternary Geology of Alaska. United States Government Printing Office, Washington.

Popp S, Diekmann B, Meyer H, Siegert C, Syromyatnikov I, Hubberten HW (2006) Palaeoclimate signals as inferred from stable-isotope composition of ground ice in the Verkhoyansk Foreland, Central Yakutia. *Permafrost Periglac* 17:119-132.

Rooney-Varga JN, Giewat MW, Duddleston KN, Chanton JP, Hines ME (2007) Links between archaeal community structure, vegetation type and methanogenic pathway in Alaskan peatlands. *FEMS Microbiol Ecol* 60:240-251.

Schaefer H, Whiticar MJ, Brook EJ, Petrenko VV, Ferretti DF, Severinghaus JP (2006) Ice record of $\delta^{13}\text{C}$ for atmospheric CH_4 across the Younger Dryas-Preboreal Transition. *Science* 313:1110-1112.

- Schleucher J, Griesinger C, Schworer B, Thauer RK (1994) H₂-forming N⁵, N¹⁰-methylenetetrahydromethanopterin dehydrogenase from *Methanobacterium thermoautotrophicum* catalyzes a stereoselective hydride transfer as determined by 2-dimensional NMR-spectroscopy. *Biochem* 33:3986-3993.
- Schoell M (1980) The hydrogen and carbon isotopic composition of methane from natural gases of various origins. *Geochim Cosmochim Acta* 44:649-661.
- Schworer B, Fernandez VM, Zirngibl C, Thauer RK (1993) H₂-forming N⁵, N¹⁰-methylenetetrahydromethanopterin dehydrogenase from *Methanobacterium thermoautotrophicum*: Studies of the catalytic mechanism of H₂ formation using hydrogen isotopes. *Eur J Biochem*. 212:255-261.
- Smith LC, Sheng Y, MacDonald GM (2007) A first pan-Arctic assessment of the influence of glaciations, permafrost, topography and peatlands on northern hemisphere lake distribution. *Permafrost Periglac* 18:201-208.
- Sowers T (2006) Late Quaternary atmospheric CH₄ isotopic record suggests marine clathrates are stable. *Science* 311:838-840.
- Sowers T (2009) Atmospheric methane isotope records covering the Holocene period, *Quat Sci Rev* DOI 10.1016/j.quascirev.2009.05.023.
- Svedsen JJ, Astakhov VI, Bolshiyakov DYu, Demidov I, Dowdeswell JA, Gataullin V, Hjort C, Hubberten HW, Larsen E, Mangerud J, Melles M, Moeller P, Saarnisto M, Siegert MJ (1999) Maximum extent of the Eurasian ice sheets in the Barents and Kara Sea region during the Weichselian. *Boreas* 28: 234-242.
- Tarnocai C, Canadell JG, Schuur EAG, Kuhry P, Mazhitova G, Zimov S (2009) Soil organic carbon pools in the northern circumpolar permafrost region. *Global Biogeochem Cycles* 23 DOI 10.1029/2008GB003327.
- Turner H (2009) An investigation into the formation and evolution of two lakes in Fairbanks, AK. B.S. Sr. Honors Thesis, University of Southampton.
- Valentine DL, Chidthaisong A, Rice A, Reeburgh WS, Tyler SC (2004) Carbon and hydrogen isotope fractionation by moderately thermophilic methanogens. *Geochimica Cosmochim Acta* 68:1571-1590.
- Walter KM, Zimov SA, Chanton JP, Verbyla D, Chapin FS III (2006) Methane bubbling from siberian thaw lakes as a positive feedback to climate warming. *Nature* 443:71-75.
- Walter KM, Edwards ME, Grosse G, Zimov SA, Chapin FS III (2007a) Thermokarst lakes as a source of atmospheric CH₄ during the last deglaciation. *Science* 318:633-636.

Walter KM, Smith LC, Chapin FS III (2007b). Methane bubbling from northern lakes: present and future contribution to the global CH₄ budget. *Phil Trans R Soc Lond* 365:1657-1676.

Walter KM, Chanton JP, Chapin FS III, Schuur AG, Zimov SA (2008) Methane production and bubble emissions from arctic lakes: isotopic implications for source pathways and ages. *J Geophys Res* 113 DOI 10.1029/2007JG000569.

Whiticar MJ (1999) Carbon and hydrogen isotope systematic of bacterial formation and oxidation of CH₄. *Chem Geol* 161:291-31

Whiticar M, Schaefer H (2007) Contrasting past global tropospheric methane budgets with carbon and hydrogen isotope ratios in ice. *Phil Trans R Soc A* 365:1793-1828.

Figures

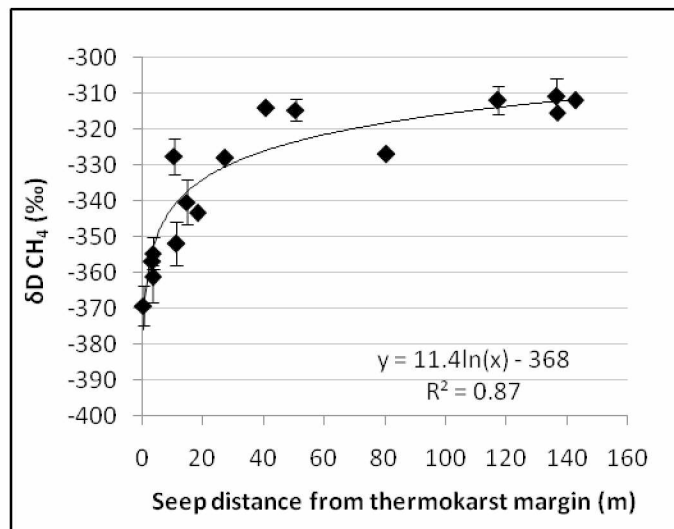


Figure 3.1: Seep CH₄ was more enriched in δD with increased distance from Goldstream Lake's thermokarst margin, indicating a reduction in H contributions from permafrost melt water and an increase in lake water H contributions.

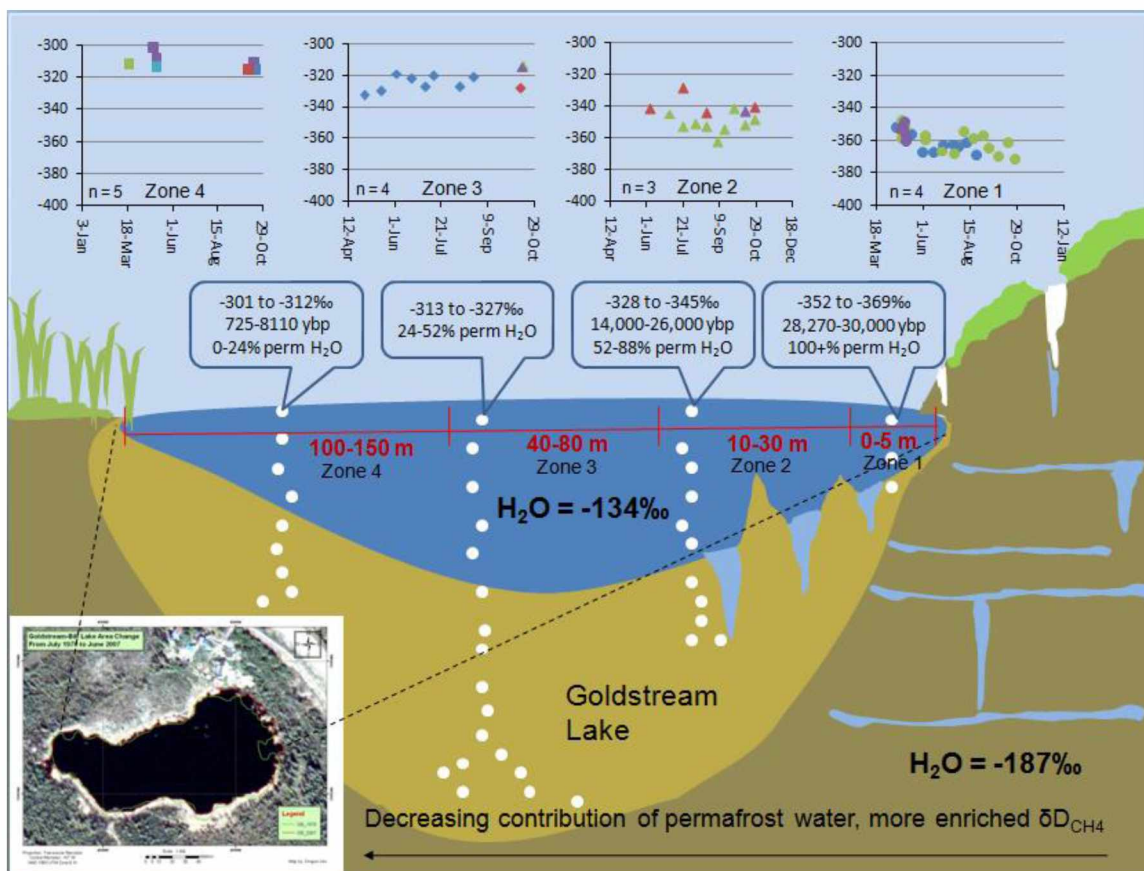


Figure 3.2: Schematic of Goldstream Lake showing varying H contributions of permafrost melt water by zone. Each zone is progressively further from the thermokarst margin and therefore receives less H input from permafrost thaw. The progressively younger CH₄ ages of bubbling from each zone also indicate a decline in ancient permafrost C contributions with distance from the thermokarst margin. Graphs above show the lack of distinctive seasonal variability in δD_{CH_4} . Different colored points represent different discrete seeps measured over time.

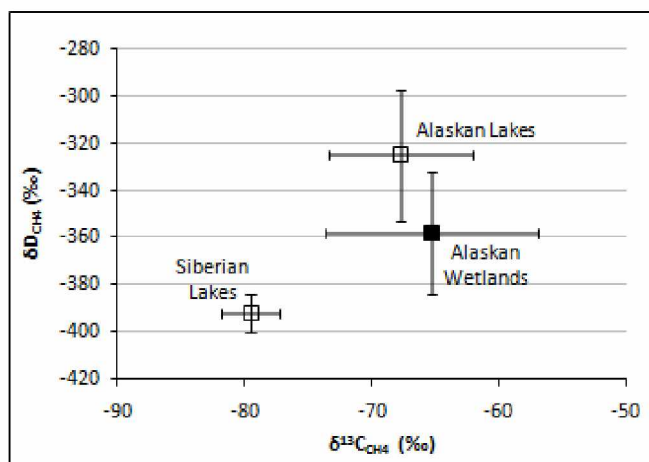


Figure 3.3: δD and $\delta^{13}\text{C}$ of CH_4 emissions from Siberian lakes (Walter et al. 2008, $n=40$), Alaskan wetlands (Chanton et al. 2006, $n=26$) and Alaskan lakes (Walter et al 2008, this study, $n=26$) plotted in isotopic space. Wetland and thermokarst lake emissions differ in their ^{14}C -depletion. Open squares indicate strong ^{14}C -depletion and closed squares indicate modern ^{14}C signatures. X- and Y-error bars show standard deviations, not absolute ranges.

Tables

Table 3.1: Source water isotopic composition

<i>Object</i>	<i>Depth (m)</i>	<i>δD (‰)</i>	<i>$\delta^{18}O$ (‰)</i>
Lake H ₂ O (25 Jun 08)	0.01	-137	-14.70
Lake H ₂ O (25 Jun 08)	2.0	-136	-14.95
Lake H ₂ O (12 Oct 08)	0.01	-133	-15.28
Lake H ₂ O (12 Oct 08)	2.0	-132	-15.16
Sediment Pore H ₂ O (A) (n =12)	-	-142 ± 1	-15.3 ± 0.2
Sediment Pore H ₂ O (C) (n =10)	-	-152 ± 4	-18.4 ± 1.1
Permafrost H ₂ O (n =1)	-	-186	-24.1

Appendix

Fickian diffusion equation: $J_s = - \phi D_s \partial C / \partial x$ (A.1)

ϕ = porosity (assumed to be 0.56 for silt loam)

D_s = the diffusion coefficient of N₂ through water ($1.6 \times 10^{-4} \text{ cm}^2 \text{ s}^{-1}$)

$\partial C / \partial x$ = the concentration gradient of N₂ over a sediment path length of 40 cm

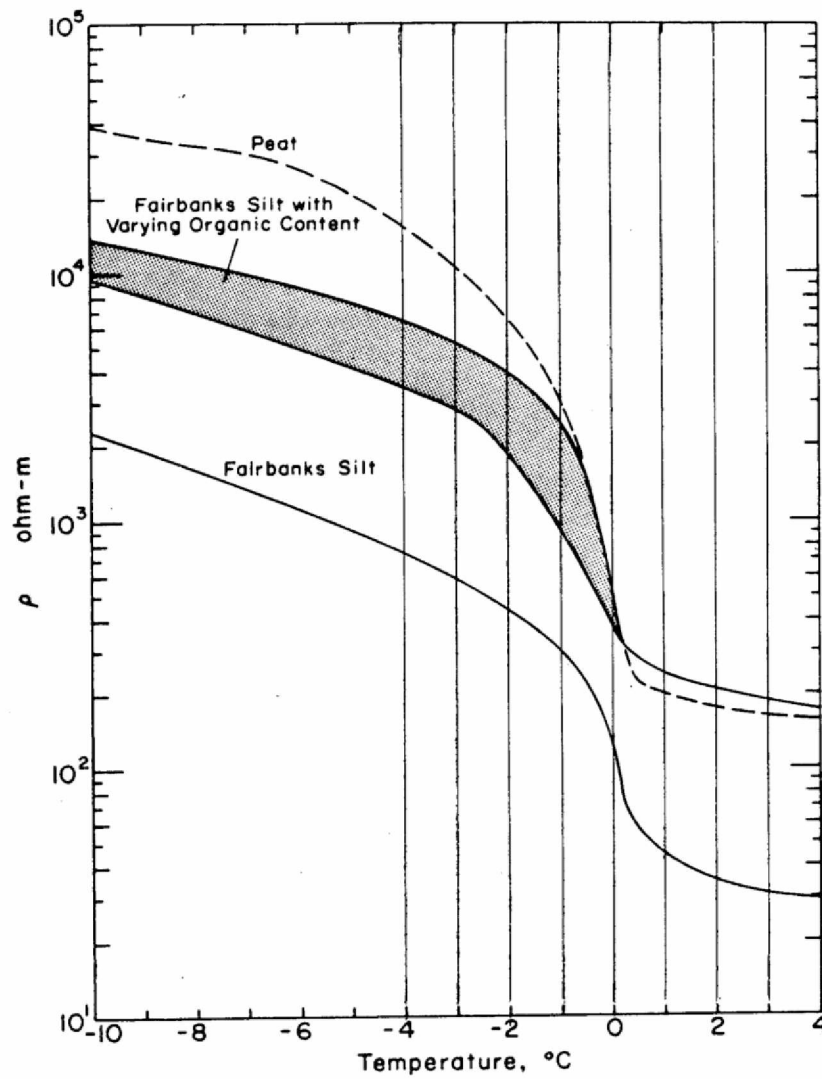


Figure A.1: The measured resistivity of Fairbanks silt is strongly dependant on temperature and the presence of liquid water even below zero (from Hoekstra et al. 1973).

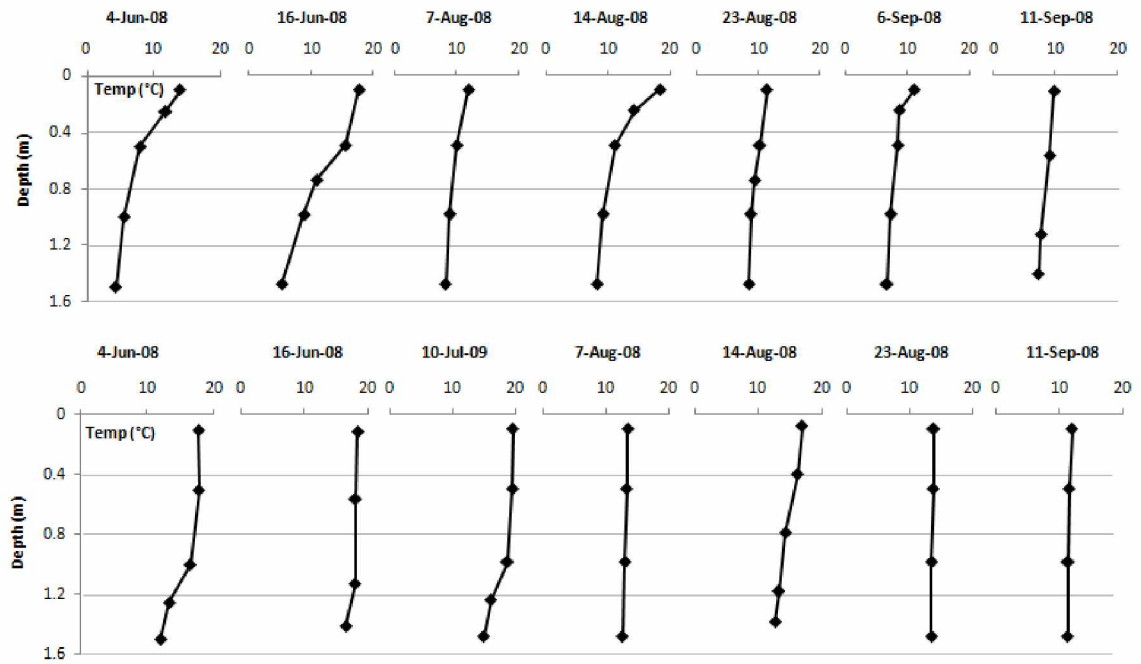


Figure A.2: Lake temperature profiles spanning the majority of the open water season 2008 for Killarney (top), and Goldstream (bottom).

Table A.1: Explanation of whole lake bubbling estimates based on ice-bubble survey transects in Chapter 2.

<i>Class</i>	<i>Killarney</i>			<i>Goldstream</i>		
	<i>Flux (mg CH₄ d⁻¹)</i>	<i>Flux (ml gas d⁻¹)</i>	<i>n</i>	<i>Flux (mg CH₄ d⁻¹)</i>	<i>Flux (ml gas d⁻¹)</i>	<i>n</i>
A	15 ± 12	37 ± 29	8	62	84	1
B	80 ± 16	151 ± 30	4	224 ± 119	209 ± 111	3
C	432 ± 268	800 ± 496	4	825 ± 348*	-	0
HS	1750 ± 356	3914 ± 796	7	5282 ± 3881	4819 ± 3541	8

* This value from Walter et al. 2008. No class C seeps were reliably measured on Goldstream Lake in this study.

To determine rates of whole lake bubbling I used data from bubbling that our lab group surveyed in 2007 and 2009. For the Killarney estimate, I averaged all six transects. For the Goldstream estimate I split the lake in half and averaged bubbling rates for the two halves. Our 2009 surveys were conducted along perpendicular transects to the thermokarst margin, thus capturing variation from the thermokarst margin to the lake center. I averaged our 2009 transects to get a representative estimate for one half, and averaged data from two lake center transects (2007) for the other half. I scaled up using measured flux and concentration data from each lake as follows. The flux rates in the table below take into account the variation in CH₄ between seep type and lake.

Table A.2: Goldstream Lake hydrological data taken during the open water season 2008.

<i>Date</i>	<i>Depth (m)</i>	<i>Temp (°C)</i>	<i>Cond (µS)</i>	<i>DO (mg/L)</i>	<i>pH</i>	<i>Sal</i>	<i>DO (% sat)</i>	<i>ORP (mV)</i>
4-Jun-08	0.1	17.8	0.058	6.60	8.1	0.28	80	311
4-Jun-08	0.5	17.8	0.581	6.44	8.1	0.28	80.3	310
4-Jun-08	1	14.8	0.681	1.40	7.8	0.31	17.9	299
4-Jun-08	1.5	10.7	1.274	0.63	7.7	0.63	6.1	291
16-Jun-08	0.1	18.3	0.693	5.12	7.2	0.33	63.8	419
16-Jun-08	0.5	18.0	0.688	5.14	8.0	0.33	63.1	415
16-Jun-08	1	18.0	0.685	5.04	8.0	0.33	62.8	411
16-Jun-08	1.25	16.4	0.979	0.69	7.8	0.49	8.7	380
10-Jul-08	0.1	19.6	0.665	6.14	8.0	0.34	67.4	374
10-Jul-08	0.5	19.4	0.665	5.99	7.9	0.34	65.5	371
10-Jul-08	1	18.7	0.693	5.35	7.5	0.36	57.7	380
10-Jul-08	1.25	16.1	0.997	3.20	7.3	0.52	32.7	200
10-Jul-08	1.5	14.9	1.045	2.22	7.3	0.55	22.1	117
7-Aug-08	0.1	13.4	0.725	9.10	8.2	0.35	84.90	495
7-Aug-08	0.5	13.3	0.726	8.71	8.2	0.35	83.40	496
7-Aug-08	1	13.0	0.726	8.30	8.1	0.35	78.00	498
7-Aug-08	1.5	12.6	0.916	1.45	7.7	0.48	27.50	490
14-Aug-08	0.1	17.0	0.713	11.15	8.5	0.35	115.60	354
14-Aug-08	0.5	16.2	0.717	10.69	8.4	0.35	107.20	359
14-Aug-08	1	14.2	0.722	7.86	8.3	0.35	75.50	366
14-Aug-08	1.5	13.2	0.787	2.49	8.0	0.37	22.00	373
14-Aug-08	1.75	12.7	0.855	1.24	7.9	0.42	10.30	247
23-Aug-08	0.1	13.8	0.743	7.13	8.1	0.36	69.60	366
23-Aug-08	0.5	13.8	0.743	6.87	8.1	0.36	66.40	364
23-Aug-08	1	13.5	0.753	6.02	8.1	0.36	58.40	364
23-Aug-08	1.5	13.5	0.794	2.58	7.9	0.37	27.00	276
6-Sep-08	0.1	12.2	0.784	6.40	8.0	0.38	59.00	305
6-Sep-08	0.5	11.7	0.784	6.22	8.0	0.38	57.00	305
6-Sep-08	1	11.6	0.784	5.99	7.9	0.38	54.40	306
6-Sep-08	1.5	11.6	0.785	4.48	7.9	0.38	32.10	307
11-Sep-08	0.1	12.0	0.790	5.84	8.0	0.38	54.30	321
11-Sep-08	0.5	11.5	0.791	5.34	8.0	0.38	49.50	324
11-Sep-08	1	11.3	0.795	4.88	7.9	0.38	45.10	327
11-Sep-08	1.5	11.3	0.801	3.09	7.9	0.39	28.50	329

Table A.3: Killarney Lake hydrological data taken during the open water season

<i>Date</i>	<i>Depth (m)</i>	<i>Temp (°C)</i>	<i>Cond (µS)</i>	<i>DO (mg/L)</i>	<i>pH</i>	<i>Sal</i>	<i>DO (% sat)</i>	<i>ORP (mV)</i>
4-Jun-08	0.1	14.0	0.311	9.43	7.7	0.15	105.6	397
4-Jun-08	0.25	11.8	0.318	8.23	7.8	0.15	92.1	287
4-Jun-08	0.5	7.9	0.314	6.14	7.7	0.15	63.4	290
4-Jun-08	1	5.5	0.335	3.05	7.7	0.15	27.7	288
4-Jun-08	1.5	4.3	0.458	0.40	7.7	0.23	3.5	284
16-Jun-08	0.1	17.7	0.340	11.80	8.1	0.16	144.6	390
16-Jun-08	0.5	15.5	0.336	18.02	8.3	0.16	199.7	388
16-Jun-08	0.75	10.9	0.340	15.20	8.2	0.16	167.5	297
16-Jun-08	1	8.9	0.340	11.95	7.7	0.16	120	310
16-Jun-08	1.5	5.3	0.530	4.07	7.5	0.25	30.4	282
7-Aug-08	0.1	11.9	0.161	7.56	7.7	0.08	66.8	431
7-Aug-08	0.5	10.1	0.164	6.73	7.7	0.08	59.1	435
7-Aug-08	1	8.9	0.190	5.13	7.7	0.09	43.8	441
7-Aug-08	1.5	8.2	0.474	3.49	7.7	0.21	24.1	440
14-Aug-08	0.1	18.4	0.177	6.15	7.8	0.09	64.3	446
14-Aug-08	0.25	14.2	0.173	5.05	7.9	0.08	50.5	439
14-Aug-08	0.5	11.2	0.175	6.22	7.8	0.08	54.8	460
14-Aug-08	1	9.3	0.372	2.11	7.8	0.15	18.2	472
14-Aug-08	1.5	8.3	0.503	1.87	7.8	0.25	10.8	449
23-Aug-08	0.1	11.5	0.282	7.60	7.9	0.13	69.2	287
23-Aug-08	0.5	10.4	0.284	5.02	7.9	0.13	49.2	291
23-Aug-08	0.75	9.4	0.283	7.32	7.9	0.13	64.3	288
23-Aug-08	1	8.9	0.302	4.62	7.8	0.14	38.7	292
23-Aug-08	1.5	8.5	0.483	3.87	7.7	0.23	14.9	295
6-Sep-08	0.1	11.2	0.347	16.54	8.1	0.16	141	291
6-Sep-08	0.25	8.8	0.347	13.48	8.0	0.16	117.3	296
6-Sep-08	0.5	8.5	0.347	12.00	7.9	0.16	102.6	296
6-Sep-08	1	7.3	0.365	3.59	7.8	0.17	30.2	302
6-Sep-08	1.5	6.8	0.382	1.31	7.6	0.18	11.3	215
11-Sep-08	0.1	9.9	0.366	14.59	8.1	0.17	129.3	328
11-Sep-08	0.5	9.1	0.367	12.26	8.0	0.17	106.6	334
11-Sep-08	1	7.8	0.381	4.40	7.8	0.18	37.1	342
11-Sep-08	1.25	7.3	0.393	1.67	7.8	0.19	13.6	343

Table A.4: Isotopic and elemental composition of all bubbling seeps sampled in our two study lakes in 2008

Lake	Source	Class	n	CO ₂ (%)	CH ₄ (%)	CH ₄ Std (%)	O ₂ (%)	N ₂ (%)	δ ¹³ C-CH ₄	δ ¹³ C-CO ₂	δD-CH ₄	Alpha C	Flux (mg/day)
Goldstream	2	HS	19	0.61	89.77	2.68	1.46	9.95	-74.4	-19.8	-361	1.062	10080
Goldstream	51	HS	12	0.36	91.04	2.71	2.46	12.98	-66.3	-16.5	-325	1.033	2229
Goldstream	3	B	10	0.25	78.79	9.81	4.72	17.49	-55.9	-21.4	-351	1.037	336
Goldstream	69	A	10	0.42	59.02	12.80	7.50	33.77	-57.2	-16.5	-363	1.045	84
Goldstream	12	HS	8	0.51	87.13	7.06	1.92	12.94	-67.1	-17.0	-337	1.057	2002
Goldstream	1	HS	5	0.31	90.31	1.13	1.21	11.06	-74.8	-28.2	-355	1.055	7500
Goldstream	14	C	4	0.47	83.38	1.31	1.91	17.31	-70.8	-21.0	-307	1.056	1601
Goldstream	3	HS	3	0.33	90.54	1.31	1.25	10.88	-74.5	-15.2	-357	1.066	3400
Goldstream	7	HS	2	0.59	91.67	1.58	0.93	10.57	-67.3	-22.8	-328	1.048	8584
Goldstream	10	HS	2	0.59	88.66	0.56	1.04	12.54	-68.6	-16.0	-337	1.057	-
Goldstream	5	B	1	0.75	95.97	-	0.72	0.67	-67.8	-13.7	-314	1.058	-
Goldstream	6	C	1	0.55	85.85	-	1.02	16.82	-71.5	-15.6	-312	1.060	-
Goldstream	8	HS	1	0.55	87.67	-	1.13	14.10	-68.5	-	-327	1.074	1157
Goldstream	15	C	1	0.17	80.43	-	2.82	18.33	-72.2	-13.0	-313	1.064	-
Goldstream	67	B	1	0.63	89.05	-	1.33	12.34	-67.6	-20.7	-315	1.050	161
Goldstream	85	B	1	0.66	91.36	-	1.87	10.00	-58.9	-17.0	-344	1.045	130
Goldstream	87	B	1	0.57	93.05	-	0.96	8.98	-67.7	-16.6	-315	1.055	-
Goldstream	23	HS	1	-	-	-	-	-	-70.1	-16.5	-312	1.075	-
Killamey	13	C	21	1.36	35.72	8.37	2.68	61.52	-83.8	-20.7	-296	1.069	3268
Killamey	49	HS	16	0.82	40.31	5.50	1.89	54.97	-84.8	-22.0	-301	1.065	1481
Killamey	25	C	10	0.43	35.56	3.56	2.70	61.92	-85.0	-21.9	-294	1.061	3237
Killamey	30	B	8	1.23	37.61	8.57	3.22	59.49	-80.3	-24.3	-307	1.060	473
Killamey	27	B	5	0.94	43.16	7.78	3.99	53.19	-84.9	-21.2	-311	1.071	176
Killamey	70	G	3	0.32	21.45	10.37	12.03	66.20	-77.0	-31.1	-288	1.055	88
Killamey	88	A	3	0.68	57.96	17.26	4.56	40.31	-76.3	-20.7	-342	1.060	394
Killamey	42	HS	2	0.98	28.27	1.00	1.35	72.14	-88.3	-21.2	-300	1.074	5117
Killamey	47	HS	2	2.01	45.69	2.52	1.45	52.00	-81.2	-23.0	-310	1.063	21
Killamey	55	C	2	1.06	30.42	1.09	4.20	66.98	-87.8	-23.4	-303	1.071	55
Killamey	108	A	2	0.53	41.39	8.10	4.08	56.22	-81.2	-24.2	-310	1.062	131
Killamey	117	C	2	0.73	42.98	4.76	2.96	55.78	-83.5	-25.2	-316	1.064	176
Killamey	125	C	2	0.49	30.68	9.83	4.51	66.71	-80.8	-32.2	-297	1.053	29
Killamey	132	HS	2	0.62	38.46	0.04	1.74	62.42	-84.5	-50.9	-299	1.037	3830
Killamey	11	B	1	2.03	41.75	-	1.00	55.92	-83.1	-19.8	-318	1.069	64
Killamey	12	C	1	2.16	37.35	-	0.77	60.25	-81.0	-19.2	-305	1.067	-
Killamey	19	A	1	2.86	33.53	-	2.58	62.11	-77.2	-20.0	-327	1.064	21
Killamey	21	HS	1	1.01	39.65	-	1.10	60.50	-85.0	-22.6	-309	1.068	4142
Killamey	22	HS	1	0.59	38.24	-	1.75	61.96	-85.8	-25.2	-297	1.066	4745
Killamey	32	C	1	0.84	38.15	-	1.76	61.71	-86.0	-26.8	-302	1.065	854
Killamey	68	B	1	0.49	42.49	-	4.23	55.24	-81.9	-40.2	-313	1.045	120
Killamey	77	HS	1	0.08	48.52	-	7.26	42.58	-84.3	-20.2	-291	1.070	-
Killamey	106	HS	1	0.82	36.13	-	1.70	63.39	-84.5	-19.7	-299	1.071	3061
Killamey	120	B	1	0.33	42.47	-	7.92	51.82	-76.3	-23.6	-332	1.057	10
Killamey	123	A	1	0.40	23.61	-	6.54	71.01	-75.8	-43.8	-330	1.035	5

Table A.5: Isotopic and elemental composition of all other bubbling seeps sampled in 2007 and 2008. Method column refers to either collection via submerged bubble trap ("Fresh") or capture of bubbles trapped in lake ice ("In-ice").

<i>Lake</i>	<i>Source</i>	<i>Class</i>	<i>Method</i>	<i>CO₂ (%)</i>	<i>CH₄ (%)</i>	<i>O₂ (%)</i>	<i>N₂ (%)</i>	$\delta^{13}\text{C-CH}_4$	$\delta^{13}\text{C-CO}_2$	$\delta\text{D-CH}_4$	<i>Alpha C</i>	<i>Flux (mg/day)</i>
A 27	-	C	In-ice	0.04	50.35	7.57	41.70	-68.3	-	-308	-	-
A 27	-	B	In-ice	0.07	0.27	8.08	90.79	-	-	-	-	-
A 35	-	B	In-ice	0.15	3.01	19.89	75.16	-12.4	-16.3	-	-	-
A 35	-	A	In-ice	0.03	42.36	10.55	45.36	-	-12.4	-	-	-
A 35	-	B	In-ice	0.04	49.27	9.19	39.99	-71.8	-	-327	-	-
E 06	-	C	In-ice	0.41	80.30	5.84	14.78	-62.3	-14.6	-233	1.051	-
E 06	-	B	In-ice	0.36	2.68	19.74	75.32	-36.6	-18.6	-282	1.019	-
E 06	11	B	Fresh	0.04	42.82	10.26	46.70	-	4.8	-334	-	27
E 06	12	C	Fresh	0.41	57.94	7.70	33.42	-	4.4	-334	-	107
E 06	14	B	Fresh	0.24	46.26	9.60	42.99	-62.2	-13.4	-320	1.052	22
Eight Mile	18	HS	Fresh	0.29	0.07	13.99	83.67	-59.1	-20.3	-	1.041	-
Eight Mile	19	HS	Fresh	0.36	0.04	17.26	80.40	-	-	-	-	-
Eight Mile	-	B	In-ice	0.13	0.11	20.40	77.83	-	-23.0	-	-	-
Eight Mile	-	B	In-ice	0.10	0.11	18.86	79.56	-	-	-	-	-
El Fuego	-	B	In-ice	0.08	44.00	6.77	47.71	-72.1	-14.6	-323	1.062	-
El Fuego	1	HS	Fresh	0.03	52.85	8.87	36.19	-	-	-	-	-
El Fuego	2	HS	Fresh	0.11	84.47	2.74	12.02	-76.3	-18.1	-319	1.063	-
Fog 01	-	C	In-ice	0.10	82.18	3.82	13.76	-	-	-	-	-
NE 14	-	B	In-ice	0.04	0.00	7.60	25.08	-	-11.3	-	-	-
NE 14	-	B	In-ice	0.03	0.44	20.14	76.23	-70.0	-46.6	-349	1.025	-
NE 02	-	B	In-ice	0.34	70.26	4.92	23.69	-72.6	-	-299	-	-
NE 02	-	B	In-ice	0.06	40.99	7.92	49.25	-	-40.8	-	-	-
NE 02	8	A	Fresh	0.11	10.85	14.84	73.66	-62.5	-25.0	-	1.040	10
NE 02	9	A	Fresh	0.13	8.25	10.31	80.18	-58.3	-25.1	-	1.035	2
NE 02	7	A	Fresh	0.15	19.44	13.45	66.03	-64.0	-14.5	-321	1.053	3
Toolik	20	C	Fresh	0.13	26.11	5.44	67.45	-59.3	-16.7	-298	1.045	2
Toolik	21	B	Fresh	0.14	4.02	13.02	81.53	-60.2	-26.1	-	1.036	-
Toolik	2A	A	Fresh	0.09	32.63	7.14	59.64	-63.6	-17.2	-343	1.050	13
WP1	-	B	In-ice	0.05	26.86	13.84	58.15	-	-	-	-	-
WP2	-	B	In-ice	0.21	43.76	6.60	47.58	-	-	-	-	-
Just-a-store	72	HS	Fresh	1.06	76.90	2.42	20.17	-59.9	-19.5	-361	1.048	169
Just-a-store	75	C	Fresh	1.25	74.90	2.69	22.14	-60.1	-18.4	-360	1.051	72

Table A.6: Water isotope data from lakes, sediment pore water and permafrost. Depth refers to the water depth, or depth along core or from the ground surface at which each sample was taken.

<i>Site (n)</i>	<i>Object</i>	<i>Date</i>	<i>Depth (m)</i>	δD (‰)	$\delta^{18}O$ (‰)
Goldstream (1)	Lake H ₂ O	25 Jun 08	0.01	-137	-14.7
Goldstream (1)	Lake H ₂ O	25 Jun 08	2.0	-136	-15.0
Goldstream (1)	Lake H ₂ O	12 Oct 08	0.01	-133	-15.3
Goldstream (1)	Lake H ₂ O	12 Oct 08	2.0	-132	-15.2
Killarney (1)	Lake H ₂ O	25 Jun 08	0.01	-147	-18.2
Killarney (1)	Lake H ₂ O	25 Jun 08	2.0	-146	-17.9
Killarney (1)	Lake H ₂ O	12 Oct 08	0.01	-146	-18.3
Killarney (1)	Lake H ₂ O	12 Oct 08	2.0	-145	-18.5
Goldstream Core A (12)	Pore H ₂ O	15 Apr 09	0.02 - 0.50	-152 ± 1	-18.4 ± 0.2
Goldstream Core C (10)	Pore H ₂ O	4 Nov 09	0.11 - 0.92	-142 ± 4	-15.3 ± 1.1
Killarney Core B (21)	Pore H ₂ O	8 Apr 09	0.08 - 1.68	-145 ± 2	-18.1 ± 0.4
Goldstream (1)	Permafrost H ₂ O	24 Sept 08	0.82 - 0.84	-186	-24.1
Killarney (1)	Permafrost H ₂ O	22 Sept 08	0.83 - 0.85	-150	-18.4

Table A.7: Coordinates of coring locations in both lakes.

<i>Core</i>	<i>Location</i>
Goldstream A	64°54'56.01"N, 147°50'53.66"W
Goldstream B	64°54'55.93"N, 147°50'53.08"W
Goldstream C	64°54'57.26"N, 147°50'50.85"W
Killarney A	64°52'11.52" N, 147°54'05.75"W
Killarney B	64°52'12.76" N, 147°54'08.18"W
Killarney C	64°52'12.84" N, 147°54'07.99"W